Exploring quantum features of large spin and photonic systems

Inauguraldissertation

zur
Erlangung der Würde eines Doktors der Philosophie
vorgelegt der
Philosophisch-Naturwissenschaftlichen Fakultät
der Universität Basel

von

Enky Oudot
von Frankreich

Basel, 2019

Genehmigt von der Philosophisch-Naturwissenschaftlichen Fakultät auf Antrag von
Prof. Dr. Nicolas Sangouard
Prof. Dr. Antonio Acín
Prof. Dr. Philipp Treutlein

Basel, 13. November 2018

Prof. Dr. Martin Spiess
Dekan

Creative Commons License Deed

Attribution-NonCommercial-NoDerivatives 4.0 International

This is a human-readable summary of (and not a substitute for) the license.

You are free to:

Share — copy and redistribute the material in any medium or format

The licensor cannot revoke these freedoms as long as you follow the license terms.

Under the following terms:

Attribution — You must give appropriate credit, provide a link to the license, and indicate if changes were made. You may do so in any reasonable manner, but not in any way that suggests the licensor endorses you or your use.

NonCommercial — You may not use the material for commercial purposes.

NoDerivatives — If you remix, transform, or build upon the material, you may not distribute the modified material.

No additional restrictions — You may not apply legal terms or technological measures that legally restrict others from doing anything the license permits.

Notices:

You do not have to comply with the license for elements of the material in the public domain or where your use is permitted by an applicable exception or limitation.

No warranties are given. The license may not give you all of the permissions necessary for your intended use. For example, other rights such as publicity, privacy, or moral rights may limit how you use the material.

ABSTRACT

In this thesis, we will present different theoretical tools for demonstrating the quantum features of possibly large photonic and spin systems. Our aim is not only to propose experiments demonstrating entanglement/non-locality in possibly large spin and photonic systems, but to clarify on the requirements that the detection systems need to fulfil to detect the quantum nature of these large systems. We will see that collective projections in which the subsystems are measured along the same direction, does not prevent the detection of entanglement and non-locality. Even threshold detectors with low efficiencies can be used to reveal non-classical features of states involving many photons. In parallel, we will make steps to clarify on the meaning of large/macroscopic when describing quantum states.

ACKNOWLEDGMENTS

I would like to thank all the people who spend time with me during these 4 years. First off all I would like to thank my Phd supervisor Nicolas Sangouard, his investment toward the success of my phd was priceless, his enthusiasm for physics put my moral up when it was needed. I learned more than just physicist skills at his contact.
I would like to thank my fellow doctoral students, especially Melvyn Ho for his helps for way more things than the space I have to enumerate it.
I am also grateful to my amazing postdoctoral researcher, Pavel Sekatski and Jean Daniel Bancal, I learned a lot from them.

I would like to thank my friends and my family to support me when it was needed. Last but not the least, I would like to particularly thank my brother, my mother and my girl friend for supporting me spiritually throughout writing this thesis and in my life in general.

CONTENTS

LIST OF PUBLICATIONS

1. Two-mode squeezed states as Schrödinger cat-like states
   Journal of the Optical Society of America B **32**, 2190 (2015).

2. Optimal entanglement witnesses in a split spin-squeezed Bose-Einstein condensate
   Physical Review A **95**, 052347 (2017).

3. Proposal for witnessing non-classical light with the human eye
   Quantum **1**, 7 (2017).

4. Witnessing optomechanical entanglement with photon counting
   Physical Review Letters **121**, 023602 (2018).

5. Bipartite non-locality with many-body systems
   arXiv: 1810.05636.

INTRODUCTION

In 1964, J.S. Bell proposed a concrete experiment to show the limit of classical physics and the necessity of a non-local theory for a complete description of physical reality [1]. While entanglement allows quantum theory to be non-local, it is also revolutionising applied physics and many quantum technologies including quantum communication, computing and metrology are at the heart of many academic projects and strategic developments of multinational companies. These efforts have already led to impressive experimental progress. Quantum cryptographic devices are available commercially since 2004 and the first exchange of a secret quantum key through space have been realized recently [2]. The field of quantum computing is advancing rapidly, in part, due to a race between ambitious companies to realize the first fully functioning quantum computer. Google, for example, hopes this year, or shortly after, to perform a computation that is beyond even the most powerful classical supercomputer and Microsoft aims to perform the first demonstration of topological quantum computing [3]. The advantage of using entanglement and in particular, in large systems, for applied physics is well illustrated in metrology. We quicly present this advantage here.

The aim of metrology is to measure small quantities with a very good accuracy using a fix number N of particles. For cold atoms, a typical situation is the rotation of an atom by an angle θ in a magnetic field. One then performs Ramsey-interferometry to estimate θ, in order to infer the amplitude of the magnetic field [4]. Quantum states with particles exhibiting quantum correlations, or more precisely, quantum entanglement [6], can provide a higher precision than an ensemble

of uncorrelated particles. Very general derivations lead to, at best, a variance of

$$\Delta\theta = \frac{1}{N} \tag{1}$$

for non-entangled particles. Equation (1) is called the shot-noise scaling. On the other hand, quantum entanglement makes it possible to reach a variance of

$$\Delta\theta = \frac{1}{N^2} \tag{2}$$

which is called the Heisenberg-scaling. One can see that not only does one need entanglement in order benefit from such scaling but entanglement in a large quantum system.

With this simple yet powerful example, we see a clear advantage for metrology when using entangled states with a large number of particles. The same advantage holds for quantum computation, in particular measurement-based quantum computation where one needs entanglement between all the qubits to start with, e.g in a form of a cluster state [5], before performing individual measurements. In quantum communication, the long term goal is to realise quantum networks where entanglement can be distributed in between multiple nodes so that they can share secret keys and subsequently secret communications. Entanglement in large systems is thus a key ingredient of each of these quantum technologies.

Before presenting our results, we begin by defining entangled states. The simplest scenario is the one where two parties, Alice and Bob, share a pure state $|\psi\rangle \in H_A \otimes H_B$. $|\psi\rangle$ is a product state if one can find states $|\phi\rangle_A$ and $|\phi\rangle_B$ such that

$$|\psi\rangle = |\phi_A\rangle \otimes |\phi_B\rangle \,. \tag{3}$$

To keep the notation simple, we often write the tensor product of two states as $|\phi_A\rangle \otimes |\phi_B\rangle = |\phi_A\phi_B\rangle$. A pure state is said to be entangled if it is not a product state. In the case of mixed states, if there exist a convex sum of state $\rho_i^A \otimes \rho_i^B$ with weights p_i such that

$$\rho_{sep} = \sum_i p_i \rho_i^A \otimes \rho_i^B, \tag{4}$$

the state ρ_{sep} is separable. If a state is not separable, it is said to be entangled.

With this definition in place, we now discuss tools to detect entanglement. One possible way of demonstrating entanglement is to use separability criteria [8, 9, 10, 11]. In a bipartite system, separability criteria are direct constraints on the density matrices satisfying (4). To check that a given state does not satisfy some of these constraints and is thus entangled, one usually requires extensive knowledge of the elements of the density matrix of the tested state, which can be very demanding as the dimension of the system grows. To avoid this problem, one might use an entanglement witness which is an operator $\mathbf{W}$ satisfying

$$\mathrm{Tr}(\mathbf{W}\rho_{sep}) \geq 0 \tag{5}$$

for all separable state. A schematic picture of the set of quantum states including

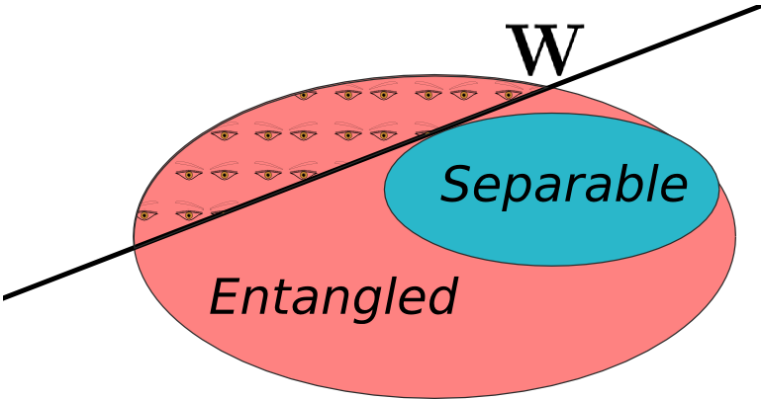

Figure 1: Schematic picture of the set of all states and the set of separable states. A tight witness $\mathbf{W}$ is represented by a black line which corresponds to an hyperplane defines by $\mathrm{Tr}(\mathbf{W}\rho) = 0$. The part of entangled states detected by the witness is represented by the red region with many eyes.

the hyperplane defined by $\mathrm{Tr}(\mathbf{W}\rho) = 0$ is represented in Fig.(1). One can directly see the advantage of using such witnesses: It allows one to detect entanglement even in a large ensemble of particles where it is only possible to perform a restricted set of measurements. A witness can simply be constructed from this restricted set of measurements. Finding witnesses of entanglement tailored to specific cases has been an active field of research in the past 20 years [12] .

Note than one can also consider more general cases involving more than 2 parties.

We say that a pure state of N parties is fully separable if it is a product state of all parties, that is, if

$$|\psi\rangle = |\phi^1\rangle \otimes |\phi^2\rangle \ldots \otimes |\phi^N\rangle \,. \tag{6}$$

A mixed state is called fully separable if it can be written as a convex combination of pure fully separable states, that is, it can be written as

$$\rho = \sum_k p_k \rho_1^k \otimes \rho_2^k \otimes \ldots \otimes \rho_N^k. \tag{7}$$

If a state is not fully separable, it contains some entanglement. This does not yet imply true genuine entanglement. Thus, we call a pure state m-separable, with $1 < m < N$, if there exists a splitting of the N parties into m parts $L1, ..., Lm$ such that

$$|\psi\rangle = |\phi^1\rangle_{L_1} \otimes |\phi^2\rangle_{L_2} \ldots \otimes |\phi^M\rangle_{L_m} \,. \tag{8}$$

holds. Note that an m-separable state still may contain some entanglement. We called mixed states m-separable, if they can be written as convex combinations of pure m-separable states, which might belong to different partitions. Finally, we call a state truly N-partite entangled when it is neither fully separable, nor m-separable, for any $m > 1$. In this multipartite scenario, entanglement witnesses again show themselves to be very useful for the characterization of entanglement [13, 14, 15, 16].

As we have seen, entanglement witnesses are useful tools for characterizing entanglement. However, the certification of entanglement using a witness usually relies on either an accurate description of the measurement device or an assumption about the Hilbert space dimension. Such assumptions typically rely on the best understanding of the physics of the measured system currently available - a physical model consistent with the history of previous experiments performed on the same setup. Nonetheless, this does not protect against interpretation bias, which can lead to erroneous conclusions, e.g. about the presence of quantum features [17]. The proper use of these assumptions is crucial in the use of entanglement witnesses.

Let us give an example to illustrate how one can make wrong conclusions if the hypotheses about the accurate description of the measurement and the dimension of the Hilbert space are not fulfilled. Two parties Alice and Bob share a state which

they assume to be a two qubit state and want to demonstrate its entanglement property. For a two qubit separable state, it is straightforward to demonstrate that

$$\langle \mathbf{W} \rangle = 1 - (\langle \sigma_x^A \sigma_x^B \rangle + \langle \sigma_y^A \sigma_y^B \rangle) \geq 0, \tag{9}$$

where σ_i^A (σ_i^B) represents a Pauli measurement in the direction i for Alice (Bob). $\mathbf{W}$ is thus a witness of entanglement. Now consider the case where they do not actually share a state of two qubits. The state of Alice and Bob could live in a higher dimension

$$\rho = \frac{1}{4} \sum_{i,j=0}^{1} |x_i, y_j\rangle \langle x_i, y_j|_A \otimes |x_i, y_j\rangle \langle x_i, y_j|_B \tag{10}$$

for example, where x_0, x_1 (y_0, y_1) correspond to the two eigenvectors of σ_x (σ_y). When Alice and Bob measure $\mathbf{W}$, they could be measuring $\sigma_x \otimes \mathbf{1}$ instead of σ_x and $\mathbf{1} \otimes \sigma_y$ instead of σ_y. They will thus find $\langle W \rangle = -1$ and conclude about the presence of entanglement even if ρ is separable. The hypothesis behind the use of this witness was wrong and thus led to wrong conclusions. This naturally raises the question of how to demonstrate entanglement in a device independent way, that is, without assumption on the description of the measurement device and on the dimension of the Hilbert space.

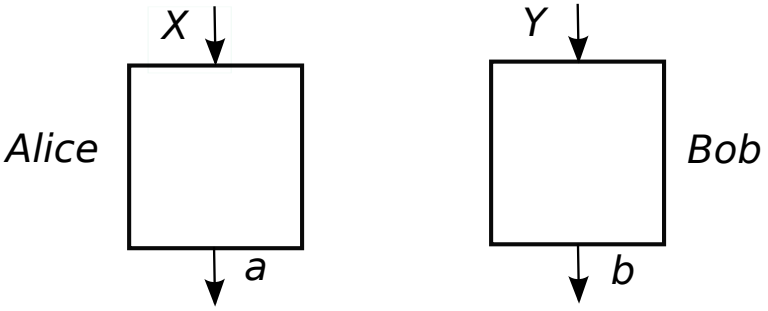

Figure 2: Schematic representation of a CHSH test where two protagonists Alice and Bob have two black boxes with inputs (X,Y) and outputs (a,b) and perform measurement in order to have access to correlators.

Fully device independent certification relies on Bell inequalities. The simplest Bell test is described in the Clauser-Horne-Shimony-Holt (CHSH) scenario, where two protagonists Alice and Bob have two black boxes with two inputs (X, Y) and two

outputs (a, b) as shown in Fig. (2). They then compute the joint probability of obtaining one output given one input $P(a, b|X, Y)$. The hypothesis of locality leads to constraints on these probabilities which we call a Bell inequality. It turns out that Bell inequalities are very powerful tools for device independent conclusions. For example, given the maximum violation of the CHSH inequality, one can certify that the state is a singlet state up to local isometry [19] and the measurement performed are Pauli matrices. Bell tests thus allow us to conclude about the presence of entanglement in scenario where we have uncharacterised measurement devices and state dimension.

As we have seen, we can make use of many tools to characterize quantum features in different systems. The aim of this work is to show how they can be used for detecting experimentally quantum features in possibly large systems, including spin and photonic systems. We also clarify on the requirements that the detection systems need to fulfil to detect the quantum nature of these large systems.

In the first step, we develop a method to witness bipartite entanglement in spin systems which is robust against noise and only requires low order moments of collective spin observables. We describe this method in **Chapter 1: Entanglement witnesses for a split many-body system.**

We then study the possibility to characterize bi-partite non locality in a many body system in **Chapter 2: Bipartite Bell non locality in many-body systems.**

So far, we have limited ourselves to the detection schemes which are used in experiments. Could we go beyond this? Can one use a noisy detector like the human eye in order to detect quantum features in a photonic state? We elaborate on that in **Chapter 3: Detection of the non-classical nature of light with the human eye.**

Optical technologies have been a very promising resource for quantum communication. We investigate in **Chapter 4** genuine entanglement in photonic systems in a scenario relevant for future quantum networks, **Genuine Entanglement in multi-partite photonic systems.**

As we consider systems with large numbers of particles, we make a concrete proposal for defining the size of a quantum state which can be applied to different systems. We detail our contribution on this in **Chapter 5: Macroscopic quantum states of light.**

CHAPTER 1

ENTANGLEMENT WITNESSES FOR A SPLIT MANY-BODY SYSTEM

We begin our investigation by being interested with the simplest form of entanglement, namely bipartite entanglement in many body systems. Let us start by noting that Bell correlations that is, correlations strong enough to violate a Bell inequality, have been demonstrated in a Bose-Einstein-Condensate (BEC) [20]. A natural question is then if it is possible to demonstrate non locality if one separates this system into two spatially separated subsystems. We propose a first step toward a Bell test by focusing on witnesses of entanglement suited for a split many-body system.

More precisely we consider the scenario of Fig. 1.1 where two parties Alice and Bob share many 1/2 spins. In practice, these spins can be physically implemented in two internal states of atoms. Due to current imaging techniques, it is very hard to address the spin of each atom individually. We thus restrict ourselves to collective measurements where each party can only address all of its atoms in the same direction. Even with collective measurements, one might further encounter an imperfect precision on the atom number distribution which constrains us to consider only low order moments of such spin operators. In any such experiment the statistics that are feasible are also finite, and thus the ability to access high order moments of collective spin observables from the distribution of the measured collective spins is limited. In practice only first and second order moments of collective spin observable can be measured with reasonable precision.

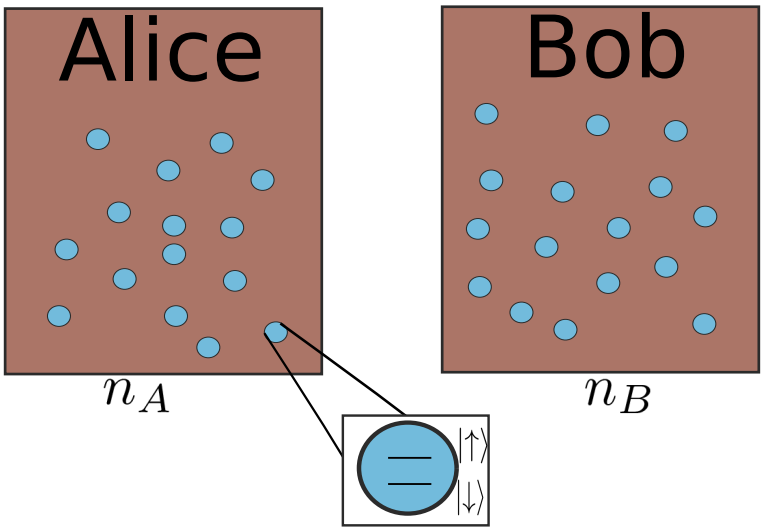

Figure 1.1: Schematic representation of the bipartite we considered. A bipartite system constitute with many qubits which can be two internal energie level of atoms.

We thus develop numerical methods to characterize the set of separable first and second order moments of collective spin observables. This method allows us to find any witness constructed by the linear combination of first and second order moments of collective spin observables, and thus conclude about entanglement only based on this knowledge. We consider a split spin squeezed state as an example to illustrate the usefulness of our method and present optimal witnesses for this state.

Paper A

Optimal entanglement witnesses in a split spin-squeezed Bose-Einstein condensate

Enky Oudot, Jean-Daniel Bancal, Roman Schmied, Philipp Treutlein, and Nicolas Sangouard

Phys. Rev. A **95**, 052347(2017)

Optimal entanglement witnesses in a split spin-squeezed Bose-Einstein condensate

Enky Oudot,[1] Jean-Daniel Bancal,[1] Roman Schmied,[2] Philipp Treutlein,[2] and Nicolas Sangouard[1,*]
[1]*Quantum Optics Theory, Department of Physics, University of Basel, Klingelbergstrasse 82, 4056 Basel, Switzerland*
[2]*Quantum Atom Optics Laboratory, Department of Physics, University of Basel, Klingelbergstrasse 82, 4056 Basel, Switzerland*
(Received 6 March 2017; published 30 May 2017)

How do we detect quantum correlations in bipartite scenarios using a split many-body system and collective measurements on each party? We address this question by deriving entanglement witnesses using either only first-order or both first- and second-order moments of local collective spin components. In both cases, we derive optimal witnesses for spatially split spin-squeezed states in the presence of local white noise. We then compare the two optimal witnesses with respect to their resistance to various noise sources operating either at the preparation or at the detection level. We finally evaluate the statistics required to estimate the value of these witnesses when measuring a split spin-squeezed Bose-Einstein condensate. Our results can be seen as a step toward Bell tests with many-body systems.

DOI: 10.1103/PhysRevA.95.052347

I. INTRODUCTION

Substantial efforts have been devoted in the past years to the characterization of many-body systems through the entanglement of their elementary bodies [1,2]. While entanglement is usually detected using entanglement witnesses in many-body systems, first theoretical [3–8] and experimental [9] steps have been taken to test a Bell inequality on a many-body system. The interest is twofold. First, the violation of a Bell inequality certifies the presence of a stronger form of quantum correlation than entanglement, namely, Bell correlations [10]. Second, Bell inequalities certify the presence of nonclassical correlations independently of the device, i.e., without assumption of the Hilbert space dimension or the structure of the measurement operation [11]. While Bell correlation witnesses have been proposed and used recently to successfully detect Bell-correlated states in a Bose-Einstein condensate [9], the device-independent detection of nonclassical correlations remains to be demonstrated in many-body systems. The main problem is that Bell tests require one to address the constituent bodies individually, which is challenging in many-body systems. A natural approach to circumvent this problem consists first in a bipartite splitting of the constituent bodies and then in applying collective measurements on each party. While the ultimate goal is to perform a Bell test, we focus on a simpler task in this paper, namely, the detection of entanglement between these two parties.

Let us clarify the scenario. We consider an ensemble of N atoms with two internal states 1 and 2 and located at location A. Let $\hat{a}_i$ and $\hat{a}_i^\dagger$ with $i \in \{1,2\}$, be the corresponding bosonic operators satisfying $[\hat{a}_i,\hat{a}_j^\dagger] = \delta_{i,j}$. To describe this ensemble of atoms, we use the picture of a collective spin, i.e., a vector of operators $\vec{J}^A$ with components

$$\hat{J}_x^A = \frac{1}{2}(\hat{a}_1^\dagger\hat{a}_2 + \hat{a}_1\hat{a}_2^\dagger), \tag{1}$$

$$\hat{J}_y^A = \frac{1}{2i}(\hat{a}_1^\dagger\hat{a}_2 - \hat{a}_1\hat{a}_2^\dagger), \tag{2}$$

$$\hat{J}_z^A = \frac{1}{2}(\hat{a}_1^\dagger\hat{a}_1 - \hat{a}_2^\dagger\hat{a}_2), \tag{3}$$

satisfying the commutation relations

$$\left[\hat{J}_i^A,\hat{J}_j^A\right] = i\epsilon_{ijk}\hat{J}_k^A, \tag{4}$$

where ϵ_{ijk} is the Levi-Civita symbol and $i,j,k \in \{x,y,z\}$. The component $\hat{J}_z^A$ of the collective spin is half the population difference between the two internal states while $\hat{J}_x^A$ and $\hat{J}_y^A$ describe the coherence between these two states. We consider the case where initially this spin points in the x direction

$$|\psi_0\rangle = \frac{1}{\sqrt{N}} e^{-i\frac{\pi}{2}\hat{J}_y^A}\hat{a}_1^{\dagger N}|0\rangle, \tag{5}$$

where $|0\rangle$ is the vacuum state for all modes and then undergoes one-axis twisting [12,13]

$$|\psi\rangle = e^{-i\chi t(\hat{J}_z^A)^2}|\psi_0\rangle. \tag{6}$$

This results in a spin-squeezed state, i.e., a state for which the variance along a certain direction $(\Delta\hat{J}_\perp^A)^2 = \langle(\hat{J}_\perp^A)^2\rangle - \langle\hat{J}_\perp^A\rangle^2$ is smaller than $\frac{1}{N}|\langle\hat{J}_x^A\rangle|^2$. This means that the mean spin projection of the state is large, and in a direction orthogonal to it, the spin variance is small. While the product of the squeezing rate χ and interaction time t could be used to quantify the amount of squeezing as in Refs. [14,15], one usually refers to the spin squeezing or Wineland parameter [16,17] $\xi^2 = \frac{N(\Delta\hat{J}_\perp^A)^2}{\langle\hat{J}_x^A\rangle^2}$. For a coherent spin state like $|\psi_0\rangle$, $\xi^2 = 1$. $\xi^2 < 1$ witnesses metrologically useful states; see, e.g., [13,18] for a detailed discussion. For the state $|\psi\rangle$, this parameter is given by

$$\xi^2 = \frac{1}{4}\cos(\chi t)^{2-2N}(3+N-(N-1)\{\cos(2\chi t)^{N-2} + \sqrt{[1-\cos(2\chi t)^{N-2}]^2 + 16\cos(\chi t)^{2N-4}\sin(\chi t)^2}\}).$$

In the rest of the paper, *we quantify spin squeezing through the quantum noise reduction in dB using* $10\log_{10}(\xi^2)$ *for* $N = 500$ *atoms*. For example, -10 dB squeezing corresponds to $\chi t = 0.0058$. Note that the existence of spin squeezing is connected to quantum correlation between the spins [14], and many entanglement witnesses have been derived for spin-squeezed states; see [12,13] for reviews.

*nicolas.sangouard@unibas.ch

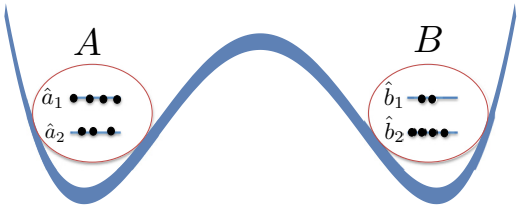

FIG. 1. Schematic representation of the four mode system of interest. The two internal states of the atoms located in A are initially prepared in a coherent spin state along the x direction [Eq. (5)] before being squeezed with one-axis twisting [Eq. (6)]. The atoms are then spatially split and distributed between A and B with a binomial distribution before being measured collectively. The aim of this paper is to propose entanglement witnesses that could be used to reveal entanglement between locations A and B in the presence of noise.

In this paper, we consider the case where the atoms are spatially split with a state-independent beamsplitter, i.e.,

$$|\phi\rangle = e^{\frac{\pi}{4}(\hat{a}_1^\dagger \hat{b}_1 + \hat{a}_2^\dagger \hat{b}_2 - \text{H.c.})} |\psi\rangle , \tag{7}$$

where $\hat{b}_i$ and $\hat{b}_i^\dagger$ are bosonic operators for the location B, see Fig. 1. Our aim is to show how to reveal entanglement between A and B using the collective spin observables given in Eqs. (1)–(3) and similarly for B. Let us mention that entanglement [19–22] and steering [23] have been studied in a different scenario where a beamsplitter interaction is applied in order to couple two spin-squeezed states. In this work, we show how to derive optimal witnesses for the state $|\phi\rangle$ in the presence of local white noise using either only first-order or both first- and second-order moments of local collective spins. Interestingly, we find in each case witnesses that are closely related to existing entanglement criteria [24–27] and we show how they could be used to reveal entanglement in a split Bose-Einstein condensate (BEC).

Concretely, we consider a two-component BEC of alkali atoms where two hyperfine states represent a pseudo-spin $\frac{1}{2}$ for each atom, see Fig. 1. Such a BEC can be prepared in one of the two hyperfine levels without discernible thermal components before being rotated with a $\pi/2$ pulse around the y axis, hence creating a coherent spin state pointing along the x direction as described by Eq. (5). To create quantum correlations between the spins, one can make use of elastic collisions in state-dependent potentials [28,29], giving rise to one-axis twisting as in Eq. (6). The spatial splitting is done by slowly raising a barrier in a state-independent potential as in Refs. [30,31]. To characterize the resulting state, the collective observables $\hat{J}_z^{A/B}$ can be accessed locally in each well by counting the number of atoms in each hyperfine state using resonant absorption imaging [32]. Projections along other spin directions are obtained by appropriate Rabi rotations in each well before the measurement. We show through a detailed feasibility study that the detection of entanglement in this system is within reach using currently available setups.

The outline of this paper is the following. In Sec. II, we derive witnesses using first-order moments of local collective spin operators, i.e., $\langle \hat{J}_i^A \rangle$, $\langle \hat{J}_i^B \rangle$, and $\langle \hat{J}_i^A \hat{J}_j^B \rangle$, where i,j label the components in the directions x, y, and z. We show in particular, the entanglement witness that is optimal regarding the tolerance to local white noise. In Sec. III, we consider the set of witnesses involving not only first-order moments of local collective operators, but also the second-order moments $\langle (\hat{J}_i^A)^2 \rangle$ and $\langle (\hat{J}_i^B)^2 \rangle$ and derive again the witness that is optimal with respect to the tolerance to local white noise. The optimal witnesses presented in Secs. II and III are then compared in Sec. IV with respect to various experimental issues operating either at the level of the state preparation or at the level of the detection. Section V is devoted to a feasibility study using a spin-squeezed Bose-Einstein condensate. We quantify in particular the statistics needed to estimate the value of our entanglement witnesses in realistic parameter regimes. We conclude in the last section.

II. ENTANGLEMENT WITNESSES USING FIRST-ORDER MOMENTS OF LOCAL COLLECTIVE SPIN OBSERVABLES

This section is divided into three subsections. The first one shows how to derive entanglement witnesses using first-order moments of local collective spin observables. The second subsection aims at identifying the witness that is optimal with respect to local white noise. The last subsection presents the result of this optimization.

A. Construction of entanglement witnesses

We first consider the case where n_a atoms are located in A and n_b in B. With this in mind, we focus on the set of expectation values of first-order moments of local collective spin observables (LCSOs). This is a real space consisting of all possible values of $\langle \hat{J}_i^A \rangle$, $\langle \hat{J}_i^B \rangle$, and $\langle \hat{J}_i^A \hat{J}_j^B \rangle$, where $i,j,k = \{x,y,z\}$. Note that the marginals $\langle \hat{J}_i^A \rangle$ and $\langle \hat{J}_i^B \rangle$ are constrained by

$$||\langle \vec{J}^A \rangle|| \leqslant \frac{n_a}{2}, \quad ||\langle \vec{J}^B \rangle|| \leqslant \frac{n_b}{2}. \tag{8}$$

This can be seen by noting that by a rotation, the vector $\langle \vec{J}^A \rangle = (\langle \hat{J}_x^A \rangle, \langle \hat{J}_y^A \rangle, \langle \hat{J}_z^A \rangle)$ can be brought to a form where one component only is nonvanishing. Since any component $\hat{J}_i^A$ has $-n_a/2$ and $n_a/2$ as eigenvalues with the largest modulus, $||\langle \vec{J}^A \rangle||$ is bounded by $n_a/2$. The same arguments apply to $||\langle \vec{J}^B \rangle||$. We call $\mathcal{U}$ the space of possible values of $\langle \hat{J}_i^A \rangle$, $\langle \hat{J}_i^B \rangle$, and $\langle \hat{J}_i^A \hat{J}_j^B \rangle$ satisfying the inequality (8).

We now consider a subspace $\mathcal{L}$ generated by the expectation values of first-order moments of LCSOs that are obtained from separable states, i.e., states of the form

$$\rho_{n_a,n_b} = \sum_k p_k \rho_{n_a}^{A(k)} \otimes \rho_{n_b}^{B(k)}, \tag{9}$$

where p_k is a probability distribution. $\mathcal{L}$ is a convex set. This can be seen by considering the sum $\Lambda \vec{X} + (1-\Lambda)\vec{Y}$ of two vectors in $\mathcal{L}$ where Λ is an arbitrary positive real number smaller than or equal to 1. The components of $\Lambda \vec{X} + (1-\Lambda)\vec{Y}$ can be written as a sum of two traces involving the same LCSO

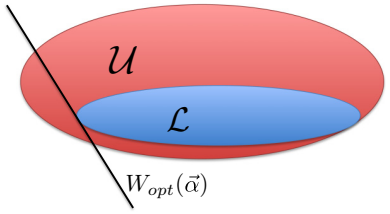

FIG. 2. Schematic representation of the set $\mathcal{U}$ of expectation values of first-order moments of local collective spin observables $\langle \hat{J}_i^A \rangle$, $\langle \hat{J}_i^B \rangle$, $\langle \hat{J}_{i,j}^{A,B} \rangle$, where $i,j,k \in \{x,y,z\}$ satisfying $||\langle \vec{J}^A \rangle|| \leqslant \frac{n_a}{2}$ and $||\langle \vec{J}^B \rangle|| \leqslant \frac{n_b}{2}$. The subset $\mathcal{L}$ is generated by the expectation values of first-order moments of local collective spin observables obtained from separable states [Eq. (9)]. Since $\mathcal{L}$ is a convex set, a family of linear witnesses is sufficient to fully characterize it. The minimum value that these witnesses can take on separable states $w(\vec{\alpha})_{n_a,n_b} - W(\vec{\alpha})_{n_a,n_b} = 0$ defines hyperplans in $\mathcal{U}$ that are tangent to $\mathcal{L}$. One of these hyperplans is drawn as a black line. The fact that some of these witnesses can be violated indicates that $\mathcal{U}$ is larger than $\mathcal{L}$.

and two different separable states. By the linearity of the trace and the convexity of the set of separable states, we deduce that $\Lambda\vec{X} + (1-\Lambda)\vec{Y}$ belongs to $\mathcal{L}$, i.e., $\mathcal{L}$ is convex. Hence, to characterize $\mathcal{L}$, it is sufficient to consider witnesses that are linear with respect to $\langle \hat{J}_i^A \rangle$, $\langle \hat{J}_i^B \rangle$, and $\langle \hat{J}_i^A \hat{J}_j^B \rangle$; see Fig. 2. Such witnesses are of the form $W(\vec{\alpha})_{n_a,n_b} = \langle \hat{W}(\vec{\alpha}) \rangle$ with

$$\hat{W}(\vec{\alpha}) = \sum_{i,j=x,y,z} \alpha_{i,j} \hat{J}_i^A \hat{J}_j^B + \bar{\alpha}_i \hat{J}_i^A + \alpha_i \hat{J}_i^B \tag{10}$$

the corresponding operators. These witnesses can be parametrized by a vector $\vec{\alpha} = (\alpha_{i,j}, \bar{\alpha}_i, \alpha_i)$ with 15 elements. Each vector $\vec{\alpha}$ defines one particular direction in the space $\mathcal{U}$ and the maximum value that a given $W(\vec{\alpha})$ can take over the set of separable states defines the boundary of $\mathcal{L}$ in the direction $\vec{\alpha}$. For any product state $\rho_{n_a}^{A(k)} \otimes \rho_{n_b}^{B(k)}$, we have

$$W(\vec{\alpha})^{(k)}_{\text{prod},n_a,n_b} = \left(\sum_{i,j=x,y,z} \alpha_{i,j} \langle \hat{J}_i^{A(k)} \rangle \langle \hat{J}_j^{B(k)} \rangle + \bar{\alpha}_i \langle \hat{J}_i^{A(k)} \rangle + \alpha_i \langle \hat{J}_i^{B(k)} \rangle \right),$$

where $\langle \hat{J}_i^{A(k)} \rangle = \text{tr}(\rho_{n_a}^{A(k)} \hat{J}_i^A)$ and similarly for $\langle \hat{J}_i^{B(k)} \rangle$. We deduce that for any state of the form (9), we have

$$\begin{aligned} W(\vec{\alpha})_{\text{sep},n_a,n_b} &= \sum_k p_k W(\vec{\alpha})^{(k)}_{\text{prod},n_a,n_b} \\ &\leqslant \max_k \left(\sum_{i,j=x,y,z} \alpha_{i,j} \langle \hat{J}_i^{A(k)} \rangle \langle \hat{J}_j^{B(k)} \rangle \right. \\ &\quad \left. + \bar{\alpha}_i \langle \hat{J}_i^{A(k)} \rangle + \alpha_i \langle \hat{J}_i^{B(k)} \rangle \right), \end{aligned} \tag{11}$$

where $W(\vec{\alpha})_{\text{sep},n_a,n_b}$ refers to the set of values attainable by $W(\vec{\alpha})_{n_a,n_b}$ while considering only the separable states given in Eq. (9). For a given choice of $\vec{\alpha}$, the value of k which saturates the inequality (11) defines a separable bound $w(\vec{\alpha})_{n_a,n_b}$, i.e., the maximum value that $W(\vec{\alpha})_{\text{sep},n_a,n_b}$ can take. The latter can be computed as

$$\begin{aligned} w(\vec{\alpha})_{n_a,n_b} = &\max_{||\langle \vec{J}^A \rangle|| \leqslant \frac{n_a}{2}, ||\langle \vec{J}^B \rangle|| \leqslant \frac{n_b}{2}} \\ &\times \left(\sum_{i,j=x,y,z} \alpha_{i,j} \langle \hat{J}_i^A \rangle \langle \hat{J}_j^B \rangle + \bar{\alpha}_i \langle \hat{J}_i^A \rangle + \alpha_i \langle \hat{J}_i^B \rangle \right). \end{aligned}$$

This yields the following family of witnesses:

$$w(\vec{\alpha})_{n_a,n_b} - W(\vec{\alpha})_{n_a,n_b} \geqslant 0, \tag{12}$$

which is satisfied by measurement on all separable states. Note that there is no guarantee that the previous inequality can be violated. A violation of this inequality, however, reveals the presence of entanglement.

Now consider the case in which N spins are split leading to a fluctuating number of particles between the two locations A and B at each run. Since we are only considering local spin observable measurements, the coherence between different atom numbers on each side cannot be probed and only the distribution of the particles $p(n_a, N-n_a)$ between the two wells matters. Following the same line of thought we get a separable bound for any distribution of particles across the two wells, including the case where the atomic fluctuations during the splitting result in reduced fluctuations of the relative atom number between A and B. That is, $w(\vec{\alpha}) = \sum_{n_a} p(n_a, N-n_a) w(\vec{\alpha})_{n_a,N-n_a}$. Since we are considering the splitting given in Eq. (7) leading to a binomial distribution of particles, we end up with the separable bound

$$w(\vec{\alpha}) = \sum_{n_a} \frac{1}{2^N} \binom{N}{n_a} w(\vec{\alpha})_{n_a,N-n_a} \tag{13}$$

and the corresponding entanglement witnesses

$$w(\vec{\alpha}) - W(\vec{\alpha}) \geqslant 0 \tag{14}$$

with $W(\vec{\alpha})$ the expectation value of $\hat{W}(\vec{\alpha})$ given in Eq. (10), evaluated on the state (7) which involves variable local atom numbers.

B. Optimal witness with respect to local white noise

Now that a family of witnesses is available, we want to find the one that is the most relevant for the scenario described in the Introduction. In particular, we consider the general case where the split spin-squeezed state $|\phi\rangle$ experiences local white noise in each location, i.e., we consider the state

$$\rho_{\text{noisy}} = p\,|\phi\rangle\langle\phi| + \sum_{k=0}^{N} \frac{(1-p)}{(k+1)(N-k+1)} \binom{N}{k} \mathbb{I}_k \otimes \mathbb{I}_{N-k}, \tag{15}$$

where $\mathbb{I}_k$ is the identity for k particles in the symmetric subspace and we look for the witness that can detect entanglement for the smallest value of p. Note first that $W(\vec{\alpha})_{\rho_{\text{noisy}}} = \text{tr}(\hat{W}(\vec{\alpha})\rho_{\text{noisy}}) = p\,\text{tr}(\hat{W}(\vec{\alpha})\,|\phi\rangle\langle\phi|) = p\,W(\vec{\alpha})_{|\phi\rangle}$. For a given choice of $\vec{\alpha}$, we define $W(\vec{\alpha})^{\text{opt}}_{|\phi\rangle}$ as the maximal value of $W(\vec{\alpha})_{|\phi\rangle}$ over all possible local rotations. Since entanglement is by definition invariant under local rotation, the resistance to noise

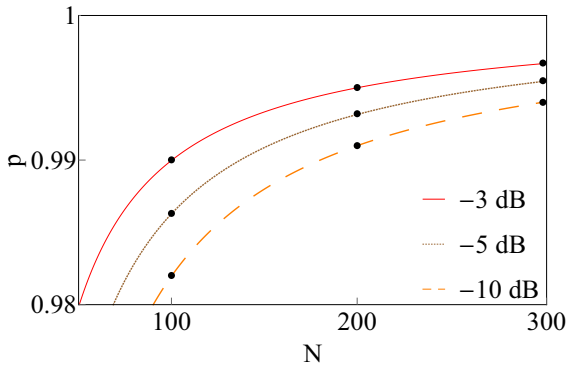

FIG. 3. Tolerable noise as a function of the number of atoms for the criterion (17) for different squeezing. The black dots correspond to the results of the numerical optimization, which have been obtained following the procedure described in Sec. II B.

of the witness corresponding to the direction $\vec{\alpha}$ is given by the value of p such that

$$p W(\vec{\alpha})^{\text{opt}}_{|\phi\rangle} = w(\vec{\alpha}). \tag{16}$$

We emphasize here that $w(\vec{\alpha})/W(\vec{\alpha})^{\text{opt}}_{|\phi\rangle} = p_{\text{min}} < 1$ implies that the witness $w(\vec{\alpha}) - W(\vec{\alpha})^{\text{opt}}_{|\phi\rangle} \geqslant 0$ parametrized by the direction $\vec{\alpha}$ detects entanglement in state ρ_{noisy} [Eq. (15)] for p going from p_{min} to 1. The optimal witness is thus associated with the particular direction $\vec{\alpha}$ such that the ratio $w(\vec{\alpha})/W(\vec{\alpha})^{\text{opt}}_{|\phi\rangle}$ takes the smallest possible value. Since the state $|\phi\rangle$ depends on χt and N, the procedure needs to be repeated when changing these two parameters. The result of this optimization is given in the next subsection.

C. Result of the optimization

To find the witness admitting the largest amount of noise, we minimized numerically the value of the ratio $w(\vec{\alpha})/W(\vec{\alpha})^{\text{opt}}_{|\phi\rangle}$ over all choices of $\vec{\alpha}$ and of local unitaries. We display the results of this optimization (black dots) in Fig. 3 where we plot the resistance of noise vs the spin number for various squeezing parameters. For comparison, we also plot the resistance of the criterion S (solid, dashed, and dotted lines) whose precise form is given below in a basis where the state $|\phi\rangle$ is rotated by the squeezing angle around the x axis before the beamsplitter so that z corresponds to the squeezed direction [13]

$$S = \langle \hat{J}^A_x \hat{J}^B_x \rangle + \langle \hat{J}^A_y \hat{J}^B_y \rangle - \langle \hat{J}^A_z \hat{J}^B_z \rangle \leqslant \frac{N(N-1)}{16}. \tag{17}$$

The previous inequality holds for any separable state. It is closely connected to the minimization of the scalar product between $\vec{J}^A$ and $\vec{J}^B$ [27] (see also [33,34]) which requires correlations between the two parties to be violated, namely, entanglement. This inequality is violated by a split spin-squeezed state. The comparison in Fig. 3 shows that it is actually the witness involving first-order moments of LCSOs that can tolerate the largest amount of white noise when considering spin-squeezed states. We will show in Sec. IV B, that any symmetric state having a second moment of a collective spin (in any direction) which is smaller than the one of a coherent spin state (with the same mean number of spins) leads to a violation of the inequality (17) after splitting. A split Dicke state with $N/2$ excitations leads to $S = N(N+1)/16$ and provides the maximum violation.

III. ENTANGLEMENT WITNESSES USING SECOND-ORDER MOMENTS OF LOCAL COLLECTIVE SPIN OBSERVABLES

In this section, we follow the line of thought presented in the previous section to develop entanglement witnesses involving higher-order moments. We start by considering the real space consisting of all possible values of $\langle \hat{J}^A_i \rangle$, $\langle \hat{J}^B_i \rangle$, $\langle \hat{J}^A_i \hat{J}^B_j \rangle$, $\langle (\hat{J}^A_i)^2 \rangle$, and $\langle (\hat{J}^B_i)^2 \rangle$ satisfying the constraints

$$||\langle \vec{J}^A \rangle|| \leqslant \frac{n_a}{2}, \tag{18}$$

$$\langle (\hat{J}^A_x)^2 \rangle + \langle (\hat{J}^A_y)^2 \rangle + \langle (\hat{J}^A_z)^2 \rangle \leqslant \frac{n_a}{2}\left(\frac{n_a}{2}+1\right), \tag{19}$$

$$(\Delta \hat{J}^A_i)^2 = \langle (\hat{J}^A_i)^2 \rangle - \langle \hat{J}^A_i \rangle^2 \geqslant 0, \tag{20}$$

$$(\Delta \hat{J}^A_i)^2 + (\Delta \hat{J}^A_j)^2 - |\langle \hat{J}^A_k \rangle| \geqslant 0, \tag{21}$$

and similarly for B and $i,j,k \in \{x,y,z\}$. Note that we do not consider higher-order moments like $\langle (\hat{J}^A_i)^2 \hat{J}^B_j \rangle$ because they often require more experimental runs to be evaluated. According to angular momentum theory, the second and the third constraints are valid for all quantum states, the fourth one comes from the Heisenberg inequality. Since the space of first- and second-order moments of LCSOs is convex, we look again for witnesses that are linear in the parameters given above. Let us consider the quantity

$$W_2(\vec{\alpha})_{na,nb} = \sum_{i,j=x,y,z} \left(\alpha_{i,j}\langle \hat{J}^A_i \hat{J}^B_j \rangle + \bar{\alpha}_i \langle \hat{J}^A_i \rangle + \alpha_i \langle \hat{J}^B_i \rangle + \bar{\alpha}^{(2)}_i \langle (\hat{J}^A_i)^2 \rangle + \alpha^{(2)}_i \langle (\hat{J}^B_i)^2 \rangle\right).$$

Here $\vec{\alpha}$ is a vector with 21 elements $(\alpha_{i,j}, \bar{\alpha}_i, \alpha_i, \bar{\alpha}^{(2)}_i, \alpha^{(2)}_i)$. When the expectation values are taken on the set on separable states, the previous quantity can be upper bounded by

$$w_2(\vec{\alpha})_{na,nb} = \max_{\vec{J}^A, \vec{J}^B} \sum_{i,j=x,y,z} \left(\alpha_{i,j}\langle \hat{J}^A_i \rangle \langle \hat{J}^B_j \rangle + \bar{\alpha}_i \langle \hat{J}^A_i \rangle + \alpha_i \langle \hat{J}^B_i \rangle + \bar{\alpha}^{(2)}_i \langle (\hat{J}^A_i)^2 \rangle + \alpha^{(2)}_i \langle (\hat{J}^B_i)^2 \rangle\right), \tag{22}$$

where the maximum is computed from the set of vectors $\vec{J}^A$, $\vec{J}^B$ satisfying Eqs. (18)–(21). This yields the following family of entanglement witnesses suited for spins distributed binomially between the locations A and B:

$$w_2(\vec{\alpha}) - W_2(\vec{\alpha}) \geqslant 0, \tag{23}$$

where

$$w_2(\vec{\alpha}) = \sum_{n_a} \frac{1}{2^N} \binom{N}{n_a} w_2(\vec{\alpha})_{n_a, N-n_a} \tag{24}$$

and $W_2(\vec{\alpha}) = \langle \hat{W}_2(\vec{\alpha}) \rangle$ with

$$\hat{W}_2(\vec{\alpha}) = \sum_{i,j=x,y,z} \left(\alpha_{i,j} \hat{J}^A_i \hat{J}^B_j + \bar{\alpha}_i \hat{J}^A_i + \alpha_i \hat{J}^B_i + \bar{\alpha}^{(2)}_i (\hat{J}^A_i)^2 + \alpha^{(2)}_i (\hat{J}^B_i)^2\right). \tag{25}$$

(26)

Now consider states of the form in Eq. (15). As before, we optimize $W_2(\vec{\alpha})_{|\phi\rangle} = \mathrm{tr}(\hat{W}_2(\vec{\alpha})|\phi\rangle\langle\phi|)$ over all possible local rotations for a given choice $\vec{\alpha}$. This defines $W_2(\vec{\alpha})^{\mathrm{opt}}_{|\phi\rangle}$. We then extract the minimum value of p for each witness from the equation

$$p W_2(\vec{\alpha})^{\mathrm{opt}}_{|\phi\rangle} + (1-p)\sum_{i=x,y,z}\frac{\alpha_i^{(2)}+\bar{\alpha}_i^{(2)}}{12}N(N+5) = w_2(\vec{\alpha}), \tag{27}$$

where the second term in the left-hand side comes from the mean values of second-order moments of LCSOs on local white noise. The optimal witness is then obtained by looking for the direction $\vec{\alpha}$ leading to the minimum value of p. Note that this optimization is not particularly easy as it is a nonlinear optimization and the space of possible values of first- and second-order moments of LCSOs has a dimension 21. To make it simpler, we restrict our interest to symmetric witnesses only; note that the state on which we are optimizing is also symmetric under exchange of parties. Over 6000 numerical optimizations with $N = 26$ atoms and a squeezing corresponding to $\chi t = 0.0058$ before splitting, we found the following optimal witness twice:

$$D = \left\langle\left(\hat{J}_y^A - \hat{J}_y^B\right)^2\right\rangle + \left\langle\left(\hat{J}_z^A + \hat{J}_z^B\right)^2\right\rangle - \left\langle\hat{J}_x^A + \hat{J}_x^B\right\rangle \geqslant 0. \tag{28}$$

This witness is satisfied for all separable states. We have not been able to find a better witness for any value of χt corresponding to squeezing parameters between -1 and -10 dB for 500 atoms and for any atom number between 25 and 100 atoms.

The witness (28) is again given in a basis where $|\phi\rangle$ is rotated by the squeezing angle around the x axis before the beamsplitter so that z corresponds to the squeezing direction. Note that this criterion can be seen as a linear form of the well-known Duan [24] and Simon [25] criteria that have been successfully used for witnessing continuous-variable entanglement more than 15 years ago [35]; see also the generalization in Ref. [26]. By linear, we mean that D involves the mean values $\langle\hat{J}_i^A\rangle$, $\langle\hat{J}_i^B\rangle$, $\langle\hat{J}_i^A\hat{J}_j^B\rangle$, $\langle(\hat{J}_i^A)^2\rangle$, and $\langle(\hat{J}_i^B)^2\rangle$ only while the criteria [24–26] also use the square of these mean values. We will gain insight in Sec. IV B about symmetric states violating the inequality (28) after splitting.

IV. COMPARISONS OF ENTANGLEMENT WITNESSES USING FIRST- AND SECOND-ORDER MOMENTS OF LOCAL COLLECTIVE SPIN OBSERVABLES

The aim of this section is to compare the two optimal witnesses (17) and (28) that we found in the two previous sections. We first evaluate the amount of local white noise that can be tolerated to maintain a violation of these inequalities. We then repeat this evaluation for preparation noise and measurement noise.

A. Local white noise

As a first comparison, we focus on the resistance of the optimal witnesses using first- and second-order moments of LCSOs to local white noise. We compute the maximal amount of noise that can be tolerated by fixing $\chi t = 0.0058$ and varying the atom number. The result is shown in Fig. 4 where the resistance of the witness (17) is drawn in orange (dashed line) and the resistance of the witness (28) is shown in blue (solid line). Let us recall that smaller p translates into a better resistance to noise. Note also that adding 0.1% (0.5%) of local white noise to a spin-squeezed state with 500 atoms and -10 dB squeezing effectively reduces the squeezing to -5.6 dB (-0.15 dB). We can fairly say that the witness using second-order moments of LCSOs has a better resistance to local white noise.

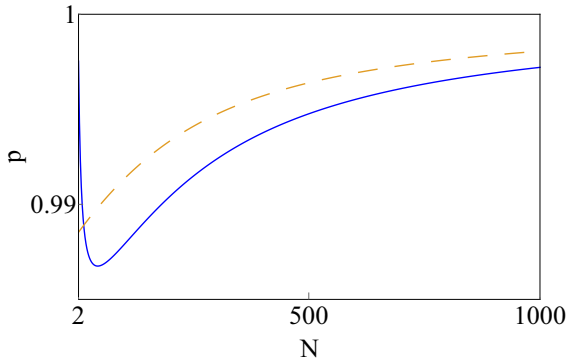

FIG. 4. Maximum tolerable local white noise for the optimal witnesses given in Eqs. (17) (orange dashed line) and (28) (blue solid line) as a function of the total number of spins. The state that is considered here is a mixture between a spin-squeezed state [with a squeezing parameter χt given by $10\log_{10}(\xi^2) = -10$ dB for 500 atoms] with probability p and local white noise with probability $1-p$, see Eq. (15). We conclude that the witness (28) is more resistant to local white noise when $N \geqslant 30$ for any squeezing between -1 and -10 dB for 500 atoms and any atom number between 2 and 500.

While local white noise often corresponds to a worst case scenario, more specific noises are often relevant when one wants to model experiments in detail. In the next section, we compare the two witnesses (17) and (28) with respect to noises that are relevant in experiments using Bose-Einstein condensates.

B. Preparation noise

To compare the resistance to noise at the preparation level, i.e., before the splitting, we apply the unitary shown in Eq. (7) back into the observables involved in (17) and (28) to get an expression of these witnesses before the splitting. For the witness (17), we get

$$\begin{aligned} S &\leqslant \frac{N(N-1)}{16} \\ &\Longleftrightarrow \frac{\left\langle\left(\hat{J}_x^A\right)^2\right\rangle + \left\langle\left(\hat{J}_y^A\right)^2\right\rangle - \left\langle\left(\hat{J}_z^A\right)^2\right\rangle}{4} - \frac{N}{16} \leqslant \frac{N(N-1)}{16}. \end{aligned} \tag{29}$$

Here, the expectation values are to be understood on the state before the beamsplitter. When considering the subspace that

is symmetric under particle interchange, this reduces to

$$S \leqslant \frac{N(N-1)}{16} \Longleftrightarrow \left\langle \left(\hat{J}_z^A\right)^2 \right\rangle \geqslant \frac{N}{4}. \tag{30}$$

This shows that any symmetric state having a second moment of a collective spin (in any direction) that is smaller than the one of a coherent spin state with the same mean number of spins leads to entanglement after splitting. Moreover, this entanglement is always detected by the witness (17).

For the witness (28), we have

$$D \geqslant 0 \Longleftrightarrow \left\langle \left(\hat{J}_z^A\right)^2 \right\rangle \geqslant \left\langle \hat{J}_x^A \right\rangle - \frac{N}{4}. \tag{31}$$

As the maximum value of $\langle \hat{J}_x^A \rangle$ for N spins is $\frac{N}{2}$ [Eq. (8)], any state violating Eq. (31) also violates Eq. (29). Therefore the first-order witness (17) is more robust than the criterion (28) for any kind of noise before the splitting that keeps the state in the symmetric subspace.

C. Measurement noise: Coarse-graining

As said in the Introduction, the local collective observable $\hat{J}_z^A$ is measured by counting the number of atoms in each state 1 and 2, i.e., $\hat{J}_z^A = \frac{\hat{a}_1^\dagger \hat{a}_1 - \hat{a}_2^\dagger \hat{a}_2}{2} = \frac{\hat{n}_1^A - \hat{n}_2^A}{2}$ where $\hat{n}_i^A$ is the atom number at location A in state i. Projections along other spin directions are obtained by appropriate Rabi rotations before the measurement. We here consider the case where the collective spin measurements are coarse-grained due to imperfect atom number measurements. In particular, we assume that the measurement noise leads to an unbiased Gaussian distribution of atom number, i.e., $\hat{n}_i^A$ is replaced by $(\hat{n}_i^A + \epsilon)$ with probability density $g_{\sigma_c}(\epsilon)$, where σ_c^2 is the variance of the Gaussian noise distribution and similarly for $\hat{n}_i^B$.

Under the assumption that the measurement noise at location A is uncorrelated with the noise in B, the witnesses involving first-order moments of LCSOs are insensitive to this noise. Therefore witness (17) is insensitive to a coarse-graining of the measurement outcome.

On the contrary, assuming also that the noises on $\hat{n}_1^A$ and $\hat{n}_2^A$ are uncorrelated (similarly in B), the witness involving second-order moments of LCSOs yields

$$\left\langle \left(\hat{J}_y^A - \hat{J}_y^B\right)^2 \right\rangle + \left\langle \left(\hat{J}_z^A + \hat{J}_z^B\right)^2 \right\rangle - \left\langle \left(\hat{J}_x^A + \hat{J}_x^B\right) \right\rangle \geqslant -2\sigma_c^2 \tag{32}$$

for all separable states. This means, for example, that for an uncertainty corresponding to five atoms ($\sigma_c = 5$), a minimum squeezing of ~ -2 dB is required to reveal entanglement in a set of 500 atoms with the witness (28).

D. Measurement noise: Phase noise

Due to the difference in energy between the states 1 and 2, the collective spin state $|\psi\rangle$ rotates around the z axis. The spin projections discussed so far are thus implemented in a rotating frame, i.e., the frame of the state is taken as a reference frame. Phase noise refers to a mismatch between the frame of the state and the frame of the measurements which can be due to magnetic field fluctuations. In the present case, we consider uncorrelated phase noise between the wells. To take this phase noise into account, the spin projections are not calculated on $|\phi\rangle$ but on

$$\rho_\sigma = \int d\theta_A \, d\theta_B \, g_{\sigma_p}(\theta_A) g_{\sigma_p}(\theta_B) R_A R_B |\phi\rangle\langle\phi| R_A^{-1} R_B^{-1} \tag{33}$$

with $R_A = e^{i\theta_A \hat{J}_z^A}$, $R_B = e^{i\theta_B \hat{J}_z^B}$, and $g_{\sigma_p}(\theta_A)$ and $g_{\sigma_p}(\theta_B)$ are unbiased Gaussian distributions with a standard deviation σ_p.

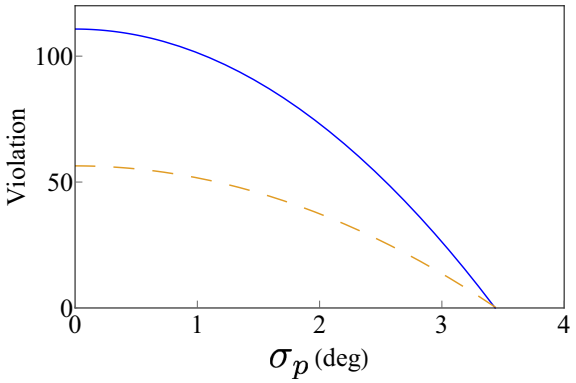

FIG. 5. The orange dashed line (blue line) gives $S - \frac{N(N+1)}{16}$ (D), i.e., the violation of the witness (17) [(28)], as a function of the phase noise (in degrees).

Figure 5 shows the violations, i.e., the values of $S - \frac{N(N+1)}{16}$ and D for -10 dB squeezing and $N = 500$ spins as a function of the standard deviation σ_p. We see that the witnesses (17) and (28) have essentially the same resistance to phase noise. In particular for phase noise of $\pm 3.4^\circ$, the violation disappears and neither of the witnesses can detect entanglement. We have been able to explore several parameter regimes; and for any χt between 0.00046258 and 0.0058 which correspond to squeezing between -1 and -10 dB for 500 atoms and any spin number between 2 and 1000, we found that the violation of both witnesses disappears for the same uncertainties on the phase. We conclude that their resistance to phase noise is thus comparable.

V. REQUIRED STATISTICS

In this section, we give an estimation of the number of experimental runs that would be necessary to estimate the quantities in Eqs. (17) and (28). Let us first consider the witness (17). We assume that the spin projections $\hat{J}_i^A \hat{J}_i^B$ are independent quantities that are measured N_m times [36]. Let $\bar{X}_k$, $\bar{Y}_k$, and $\bar{Z}_k$ be the values that $\hat{J}_i^A \hat{J}_i^B$ take at the run k for $i = x, y$, and z, respectively. The estimator of S after N_m runs is given by

$$\bar{S} = \frac{1}{N_m} \sum_{k=1}^{N_m} \bar{X}_k + \frac{1}{N_m} \sum_{i=1}^{N_m} \bar{Y}_k - \frac{1}{N_m} \sum_{k=1}^{N_m} \bar{Z}_k, \tag{34}$$

and the fluctuations of this mean value are parametrized by

$$\sigma_{\bar{S}} = \frac{1}{\sqrt{N_m}} \sqrt{\sigma_X^2 + \sigma_Y^2 + \sigma_Z^2}, \tag{35}$$

where σ_X is the standard deviation of variables $\bar{X}_k$ and similarly for σ_Y and σ_Z. Here we assumed that the runs are independent and identically distributed. Let us consider an

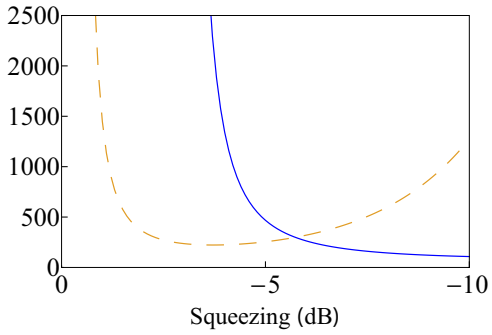

FIG. 6. Number of evaluations of the witnesses which are required in order to be 3σ less than the violation as functions of the initial squeezing in dB. The blue line represents the criterion D and the orange dashed line the criterion S.

experiment performed on the state $\bar{\rho}$. The mean value of $\bar{S}$ after N_m runs is given $\bar{S}_q = \mathrm{tr}(\bar{\rho}(\hat{J}_x^A \hat{J}_x^B + \hat{J}_y^A \hat{J}_y^B - \hat{J}_z^A \hat{J}_z^B))$ while σ_X^2 is given by $\sigma_{X,q}^2 = \mathrm{tr}(\bar{\rho}(\hat{J}_x^A \hat{J}_x^B)^2) - [\mathrm{tr}(\bar{\rho} \hat{J}_x^A \hat{J}_x^B)]^2$ and similarly for σ_Y^2 and σ_Z^2. The number of runs that is needed to estimate the value of the witness with a precision 3 times smaller than the distance to the separable bound can thus be estimated by solving

$$\left| \bar{S}_q - \frac{N(N+1)}{16} \right| = \frac{3}{\sqrt{N_m}} \sqrt{\sigma_{X,q}^2 + \sigma_{Y,q}^2 + \sigma_{Z,q}^2}. \tag{36}$$

We follow the same line of thought for the criterion D by considering the estimator

$$\tilde{D} = \frac{1}{N_m} \sum_{k=1}^{N_m} \bar{\bar{X}}_k + \frac{1}{N_m} \sum_{i=1}^{N_m} \bar{\bar{Y}}_k + \frac{1}{N_m} \sum_{k=1}^{N_m} \bar{\bar{Z}}_k, \tag{37}$$

where $\bar{\bar{X}}_k$, $\bar{\bar{Y}}_k$, and $\bar{\bar{Z}}_k$ are the values of $-\hat{J}_x^A - \hat{J}_x^B$, $(\hat{J}_y^A - \hat{J}_y^B)^2$, and $(\hat{J}_z^A + \hat{J}_z^B)^2$ at the run k.

For concreteness, we consider a spin-squeezed state made with $N = 500$ spins with an uncertainty on the phase of $\pm 1^\circ$ and a measurement coarse-graining of ± 5 atoms. As a function of the initial squeezing parameter, we compute the number of runs needed to observe a value of the witnesses (17) and (28) exceeding the separable bound by 3 standard deviations. The result is shown in Fig. 6. We see that one needs fewer runs to estimate the criterion S with an accuracy of 3σ if the initial squeezing $\xi^2 > -6$ dB mostly because of the insensibility with respect to detection noise.

VI. CONCLUSION

The aim of this work was to clarify the requirements to reveal entanglement between the two parts of a spatially split spin-squeezed Bose-Einstein condensate. We focused on two families of witnesses. The first one uses first-order moments of local collective spin operators, i.e., $\langle \hat{J}_i^A \rangle$, $\langle \hat{J}_i^B \rangle$, and $\langle \hat{J}_i^A \hat{J}_j^B \rangle$, where i, j labels the components in the directions x, y, and z. The second family of witnesses involves not only first-order moments of local collective operators, but also the second-order moments $\langle (\hat{J}_i^A)^2 \rangle$ and $\langle (\hat{J}_i^B)^2 \rangle$. In both cases, we found the witness that is the most resistant to local white noise. In the first case, we found a witness closely connected to the scalar product given in Ref. [27]. In the second case, the best linear witness regarding local white noise turns out to be a linear form of the Duan [24,25] criteria for spins. We then compared these two optimal witnesses with respect to their robustness to various noises and we finally gave an estimate of the statistics needed for their experimental measurement. This work lays the theoretical ground that is needed for an ambitious experiment aiming to detect entanglement in a split Bose-Einstein condensate. The next step will be to show how to violate a Bell inequality in this scenario—a milestone to extend the field of device-independent quantum information processing to many-body physics.

ACKNOWLEDGMENTS

We thank B. Allard, P. Drummond, M. Fadel, A. Peter, M. Reid, P. Sekatski, and T. Zibold for valuable discussions and/or comments on the paper. This work was supported by the Swiss National Science Foundation (SNSF), through the NCCR QSIT and Grant No. PP00P2-150579. N.S. acknowledges the Army Research Laboratory Center for Distributed Quantum Information via the project SciNet.

[1] L. Amico, R. Fazio, A. Osterloh, and V. Vedral, Rev. Mod. Phys. **80**, 517 (2008).
[2] I. Bloch, J. Dalibard, and W. Zwerger, Rev. Mod. Phys. **80**, 885 (2008).
[3] W. J. Mullin and F. Laloë, Phys. Rev. A **78**, 061605(R) (2008).
[4] F. Laloë and W. J. Mullin, Eur. Phys. J. B **70**, 377 (2009).
[5] C. Gneiting and K. Hornberger, Phys. Rev. Lett. **101**, 260503 (2008).
[6] R. J. Lewis-Swan and K. V. Kheruntsyan, Phys. Rev. A **91**, 052114 (2015).
[7] S. Pelisson, L. Pezzè, and A. Smerzi, Phys. Rev. A **93**, 022115 (2016).
[8] J. Tura, R. Augusiak, A. B. Sainz, T. Vertesi, M. Lewenstein, and A. Acín, Science **344**, 1256 (2014).
[9] R. Schmied, J-D. Bancal, B. Allard, M. Fadel, V. Scarani, P. Treutlein, and N. Sangouard, Science **352**, 441 (2016).
[10] N. Brunner, D. Cavalcanti, S. Pironio, V. Scarani, and S. Wehner, Rev. Mod. Phys. **86**, 419 (2014).
[11] V. Scarani, Acta Phys. Slovaca **62**, 347 (2012).
[12] J. Ma, X. Wang, C. P. Sun, and F. Nori, Phys. Rep. **509**, 89 (2011).
[13] L. Pezzè, A. Smerzi, M. K. Oberthaler, R. Schmied, and P. Treutlein, arXiv:1609.01609
[14] M. Kitagawa and M. Ueda, Phys. Rev. A **47**, 5138 (1993).
[15] A. Sørensen, L.-M. Duan, J. I. Cirac, and P. Zoller, Nature **409**, 63 (2001).
[16] D. J. Wineland, J. J. Bollinger, W. M. Itano, F. L. Moore, and D. J. Heinzen, Phys. Rev. A **46**, R6797(R) (1992).

[17] D. J. Wineland, J. J. Bollinger, W. M. Itano, and D. J. Heinzen, Phys. Rev. A **50**, 67 (1994).
[18] K. Hammerer, A. Sørensen, and E. Polzik, Rev. Mod. Phys. **82**, 1041 (2010).
[19] Q. Y. He, P. D. Drummond, M. K. Olsen, and M. D. Reid, Phys. Rev. A **86**, 023626 (2012).
[20] Q. Y. He, M. D. Reid, T. G. Vaughan, C. Gross, M. Oberthaler, and P. D. Drummond, Phys. Rev. Lett. **106**, 120405 (2011).
[21] N. Bar-Gill, C. Gross, I. Mazets, M. Oberthaler, and G. Kurizki, Phys. Rev. Lett. **106**, 120404 (2011).
[22] H. Kurkjian, K. Pawłowski, A. Sinatra, and P. Treutlein, Phys. Rev. A **88**, 043605 (2013).
[23] B. Opanchuk, Q. Y. He, M. D. Reid, and P. D. Drummond, Phys. Rev. A **86**, 023625 (2012).
[24] L.-M. Duan, G. Giedke, J. I. Cirac, and P. Zoller, Phys. Rev. Lett. **84**, 2722 (2000).
[25] R. Simon, Phys. Rev. Lett. **84**, 2726 (2000).
[26] M. G. Raymer, A. C. Funk, B. C. Sanders, and H. de Guise, Phys. Rev. A **67**, 052104 (2003).
[27] G. A. Durkin and C. Simon, Phys. Rev. Lett. **95**, 180402 (2005).
[28] M. F. Riedel, P. Böhi, Y. Li, T. W. Hänsch, A. Sinatra, and Philipp Treutlein, Nature **464**, 1170 (2010).
[29] C. Gross, T. Zibold, E. Nicklas, J. Estève, and M. K. Oberthaler, Nature **464**, 1165 (2010).
[30] Y. Shin, M. Saba, T. A. Pasquini, W. Ketterle, D. E. Pritchard, and A. E. Leanhardt, Phys. Rev. Lett. **92**, 050405 (2004).
[31] T. Schumm, S. Hofferberth, L. M. Anderson, S. Wildermuth, S. Groth, I. Bar-Joseph, J. Schmiedmayer, and P. Kruger, Nat. Phys. **1**, 57 (2005).
[32] G. Reinaudi, T. Lahaye, Z. Wang, and D. Guery-Odelin, Opt. Lett. **32**, 3143 (2007).
[33] G. Tóth, Phys. Rev. A **70**, 010301(R) (2004).
[34] G. Tóth, Appl. Phys. B **82**, 237 (2006).
[35] B. Julsgaard, A. Kozhekin, and E. S. Polzik, Nature **413**, 400 (2001).
[36] We emphasize that N_m is the number of runs assuming that $\hat{J}_x^A \hat{J}_x^B, \hat{J}_y^A \hat{J}_y^B$, and $\hat{J}_z^A \hat{J}_z^B$ are measured at each run. When these quantities are measured separately, $3N_m$ gives a conservative estimation of the statistics needed to estimate the considered witnesses.

CHAPTER 2

BIPARTITE BELL NON LOCALITY IN MANY-BODY SYSTEMS

In the previous chapter, we have investigated witnesses in split spin systems and show that they can be used to demonstrate entanglement in such systems. Actually, witnesses of various kinds have been very useful in revealing different families of quantum correlations in many-body systems including entanglement, EPR steering and Bell correlations [22, 23, 24]. These witnesses rely however, on assumptions on the proper calibration of measurement devices and/or on the dimension of the underlying Hilbert space. The next natural step would be to violate a Bell inequality in a many-body system, hence demonstrating Bell non-locality between two mesoscopic objects. In the quantum framework, the violation of a Bell inequality would also serve as a witness for detecting entanglement in a device independent way.

We consider a scenario where a state of many spins is separated between two parties, each party performing collective spin measurements, that is, projections of all spins in the same direction. We first consider single particle resolution and show that, in this case, it is possible to violate the CHSH inequality for different class of states including the GHZ state, the spin squeezed state and the W state. In particular, we show that for the W state, one only needs to distinguish one eigenvalue from the rest. This might be interesting in practice as this sort of measurements has been already performed on a W state of 40 atoms [21].

To go further in our study of non-locality in bipartite many-body systems, we limit ourself to low order moments of collective spin observable in order to match the experimental requirement. Considering only first order moments of collective spin observables, we numerically prove that no Bell inequality can be violated for less than 6 settings for any quantum state. This suggests that in order to violate a Bell inequality with large a large spin number, single particle resolution might be necessary.

Paper B

Bipartite non-locality with many-body systems

Enky Oudot, Jean-Daniel Bancal, Pavel Sekatski and Nicolas Sangouard

arXiv: 1810.05636

Bipartite nonlocality with a many-body system

Enky Oudot, Jean-Daniel Bancal, Pavel Sekatski, and Nicolas Sangouard
Quantum Optics Theory Group, University of Basel, CH-4056 Basel, Switzerland
(Dated: October 15, 2018)

We consider a bipartite scenario where two parties hold ensembles of 1/2-spins which can only be measured collectively. We give numerical arguments supporting the conjecture that in this scenario no Bell inequality can be violated for arbitrary numbers of spins if only first order moment observables are available. We then give a recipe to achieve a significant Bell violation with a split many-body system when this restriction is lifted. This highlights the strong requirements needed to detect bipartite quantum correlations in many-body systems device-independently.

I. INTRODUCTION

In a Bell test, distinct parties initially share a resource such as a quantum state. They are then given measurement settings that they use to obtain measurement outcomes. The joint statistics of their outcomes, conditioned on the settings, can then be used to reveal a number of properties. For instance, it can be shown that certain statistics are not compatible with pre-established agreements, as highlighted by the violation of a Bell inequality [1]. Recently, a theoretical demonstration showed that some many-body quantum states are able to violate multipartite Bell inequalities [2–4]. So far, no violation of these inequalities could be observed experimentally due to the challenge of addressing individual spins in a large ensemble. Nevertheless, witnesses were constructed and used to demonstrate the presence of Bell correlations in such states, i.e. their capacity to violate a Bell inequality [5–7]. While such states are quite different from the quantum states often considered in the studies of Bell nonlocality, they are of particular relevance to many-body physics. It is then a natural question to ask whether a true Bell violation could be observed with such states.

Here, we make a step in this direction by considering the simple scenario in which hundreds of 1/2-spins are split among just two protagonists, Alice and Bob. We then ask whether a Bell violation could be observed when the parties are restricted to perform collective measurements on their 1/2-spin ensembles. Such a violation would provide a strong demonstration that mesoscopic systems can behave differently from the predictions of classical physics. Indeed, this conclusion would hold without the need to assume a quantum description of the setup. In particular, this conclusion would be independent of the Hilbert space dimension and of the proper calibration of the measurement device. For this reason, Bell tests performed on systems involving many spins are particularly appealing to show the limit of classical physics for describing mesoscopic systems.

Bell tests involving collective measurements on many-body states could in principle be realized with a Bose-Einstein condensate. The basic idea is to use controlled interactions between the constituent bodies to create non-classical correlations between the internal states of these constituents [8, 9], the later being essentially 1/2-spins. These spins could then be distributed [10, 11] between Alice and Bob – n_A spins for Alice and n_B for Bob – before being measured, see Fig. 1. The experiment would then be repeated many times so that Alice and Bob can assess the expectation values of measurement results and demonstrate the Bell violation. In such a system, however, each protagonist can only measure his ensemble of particles collectively, that is, Alice can perform measurements of the form

$$\hat{J}^l_\alpha = \frac{1}{2}\sum_{k=1}^{n_l} \vec{\alpha}.\vec{\sigma}^{(k)}_l, \text{ with } l = A. \tag{1}$$

$\vec{\sigma}^{(k)}_l$ is a vector having the 3 Pauli matrices as components and $\vec{\alpha}$ is a unit length vector with components α^x, $x = \{1, 2, 3\}$ fixing the measurement setting. The form of Bob's measurements, with $l = B$, is the same but the direction is labeled by $\vec{\beta}$. The eigenvalues of $\hat{J}^l_{\alpha/\beta}$ are $-\frac{n_l}{2}, ..., \frac{n_l}{2}$ and correspond to the possible measurement outcomes. The remaining question is what is the Bell inequality to be tested in such a scenario? We first focus on the simplest case where only first order moments of local collective spin observables, that is, $\langle \hat{J}^A_\alpha \rangle$, $\langle \hat{J}^B_\beta \rangle$ and $\langle \hat{J}^A_\alpha \hat{J}^B_\beta \rangle$ can be evaluated. We then extend our analysis beyond this restriction.

While entanglement witnesses have been intensively studied in this scenario with first order moments [12–14], few results are known with respect to Bell nonlocality. One noticeable exception is Ref. [15] where authors showed that bipartite correlations issued from first order collective measurements can be reproduced by a local model if the number of measurement settings is smaller or equal to n_A for Alice and n_B for Bob. Beyond first order moments, it is worth noting that the use of collective measurements to violate a Bell inequality was also considered recently for a specific class of state with a strong tensor structure [16, 17]. The state that we are interested in here are however very different: they do not admit any tensor structure but rather are typically symmetric under spin exchange.

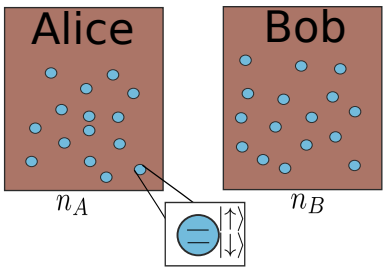

Figure 1: Schematic representation of the scenario we consider, Alice and Bob have respectively n_A and n_B indistinguishable spin $\frac{1}{2}$ and can measure them collectively with observables $\hat{J}^A_\alpha$ and $\hat{J}^B_\beta$.

In section II, we give numerical arguments suggesting that such a bipartite Bell violation may not be possible when considering only first order moments. We then show in section III that a Bell inequality can be violated if each party performs parity measurements. We conclude in section IV.

II. ATTEMPTS TO FIND A BI-PARTITE BELL CORRELATION WITNESS INVOLVING ONLY FIRST ORDER MOMENTS OF LOCAL COLLECTIVE SPIN COMPONENTS

A. Bell inequalities and Bell-correlation witnesses

Let us focus on a Bell scenario in which Alice and Bob each have a measurement box with m inputs A_i and B_j $i,j \in [1,\dots,m]$ and N spins locally, i.e. $N+1$ possible outcomes $-\frac{N}{2}, -\frac{N}{2}+1\dots,\frac{N}{2}$. We consider Bell inequalities of the form

$$B^{\hat{w},\vec{v}_a,\vec{v}_b}_{N,m} = \sum_{i,j}^{m} w_{ij}\langle A_i B_j\rangle + \sum_{i}^{m} v_{a_i}\langle A_i\rangle + \sum_{j}^{m} v_{b_j}\langle B_j\rangle \leq \ell^{\hat{w},\vec{v}_a,\vec{v}_b}_{N,m}. \quad (2)$$

$\langle A_i\rangle$ for example is the expectation value of outcomes for Alice's measurement corresponding to the input A_i. w_{ij}, v_{a_i} and v_{b_j} are weights, all taken in the interval {-1,1} without lost of generality. $\ell^{\hat{w},\vec{v}_a,\vec{v}_b}_{N,m}$ is the local bound, that is, the maximum value that the left hand side can take when considering bi-partite correlations steming from local models. This bound depends on the number of inputs and outcomes and on the weights, possibly in a non-trivial way, c.f. below.

Note that if we assign to each input an observable $A_i \to \hat{J}^A_{\alpha_i}$, one can associate to each instance of the inequality (2) a Bell operator

$$\mathscr{B}^{\hat{w},\vec{v}_a,\vec{v}_b}_{N,m} = \sum_{i,j}^{m} w_{ij}\hat{J}^A_{\alpha_i}\hat{J}^B_{\alpha_j} + \sum_{i}^{m} v_{a_i}\hat{J}^A_{\alpha_i} + \sum_{j}^{m} v_{b_j}\hat{J}^B_{\beta_j} \quad (3)$$

so that a violation of

$$\langle \mathscr{B}^{\hat{w},\vec{v}_a,\vec{v}_b}_{N,m}\rangle - \ell^{\hat{w},\vec{v}_a,\vec{v}_b}_{N,m} \leq 0 \quad (4)$$

witesses bi-partite Bell correlations. Interestingly, the expression $\langle \mathscr{B}^{\hat{w},\vec{v}_a,\vec{v}_b}_{N,m}\rangle$ might be simpler to evaluate experimentally than $B^{\hat{w},\vec{v}_a,\vec{v}_b}_{N,m}$. As an example, consider the simplest case $N=1$, $m=2$, $w_{ij}=(-1)^{i+j-1}$ and $v_{a_i}=v_{b_j}=0\ \forall i,j$ leading to the well known Clauser, Horne, Shimony, and Holt (CHSH) inequality [18] for which the local bound is 2, that is,

$$\langle A_1B_1\rangle + \langle A_2B_1\rangle + \langle A_1B_2\rangle - \langle A_2B_2\rangle \leq 2. \quad (5)$$

Assigning A_1 to σ_x, A_2 to σ_z, and $B_{1/2}$ to $(\sigma_x \pm \sigma_z)\sqrt{2}$ which correspond to the setting choice maximizing the CHSH value for the singlet, we get the Bell-correlation witness

$$\langle \sigma_x\sigma_x\rangle + \langle \sigma_z\sigma_z\rangle \leq \sqrt{2}. \quad (6)$$

The latter can be evaluated with two collective measurements while the former requires the assessment of four correlators.

Recently, such a reduction in the number of measurements, applicable when assuming that the measurements are known and trusted, was used to transform a Bell inequality involving an unbounded number of settings into a witness with only two global measurements [3]. It was also used to show that the Svetlichny inequality [19], which is a Bell inequality for N parties requiring the measurement of 2^N correlators, reduces to a negativity condition on the mean value of an observable that can be evaluated with 2 measurement settings only [7].

There are thus at least two reasons for looking for Bell inequalities of the form (2) despite the result from [15] stating that no such inequality can be violated in our setting when the number of settings is less than the number of local spins, i.e. $m \leq N$. First, for every fixed value of N, there can exist a finite value of $m > N$ potentially allowing for a Bell violation. Second, in a scenario in which one would be happy to trust the quantum description of the measurements, a Bell inequality with $m > N$, although involving a large number of settings could lead to a witness for bipartite Bell correlations that would require a maximum of three measurements per party. Such a witness would allow for the detection of a strong form of quantum correlations in many-body systems. Compared to previously known Bell correlation witnesses which only demonstrate the presence of some form of Bell correlations among a large

number of spins, this witness would demonstrate Bell correlations between two well-identified spin ensembles: between Alice's set of spins and Bob's. We show in the next two subsections how to compute the local and quantum bounds respectively.

B. Local bound

In order to determine the local bound $\ell_{N,m}^{\hat{w},\vec{v}_a,\vec{v}_b}$ of the inequality (2), one has to consider all possible local deterministic strategies, that is, strategies assigning locally an outcome taken from $\{-\frac{N}{2}, -\frac{N}{2}+1, ..., \frac{N}{2}\}$ for each of the m settings. The local bound is simply the largest value that can be obtained from these deterministic strategies. On paper, it is sufficient to list all possible deterministic strategies to find the local bound. However, there are $(N+1)^{2m}$ deterministic strategies, which makes the computation of the local bound complicated even for small N and m.

The number of relevant deterministic strategies is strongly reduced given the linearity of the inequality (2) with respect to the outcomes of Alice and Bob. To see this, let us consider an arbitrary deterministic strategy fixing the outcomes of Bob. The value of $B_{N,m}^{\hat{w},\vec{v}_a,\vec{v}_b}$ is obtained from a quantity of the form

$$\sum_i^m \alpha_i \langle A_i \rangle + C \tag{7}$$

where $\alpha_i = v_{a_i} + \sum_j w_{ij}\langle B_j\rangle$ and $C = \sum_j^m v_{b_j}\langle B_j\rangle$. The maximum value of (7) is achieved for $A_i = \text{sign}(\alpha_i)\frac{N}{2}$ and the same holds for Bob. This means that the optimal deterministic strategy is such that $A_i, B_j = \pm\frac{N}{2}$ $\forall i,j$. In other words, the vertices of the local polytope are strategies assigning $\pm\frac{N}{2}$ to all A_i, B_j. The number of these strategies is 2^{2m}, which is independent of the number of spins N.

In order to make the local bound independent of the number of spins we rescale the possible outcomes of A_i and B_j by N, defining $a_i = A_i/N$, $b_j = B_j/N$. This means that we now consider Bell inequalities of the form

$$\begin{aligned} B_{N,m}^{\prime\hat{w}',\vec{v}'_a,\vec{v}'_b} &= \sum_{i,j}^m w'_{ij}\langle a_i b_j\rangle + \sum_i^m v'_{a_i}\langle a_i\rangle + \sum_j^m v'_{b_j}\langle b_j\rangle \\ &\leq \ell_m^{\prime\hat{w}',\vec{v}'_a,\vec{v}'_b}, \end{aligned} \tag{8}$$

where this time the $N+1$ possible outcomes of Alice and Bob take value in $-\frac{1}{2}, -\frac{1}{2}+\frac{1}{N}, \ldots, \frac{1}{2}$. For some parameters $\hat{w}', \vec{v}'_a, \vec{v}'_b$, the local bound $\ell_m^{\prime\hat{w}',\vec{v}'_a,\vec{v}'_b}$ of this Bell expression is achieved by considering the 2^{2m} local strategies for which $a_i, b_j = \pm\frac{1}{2}$. This bound remains valid for all N. The local bound of the un-normalized Bell inequality (2) is then given by $\ell_{N,m}^{\hat{w},\vec{v}_a,\vec{v}_b} = \ell_m^{\prime N^2\hat{w},N\vec{v}_a,N\vec{v}_b}$.

The Bell operator corresponding to this inequality can be built in terms of the re-normalized spin operators

$$\hat{j}_\alpha^l = \frac{1}{N}\hat{J}_\alpha^l = \vec{\alpha}\cdot\vec{s}_l, \tag{9}$$

with eigenvalues between $-\frac{1}{2}$ and $\frac{1}{2}$, where

$$\vec{s}_l = \frac{1}{2N}\sum_{k=1}^N \vec{\sigma}_l^{(k)} \tag{10}$$

are the normalized spin projections:

$$\mathscr{B}_{N,m}^{\prime\hat{w}',\vec{v}'_a,\vec{v}'_b} = \sum_{i,j}^m w'_{ij}\hat{j}_{\alpha_i}^A\hat{j}_{\alpha_j}^B + \sum_i^m v'_{a_i}\hat{j}_{\alpha_i}^A + \sum_j^m v'_{b_j}\hat{j}_{\beta_j}^B. \tag{11}$$

This operator is such that a violation of the inequality

$$\langle\mathscr{B}_{N,m}^{\prime\hat{w}',\vec{v}'_a,\vec{v}'_b}\rangle - \ell_m^{\prime\hat{w}',\vec{v}'_a,\vec{v}'_b} \leq 0 \tag{12}$$

witnesses Bell correlations.

We thus focus now on Bell inequalities of the form (8). This form has the advantage that the local bound is independent of N. Once the local bound of such a Bell inequality is found, we want to show that it is a non-trivial Bell inequality by checking that it can be violated, that is, it admits a quantum value larger than its local bound.

C. Collective qubit bound

The maximal value of the inequality achievable by a quantum states of N plus N $\frac{1}{2}$-spins with local collective measurements $\max_{\rho_N}\text{Tr}\left(\rho_N\mathscr{B}_{N,m}^{\prime\hat{w}',\vec{v}'_a,\vec{v}'_b}\right)$ can be obtained by finding the maximum eigenvalue of the operator $\mathscr{B}_{N,m}^{\prime\hat{w}',\vec{v}'_a,\vec{v}'_b}$ for all possible setting choice α_i, β_j. As we show below, the quantum bound $\langle\mathscr{B}_{N,m}^{\prime\hat{w}',\vec{v}'_a,\vec{v}'_b}\rangle$ decreases with N. Given this and the fact that the local bound is independent of N, we focus on the case $N=2$. Finding no Bell violation for $N=2$ and an arbitrary number of settings is sufficient to show that there is no non-trivial Bell inequality for any N. We start by showing that indeed, the quantum bound $\langle\mathscr{B}_m^{\hat{w},\vec{v}_a,\vec{v}_b}\rangle$ decreases with N.

The Bell operator $\mathscr{B}_{N,m}^{\prime\hat{w}',\vec{v}'_a,\vec{v}'_b}$ can be written in terms of the normalized spin projections as

$$\mathscr{B}_{N,m}^{\prime\hat{w}',\vec{v}'_a,\vec{v}'_b} = \vec{s}_A\cdot\hat{W}\cdot\vec{s}_B + \vec{s}_A\cdot\vec{V}_A + \vec{s}_B\cdot\vec{V}_B \tag{13}$$

where $\hat{W}$ is a 3×3 matrix having elements W^{xy} given by

$$W^{xy} = \sum_{i,j=1}^m w'_{ij}\alpha_i^x\beta_j^y, \tag{14}$$

$\vec{V}_A$ is a vector with 3 components defined by $V_A^x = \sum_i v'_{a_i} \alpha_i^x$ and similarly for $\vec{V}_B$.

We now use $\vec{k} = (k_1, k_2, \ldots, k_M)$ with $1 \leq k_i < k_{i+1} \leq N$ to denote a subset of $M < N$ spins and introduce the normalized spin observables over these spins

$$\vec{u}_l^{\vec{k}} = \frac{1}{2M} \sum_{i=1}^{M} \vec{\sigma}_l^{(k_i)}. \tag{15}$$

This allows us to write our Bell operator for two sets $\vec{k}$ and $\vec{k}'$ of M spins as

$$O^{\vec{k},\vec{k}'} = \vec{u}^{\vec{k}} \cdot \hat{W} \cdot \vec{u}^{\vec{k}'} + \vec{u}^{\vec{k}} \cdot \vec{V}_A + \vec{u}^{\vec{k}'} \cdot \vec{V}_B. \tag{16}$$

Noticing that the spin projections for M spins satisfy

$$\begin{aligned} \sum_{\vec{k}} \vec{u}_l^{\vec{k}} &= \frac{1}{2M} \sum_{\vec{k}} \sum_{i=1}^{M} \vec{\sigma}_l^{(k_i)} \\ &= \frac{1}{2M} \binom{N-1}{M-1} \sum_{k=1}^{N} \vec{\sigma}_l^{(k)} \\ &= \binom{N}{M} \vec{s}_l \end{aligned} \tag{17}$$

where the sum on $\vec{k}$ runs over all choices of M spins within the N spins, we obtain

$$\sum_{\vec{k},\vec{k}'} O^{\vec{k},\vec{k}'} = \binom{N}{M}^2 \mathscr{B}_{N,m}^{\prime\hat{w}',\vec{v}'_a,\vec{v}'_b}. \tag{18}$$

Therefore, the maximum quantum value of the Bell operator for $M < N$ spins per side bounds the value of the Bell operator with N spins:

$$\begin{aligned} \max_{\rho_N} \mathrm{Tr}\Big(\rho_N \mathscr{B}_{N,m}^{\prime\hat{w}',\vec{v}'_a,\vec{v}'_b}\Big) &= \binom{N}{M}^{-2} \max_{\rho_N} \mathrm{Tr}\left(\rho_N \sum_{\vec{k},\vec{k}'} O^{\vec{k},\vec{k}'}\right) \\ &= \binom{N}{M}^{-2} \max_{\rho_N} \sum_{\vec{k},\vec{k}'} \mathrm{Tr}\Big(\rho_N O^{\vec{k},\vec{k}'}\Big) \\ &\leq \binom{N}{M}^{-2} \sum_{\vec{k},\vec{k}'} \max_{\rho_N} \mathrm{Tr}\Big(\rho_N O^{\vec{k},\vec{k}'}\Big) \\ &= \max_{\rho_N} \mathrm{Tr}\Big(\rho_N O^{\vec{k},\vec{k}'}\Big) \\ &= \max_{\rho_M} \mathrm{Tr}\Big(\rho_M \mathscr{B}_{M,m}^{\prime\hat{w}',\vec{v}'_a,\vec{v}'_b}\Big), \end{aligned} \tag{19}$$

where to go from the second to the third line, we let the optimization over the state be independent for each term in the sum. This shows that the maximal value of $\langle \mathscr{B}_m^{\prime\hat{w}',\vec{v}'_a,\vec{v}'_b} \rangle$ achievable with collective 1/2-spin measurements can only decrease with the number of spins N.

D. Numerical results

Let us start this subsection by a summary of the two previous subsections: (i) The local bound of an inequality of the form (8) is independent of the number of possible outcomes (ii) Assuming collective measuremens on $\frac{1}{2}$-spins, the quantum bound decreases while increasing the number of spins (or outcomes). Together, these two statements imply that if a Bell inequality of the form (8) cannot be violated by performing collective measurements on an arbitrary state containing N particles on each side, then it is also impossible to violate it by performing collective measurements on a state with more than N particles on each side. Since the CHSH inequality is a non-trivial Bell inequality with $N = 1$ spin locally, we focus on the case with $N = 2$ spins locally. We know from Ref. [15] that in this case, one needs at least 3 measurements settings locally to circumvent known local models and thus possibly violate a Bell inequality of the form (8) with collective measurements.

In the case of 3 measurement settings with 2 outcomes, there is only one relevant Bell inequality [20]. Interpreting this inequality in terms of the normalized correlators of Eq. (8), we easily compute the maximum quantum value that a state of 4 particles (2 at each location) can achieve for this inequality by optimizing the maximal eigenvalue of the corresponding Bell operator as a function of the measurement settings. We find that this inequality is not violated (up to the accuracy of the computation) with collective spin measurement of 2 particles at each side. This implies that this inequality is likely not to admit a violation with collective spin measurement irrespectively of the number of spins per side.

We now consider the case of 4 measurement settings and 2 outcomes. In this case, the full polytope has also been recently solved [21]. Ref. [22] indeed shows that this polytope contains 175 different orbits up to relabellings of parties, inputs and outputs. A list of exactly 175 inequalities which are inequivalent under these relabelings can be found in [23–25]. They thus provide a full description of the polytope. For completeness, we provide a list containing all of these inequalities in a unified format in the appendix. Focusing on these inequalities we computed the quantum bound as before with $N = 2$ spins locally but with 4 measurements locally. We did not find any violation, which suggests that no inequality of the form (8) with $m = 4$ can be violated by collective spin observables. Note that inequalities of the form (8) could however potentially involve more than two outcomes in a nontrivial way.

For the case of 5 settings, the local polytope is not known even for the simplest case of binary outcomes. We thus proceed differently. This time, we sample different

inequalities of the form (8), that is, we choose ω'_{ij}, v'_{a_i} and v'_{b_j} at random and computed both the local bound and the quantum bound. Note that this time we are not restricting ourselves to binary outcomes. We test 400 000 Bell inequalities with $4\omega'_{ij}$, $2v'_{a_i}$ and $2v'_{b_j}$ distributed uniformly in $[-1, 1]$. We do not find any violation. Repeating the same procedure for 6 settings locally, we again don't find any non-trivial Bell inequality. 6 settings is the maximum we succeeded to do because it becomes increasingly expensive to find the maximum quantum value. Also the parameter space increases with the number of settings, so one would require more and more random trials to span the space of inequalities when the number of settings increases. Still, altogether this suggests that none of the inequalities of the form (8) can be violated by collective spin measurements when $N \geq 2$.

We have presented numerical arguments suggesting that it is not possible to violate an inequality of the form (8) with collective spin measurements with 3, 4, 5 and 6 measurements settings whenever the number of spins locally is larger than two. In the next section, we show that the violation of a bipartite Bell inequality is possible when parity measurements are performed locally, for all spin number N.

III. PROPOSAL FOR THE VIOLATION OF A BI-PARTITE BELL INEQUALITY WITH PARITY MEASUREMENTS

A. The scenario

The scenario is similar to the one before. An ensemble of 1/2-spins is created in a quantum state before being shared between Alice and Bob. Each of them performs collective measurements of their spins $\hat{J}^l_\alpha$ but in opposition to the scenario of the previous section, there is no limit on the order of moments of collective spin components that can be measured. We assume in particular that Alice and Bob can assess precisely the parity of the measurement outcome at each run.

Concretely, we consider an ensemble of N 1/2-spins encoded in the internal degree of atoms, that is, two atomic states 1 and 2. These spins are located in Alice's location. We thus call $\hat{a}_i$ and $\hat{a}^\dagger_i$ with $i \in \{1, 2\}$ the bosonic operators associated to each spin states so that the collective spin projections can be written as

$$\hat{J}^A_x = \frac{1}{2}(\hat{a}^\dagger_1\hat{a}_2 + \hat{a}_1\hat{a}^\dagger_2), \tag{20}$$

$$\hat{J}^A_y = \frac{1}{2i}(\hat{a}^\dagger_1\hat{a}_2 - \hat{a}_1\hat{a}^\dagger_2), \tag{21}$$

$$\hat{J}^A_z = \frac{1}{2}(\hat{a}^\dagger_1\hat{a}_1 - \hat{a}^\dagger_2\hat{a}_2). \tag{22}$$

We further consider that initially the spins point in the x direction and then undergoes one-axis twisting [26, 27]. This results in a spin-squeezed state

$$|\psi\rangle = \frac{1}{\sqrt{N}} e^{-i\chi t(\hat{J}^A_z)^2} e^{-i\frac{\pi}{2}\hat{J}^A_y} \hat{a}^{\dagger N}_1 |0\rangle \tag{23}$$

where $|0\rangle$ is the vacuum state for all modes. The particles are then shared between Alice and Bob with a beam splitter type Hamiltonian, that is

$$|\phi\rangle = e^{\frac{\pi}{4}(\hat{a}^\dagger_1\hat{b}_1 + \hat{a}^\dagger_2\hat{b}_2 - \text{h.c.})} |\psi\rangle . \tag{24}$$

Here $\hat{b}_i$ and $\hat{b}^\dagger_i$ are bosonic operators for the spins located at Bob's location. In practice, each of these steps can be realized with a Bose-Einstein condensate where spin squeezing can be created using elastic collisions in state dependent potentials [8, 9]. The spatial splitting can then be done by slowly raising a barrier in a state-independent potential as in Refs. [10, 11].

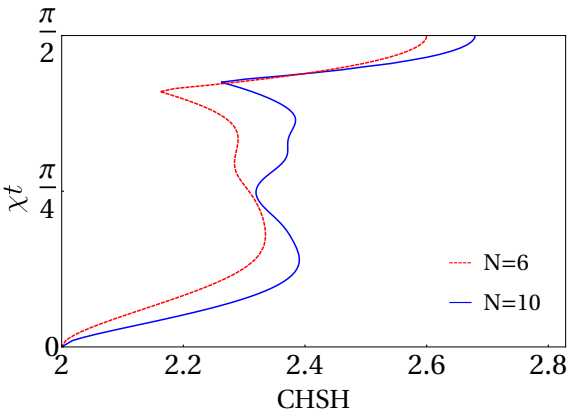

Figure 2: Violation of inequality (5) for a spin squeezed state $|\phi\rangle$ with 6 and 10 atoms as a function of the squeezing parameter χt

B. Probability distribution

Alice and Bob are sharing the state $|\phi\rangle$ and want to compute the value of the CHSH quantity using measurements $\hat{J}^A_\alpha$ and $\hat{J}^B_\beta$ where each setting is specified by two angles $\{\theta_l, \phi_l\}$ via $\vec{\alpha} = (\sin\theta_\alpha\cos\phi_\alpha, \sin\theta_\alpha\sin\phi_\alpha, \cos\theta_\alpha)$ and similarly for $\vec{\beta}$. Let $|m_a, n_a - m_a\rangle$ be the state of Alice with a total spin number n_a and m_a excitations in the state 2. Since $\hat{J}^A_z$ is half the population difference between the spin states 1 and 2, we have $\hat{J}^A_z|m_a, n_a - m_a\rangle = \frac{1}{2}(n_a - 2m_a)|m_a, n_a - m_a\rangle$. Since any operators $\hat{J}^A_\alpha$ is linked to $\hat{J}^A_z$ by a unitary, we can express its eigenstates as a function of $|m_a, n_a - m_a\rangle$ through $|m^\alpha_a, n_a - m^\alpha_a\rangle = \sum_{k=-n_a/2}^{n_a/2} \mathcal{D}^{n_a}_{k,m_a}(\theta_a, \phi_a)\,|\frac{n_a-2k}{2}, \frac{n_a+2k}{2}\rangle$ where $\mathcal{D}^{n_a}_{k,m_a}(\theta_a, \phi_a)$ is similar to a Wigner matrix:

$$e^{-i\phi_A k}\,\langle\frac{n_a - 2k}{2}, \frac{n_a + 2k}{2}|\, e^{-i\theta_A\hat{J}^A_y}\,|m_a, n_a - m_a\rangle\,. \tag{25}$$

The same basis $\{|m_a, n_a - m_a\rangle\}$ can also be used to express the state that Alice and Bob share, that is $|\phi\rangle$ can be written as

$$\frac{1}{2^N}\sum_{m=0}^{N}\sum_{k=0}^{m}\sum_{l=0}^{N-m} C_{m,k,l}\,|k,l\rangle_A\,|m-k, N-m-l\rangle_B \tag{26}$$

where $C_{m,k,l} = \sqrt{\binom{m}{N}\binom{k}{m}\binom{l}{N-m}}e^{-i\chi t(m-\frac{N}{2})^2}$. When Alice and Bob measure $\hat{J}^A_\alpha$ and $\hat{J}^B_\beta$ respectively, the probability with which they find the eigenvalues k^a_α and k^b_β is given by

$$P(k^a_\alpha, k^b_\beta|\hat{J}^A_\alpha, \hat{J}^B_\beta) = \sum_{n_a=0}^{N}\Big|\langle\frac{n_a-2k^a_\alpha}{2}, \frac{n_a+2k^a_\alpha}{2}| \otimes \langle\frac{N-n_a-2k^b_\beta}{2}, \frac{N-n_a+2k^b_\beta}{2}|\,\phi\rangle\Big|^2 \tag{27}$$

This probability can be efficiently calculated using Eqs. (25) and (26).

C. Results

We consider the violation of Ineq. (5) which uses two settings and two outcomes per party. While many strategies can be used to bin the measurement results, we could only find a violation for the parity binning, which corresponds to the measurement of $(-1)^{\hat{J}^A_{\theta_A,\phi_A}}$ for Alice and $(-1)^{\hat{J}^B_{\theta_B,\phi_B}}$ for Bob. We present results obtained in this case below.

First, we fix the total number of spins N and we optimize the value of (5) over the measurement settings for various values of χt. The result is shown in Fig. 2 for $N = 6$ and $N = 10$. For low χt, the violation increases until a value which depends on the number of atoms and then goes down whereas in the extreme squeezing regime the violation can go higher.

We further investigate the extreme squeezing case where $\chi t = \pi/2$. Remarkably the violation increases with the atom number and seems to saturate very close to the maximum value achievable by quantum states $2\sqrt{2}$, see Fig. 3. This implies that it is possible to self test a singlet state and Pauli measurements with collective observables. Although this result is unexpected, it is extremely challenging if not completely out of reach experimentally as the maximally squeezed state corresponds to a GHZ state when $\chi t = \pi/2$.

We thus focus on the regime where χt is small, which is the most relevant regime in practice. We fix $\chi t = 0.006$ corresponding to a Wineland squeezing parameter $10\log\xi^2 = 10$ dB for $N = 500$ atoms where $\xi^2 = \frac{N(\Delta\hat{J}^A_\perp)^2}{\langle\hat{J}^A_x\rangle^2}$ [28, 29], $\hat{J}^A_\perp$ corresponding a projection along the squeezing direction (before splitting). The resulting violation increases as a function of the atom number, as shown in Fig. 4.

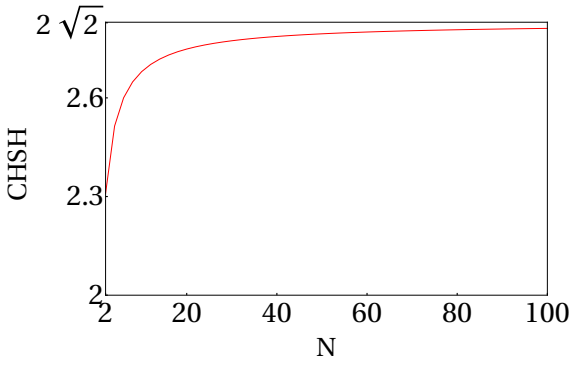

Figure 3: Violation of the inequality (5) for a spin squeezed state $|\phi\rangle$ with $\chi t = \frac{\pi}{2}$ as a function of the total number of atoms N.

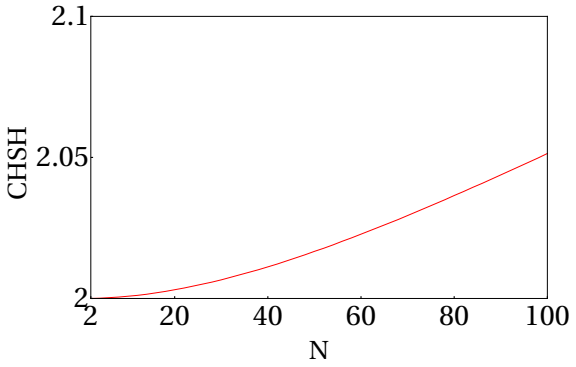

Figure 4: Violation of CHSH for a small $\chi t = 0.006$ which correspond to 10 dB of squeezing at 500 atoms. The violation is plotted with respect to the total atom number.

IV. CONCLUSION

We investigated the possibility of detecting bipartite nonlocality in many-body systems. We devoted a special attention to the experimental realization by considering realistic measurements. In particular, we focused on collective measurements only where spins are all measured in the same direction locally. We showed numerical results suggesting that no-Bell inequality with first order correlators can be violated whenever such measurements act of $N \geq 2$ spins. We then proved that the CHSH-Bell inequality can be violated with collective measurements as long as parity measurements can be performed. This suggests that parity measurements is a key ingredient – even maybe necessary – to reveal bipartite correlations in many-body systems with Bell inequalities.

Acknowledgments

This work was supported by the Swiss National Science Foundation (SNSF) through the Grant PP00P2-179109. We also acknowledge the Army Research Laboratory Center for Distributed Quantum Information via the project SciNet.

[1] N. Brunner, D. Cavalcanti, S. Pironio, V. Scarani, and S. Wehner, Rev. Mod. Phys. **86**, 419 (2014)
[2] J. Tura, R. Augusiak, A. B. Sainz, T. Vértesi, M. Lewenstein, A. Acín, Science **344**, 1256 (2014)
[3] S. Wagner, R. Schmied, M. Fadel, P. Treutlein, N. Sangouard, and J.-D. Bancal, Phys. Rev. Lett. **119**, 170403 (2017)
[4] J. Tura, G. De las Cuevas, R. Augusiak, M. Lewenstein, A. Acín, J. I. Cirac, Phys. Rev. X **7**, 021005 (2017)
[5] R. Schmied, J.-D. Bancal, B. Allard, M. Fadel, V. Scarani, P. Treutlein, and N. Sangouard, Science **352**, 441 (2016)
[6] N.J. Engelsen, R. Krishnakumar, O. Hosten, and M.A. Kasevich, Phys. Rev. Lett. **118**, 140401 (2017)
[7] F. Baccari et al. arXiv:1802.09516
[8] M.F. Riedel, P. Bohi,Y. Li, T. W. Hansch, A. Sinatra and P. Treutlein, Nature **464**, 1170-1173 (2010)
[9] C. Gross,T. Zibold, E. Nicklas, J. Esteve and M.K. Oberthaler, Nature **464**, 1165-1169 (2010)
[10] Y. Shin, M. Saba, T. A. Pasquini, W. Ketterle, D. E. Pritchard, and A.E. Leanhardt, Phys. Rev. Lett. **92**, 050405 (2004)
[11] T. Schumm, S. Hofferberth, L.M. Anderson, S. Wildermuth, S. Groth, I. Bar-Joseph, J. Schmiedmayer, and P. Kruger, Nature Phys. **1**, 57 (2005)
[12] G.A. Durkin and C. Simon, Phys. Rev. Lett. **95**, 180402 (2005)
[13] G. Tóth, Phys. Rev. A **70**, 010301(R) (2004)
[14] E. Oudot, J-D. Bancal, R. Schmied, P. Treutlein, and N. Sangouard, Phys. Rev. A **95**, 052347 (2017)
[15] R. Ramanathan, T. Paterek, A. Kay, P. Kurzyski, and D. Kaszlikowski, Phys. Rev. Lett. **107**, 060405 (2011)
[16] H. S. Poh, A. Cer, J.-D. Bancal, Y. Cai, N. Sangouard, V. Scarani, C. Kurtsiefer, Phys. Rev. A **96**, 022101 (2017)
[17] Y. Zhou, Y. Cai, J.-D. Bancal, F. Gao, V. Scarani, Phys. Rev. A **96**, 052108 (2017)
[18] J.F. Clauser, M.A. Horne, A. Shimony, and R.A. Holt, Phys. Rev. Lett. 23, 880 (1969)
[19] G. Svetlichny, Phys. Rev. D **35**, 3066 (1987)
[20] M. Froissart, Il Nuovo Cimento **64**, 241 (1981)
[21] S. Schwarz, B. Bessire, A. Stefanov, Y.-C. Liang, New J. Phys. **18**, 035001 (2016)
[22] M. Deza and M. Dutour Sikirić, Intl. Trans. in Op. Res. 23 **853-860** (2016)
[23] N. Brunner, N. Gisin. Physics Letters A **372**, 3162 (2008)
[24] K. F. Pal and T. Vértesi Phys. Rev. A **79**, 022120 (2009)
[25] J.D. Bancal, N. Gisin and S. Pironio J. Phys. A: Math. Theor. **43** 385303 (2010)
[26] J. Ma, X. Wang, C. P. Sun, and F. Nori, Physics Reports, **509**, 89 (2011)
[27] L. Pezzè, A. Smerzi, M.K. Oberthaler, R. Schmied, and P. Treutlein, Rev. Mod. Phys. **90**, 035005 (2018)
[28] D.J. Wineland, J.J. Bollinger, W.M. Itano, F.L. Moore, and D.J. Heinzen Phys. Rev. A **46**, R6797(R) (1992)
[29] D.J. Wineland, J.J. Bollinger, W.M. Itano, and D.J. Heinzen, Phys. Rev. A **50**, 67 (1994)

Appendix A: Complete list of facets for the local polytope in the Bell scenario $[(2,2,2,2),(2,2,2,2)]$

The local polytope for two parties and four binary settings per party was recently solved in [22]. Namely, this work showed that this polytope admits exactly 175 classes of facets under relabelling of parties, inputs and outputs. Interestingly, exactly 175 distinct classes of Bell inequalities for this scenario were discovered earlier, over a number of years, and published in various manuscripts [18, 20, 23–25]. Here we gather this information in a single place.

A Bell inequality for $m = 4$ binary settings is defined by 25 parameters. Following the main text we use the correlation picture with outcomes $a_i, b_j \in \{-1, 1\}$. A Bell inequality can then be written as

$$B \ = \delta + \sum_{i=1}^{4} \alpha_i \langle a_i \rangle + \sum_{j=1}^{4} \beta_j \langle b_j \rangle + \sum_{i,j=1}^{4} \gamma_{ij} \langle a_i b_j \rangle \geq 0$$

or equivalently, in table format

$$B = \left(\begin{array}{c|cccc} \ell & \beta_1 & \beta_2 & \beta_3 & \beta_4 \\ \hline \alpha_1 & \gamma_{11} & \gamma_{12} & \gamma_{13} & \gamma_{14} \\ \alpha_2 & \gamma_{21} & \gamma_{22} & \gamma_{23} & \gamma_{24} \\ \alpha_3 & \gamma_{31} & \gamma_{32} & \gamma_{33} & \gamma_{34} \\ \alpha_4 & \gamma_{41} & \gamma_{42} & \gamma_{43} & \gamma_{44} \end{array} \right) \geq 0, \qquad \text{(A1)}$$

In the main text we used $v'_{a_i} = -\alpha_i$, $v'_{b_j} = -\beta_j$, $w'_{ij} = -\gamma_{ij}$ and $\ell = \delta$.

The 175 classes of inequalities are given in table I. The first few inequalities are in order: the positivity, CHSH, I_{3322}, the three I_{4322} inequalities, after which come the 169 facets which truly involve all settings of each party.

Table I: List of I_{4422} inequalities

#	δ	α_1	α_2	α_3	α_4	β_1	γ_{11}	γ_{21}	γ_{31}	γ_{41}	β_2	γ_{12}	γ_{22}	γ_{32}	γ_{42}	β_3	γ_{13}	γ_{23}	γ_{33}	γ_{43}	β_4	γ_{14}	γ_{24}	γ_{34}	γ_{44}
1	1	1	0	0	0	1	1	0	0	0	0	0	0	0	0	0	0	0	0	0	0	0	0	0	0
2	2	0	0	0	0	0	1	1	0	0	0	1	-1	0	0	0	0	0	0	0	0	0	0	0	0
3	4	1	1	0	0	1	1	1	1	0	1	1	1	-1	0	0	1	-1	0	0	0	0	0	0	0
4	5	1	1	1	0	1	1	1	1	0	0	1	0	-1	0	0	1	-1	0	0	0	0	1	-1	0
5	6	0	0	0	0	1	1	1	1	0	1	-1	-1	-1	0	0	1	1	-2	0	0	1	-1	0	0
6	6	2	0	0	0	1	1	1	1	0	1	1	1	-1	0	1	1	-1	1	0	1	1	-1	-1	0
7	6	0	0	0	0	0	1	1	1	1	0	1	1	1	-1	0	1	1	-2	0	0	1	-1	0	0
8	6	1	1	0	0	0	1	-1	1	1	0	1	-1	1	-1	0	1	0	-1	0	0	0	1	1	0
9	6	1	1	0	0	1	1	1	1	0	1	1	0	-1	1	0	1	-1	-1	-1	0	0	1	-1	0
10	6	2	0	0	0	1	1	1	1	0	1	1	1	-1	0	1	1	-1	0	1	1	1	-1	0	-1
11	7	1	1	1	0	1	1	1	0	1	1	1	0	1	-1	1	-1	1	1	0	0	0	1	-1	-2
12	7	1	1	1	0	1	1	1	0	1	0	1	-1	-1	1	0	1	0	-1	-2	0	0	1	-1	0
13	7	1	1	1	0	1	1	1	1	0	0	1	1	-1	1	0	1	1	-1	-1	0	2	-2	0	0
14	7	1	1	1	0	1	1	1	1	2	1	1	1	0	-1	1	1	0	1	-1	0	0	1	-1	0
15	7	2	1	1	1	2	1	1	1	1	1	1	1	0	-1	1	1	0	-1	1	1	1	-1	1	0
16	7	2	2	1	0	2	1	1	1	1	2	1	1	1	-1	1	1	1	-1	0	0	1	-1	0	0
17	8	1	1	0	0	1	1	0	1	1	1	0	1	-1	-1	0	1	-1	-3	1	0	1	-1	1	-1
18	8	1	1	0	0	1	1	1	1	2	1	1	0	1	-1	0	1	1	1	-1	0	2	-1	-1	0
19	8	1	1	0	0	1	2	1	1	1	1	0	1	-1	-1	0	2	-1	-1	0	0	1	0	1	-2
20	8	1	1	0	0	1	2	1	2	0	1	1	2	-2	0	0	1	-1	-1	1	0	1	-1	-1	-1
21	8	1	1	1	1	1	1	2	1	-1	1	2	-2	1	0	1	1	1	0	1	1	-1	0	1	1
22	8	1	1	1	1	1	2	1	-1	1	1	1	1	1	0	0	1	-1	1	-1	0	1	-2	0	1
23	8	1	1	1	1	1	2	1	1	-1	1	1	2	-1	1	0	1	-1	-1	1	0	1	-1	0	0
24	8	2	1	1	0	1	1	2	-1	1	1	1	1	0	-1	0	1	-1	-1	1	0	1	-1	-1	-1
25	8	2	1	1	0	2	1	1	1	1	1	1	-2	1	-1	1	1	1	0	-1	0	1	-1	-1	1
26	8	2	1	1	0	2	1	1	1	1	1	1	2	-1	-1	1	1	-1	0	-1	0	1	-1	-1	1
27	8	2	1	1	0	2	1	2	1	2	1	1	-1	1	0	1	1	1	0	-1	0	1	-1	-1	1
28	8	2	1	1	0	2	1	2	2	1	1	1	1	-1	0	1	1	-1	1	0	0	1	-1	-1	1
29	8	2	2	0	0	0	1	-1	1	1	0	1	-1	1	-1	0	1	-1	-1	1	0	1	-1	-1	-1
30	8	2	2	0	0	2	1	1	1	1	2	1	1	-1	-1	0	1	-1	1	-1	0	1	-1	-1	1
31	9	1	1	1	0	1	-3	2	1	1	1	2	1	1	1	1	1	1	0	-1	0	1	1	-1	1
32	9	1	1	1	0	1	-1	2	1	1	1	2	1	0	2	1	1	0	1	-1	0	1	2	-1	-2
33	9	1	1	1	0	1	1	1	1	0	0	2	-1	-2	1	0	1	-2	2	1	0	1	-1	0	-2
34	9	1	1	1	0	1	1	1	2	1	0	2	1	-2	1	0	1	-1	1	-1	0	1	-2	0	1
35	9	1	1	1	0	1	1	1	2	1	1	1	1	2	-1	1	2	2	-3	0	0	1	-1	0	0
36	9	1	1	1	0	1	2	1	1	1	1	-2	2	1	0	1	2	1	0	-2	0	1	1	-1	1
37	9	1	1	1	0	1	2	1	1	1	1	-1	1	2	1	1	1	1	0	-1	0	1	-2	2	-1
38	9	1	1	1	0	1	2	1	1	1	1	1	1	1	-2	1	-1	2	1	1	0	1	1	-2	0
39	9	1	1	1	0	1	2	2	-2	1	1	1	1	2	1	1	1	1	1	-2	0	1	-1	0	0
40	9	2	1	0	0	1	2	1	1	1	1	2	1	1	-1	1	2	1	-2	0	0	2	-2	0	0
41	9	2	1	0	0	1	2	1	1	1	1	1	1	1	-2	1	1	1	-1	0	0	2	-2	-1	-1
42	9	2	1	0	0	1	2	1	1	1	1	2	1	1	-1	1	1	1	-1	0	0	3	-2	-1	0
43	9	2	1	1	1	1	2	1	1	-1	1	2	1	-1	1	1	0	-1	1	1	0	2	-2	0	0
44	10	0	0	0	0	0	2	2	1	1	0	2	-1	-1	-2	0	1	-1	-2	2	0	1	-2	2	1
45	10	1	1	0	0	0	2	-1	2	1	0	1	-1	-2	2	0	1	-2	-1	-2	0	1	1	-1	-1
46	10	1	1	0	0	1	1	2	1	1	1	2	0	-2	-1	0	1	-2	1	2	0	1	-1	2	-2
47	10	2	0	0	0	1	2	1	1	1	1	2	1	0	-2	1	2	0	-2	1	1	2	-2	1	0
48	10	2	0	0	0	1	2	2	2	1	1	2	-1	-1	-1	1	1	1	-2	1	1	1	-2	1	1
49	10	2	1	1	0	2	1	2	2	1	1	2	-1	1	-1	1	2	1	-2	0	0	1	-1	0	2
50	10	2	1	1	0	2	2	2	1	1	1	1	-1	2	-1	1	2	0	-2	-1	0	1	-2	0	1
51	10	2	1	1	0	2	2	2	1	1	1	2	1	-1	-1	1	0	-1	1	-1	0	2	-3	0	1
52	10	2	2	0	0	2	2	2	1	1	2	1	1	-1	-1	0	2	-2	1	-1	0	1	1	-1	-1
53	10	2	2	1	1	2	1	1	1	1	0	2	-1	1	-2	0	2	-1	-2	1	0	1	-1	1	1
54	10	3	1	0	0	2	2	1	2	1	2	1	1	-1	-1	1	2	-1	1	-1	1	2	0	-2	1
55	10	3	1	1	1	3	2	2	2	1	1	2	-1	1	-1	1	2	1	-2	0	1	1	-1	0	1
56	11	1	1	1	0	1	2	2	-1	2	0	1	1	-2	-4	0	1	-1	1	-1	0	1	-1	-1	1
57	11	2	1	0	0	1	2	-1	2	2	1	2	-1	1	-3	1	1	1	-1	0	0	1	-2	-2	1
58	11	2	1	1	1	1	3	-2	1	1	1	1	1	-1	2	1	1	1	1	0	0	3	1	-2	-2

Continued on the next page...

Table I: continued

#	δ	α_1	α_2	α_3	α_4	β_1	γ_{11}	γ_{21}	γ_{31}	γ_{41}	β_2	γ_{12}	γ_{22}	γ_{32}	γ_{42}	β_3	γ_{13}	γ_{23}	γ_{33}	γ_{43}	β_4	γ_{14}	γ_{24}	γ_{34}	γ_{44}
59	11	2	1	1	1	1	3	-2	1	1	1	2	1	-1	1	1	1	1	2	-1	0	2	1	-1	-2
60	11	2	1	1	1	2	1	2	2	1	1	2	2	-1	-2	1	1	1	-1	2	1	2	-2	1	0
61	11	2	1	1	1	2	1	2	2	1	1	2	-3	1	1	1	2	1	-1	-1	1	1	1	-1	2
62	11	2	1	1	1	2	2	1	1	2	1	3	1	1	-2	0	2	-2	-1	1	0	1	1	-2	0
63	11	2	1	1	1	2	2	1	1	2	1	3	1	1	-2	0	3	-2	-2	1	0	0	1	-1	0
64	11	2	1	1	1	2	2	2	1	1	1	1	-2	2	0	0	2	-1	-1	-2	0	1	-2	-1	2
65	11	2	1	1	1	2	2	2	1	1	1	1	-1	2	-1	0	2	-2	-1	-1	0	1	2	-1	-2
66	11	2	1	1	1	2	2	2	2	0	1	2	1	-1	1	0	3	-3	1	-1	0	1	1	-1	-1
67	11	2	2	1	0	2	2	1	1	2	2	1	1	2	-2	1	1	2	-1	-1	0	2	-2	-1	-1
68	11	3	1	1	0	2	2	1	2	1	1	3	-2	1	-1	1	3	1	-2	1	1	1	1	0	-1
69	11	3	1	1	0	2	2	2	2	0	1	2	1	-1	1	1	2	1	-1	-1	1	3	-3	1	0
70	12	1	1	0	0	1	-1	2	2	2	1	2	1	-1	-1	0	2	-1	-2	3	0	2	-1	3	0
71	12	1	1	0	0	1	-1	2	2	2	1	2	1	-1	-1	0	2	-1	4	-1	0	2	-1	-1	2
72	12	1	1	0	0	1	3	1	2	1	1	1	3	-2	-1	0	2	-2	-2	-2	0	1	-1	-2	2
73	12	1	1	1	1	1	-2	1	3	1	1	2	2	1	0	0	2	-2	2	-2	0	1	-2	1	2
74	12	1	1	1	1	1	2	-1	-2	2	1	-2	2	1	2	1	1	-2	3	1	1	2	2	1	0
75	12	1	1	1	1	1	-2	3	1	1	1	2	1	1	1	0	2	2	-3	-1	0	1	1	2	-2
76	12	1	1	1	1	1	-1	2	-2	2	1	2	3	1	-1	1	-2	1	3	1	1	2	-1	1	1
77	12	1	1	1	1	1	2	-3	3	1	1	1	2	1	1	0	2	-1	-2	1	0	2	1	1	-2
78	12	1	1	1	1	1	2	3	1	-1	1	-2	1	3	1	0	2	-2	2	-2	0	1	-1	1	1
79	12	1	1	1	1	1	2	3	2	-2	1	1	1	1	2	0	2	-2	1	-1	0	2	1	-3	0
80	12	2	1	1	0	1	1	-2	3	1	1	2	1	1	-1	0	2	-2	-2	2	0	1	-2	-1	-2
81	12	2	1	1	0	1	2	2	-1	2	1	2	1	1	-1	0	3	-3	-1	1	0	1	1	-2	-2
82	12	2	1	1	0	2	0	2	2	2	1	2	-1	2	-2	1	2	1	-1	-1	0	2	-1	0	3
83	12	2	1	1	0	2	0	2	2	2	1	2	1	-1	-1	1	2	-1	1	-1	0	2	-1	-1	4
84	12	2	1	1	0	2	1	2	3	2	1	2	2	-2	1	1	2	-1	1	-1	0	1	-2	-1	2
85	12	2	1	1	0	2	2	2	1	1	1	2	-1	-2	-2	1	1	-2	3	-1	0	1	-2	-1	2
86	12	2	1	1	0	2	2	3	1	2	1	3	-2	1	1	1	1	1	1	-2	0	2	1	-2	-1
87	12	2	1	1	0	2	2	3	2	1	1	3	-4	1	1	1	2	1	-1	-1	0	1	1	-1	1
88	12	2	2	1	1	2	2	2	1	-1	2	2	0	-2	2	1	1	-2	3	1	1	-1	2	1	1
89	12	3	1	0	0	2	2	1	2	1	2	1	2	-2	-1	1	2	-1	1	-3	1	2	-1	-1	1
90	12	3	1	0	0	2	3	1	3	1	2	2	2	-2	0	1	2	-1	-1	1	1	2	-1	0	-2
91	12	3	1	1	1	2	2	3	1	-2	2	2	1	-1	2	2	2	-2	2	0	0	1	-1	-1	-1
92	12	3	1	1	1	3	1	2	2	2	1	2	-2	-1	2	1	2	-1	1	-1	1	2	2	-1	0
93	12	3	2	1	0	3	2	2	1	2	2	1	2	-1	-2	1	2	-1	1	-1	0	2	-1	-2	1
94	12	4	1	1	0	3	2	2	1	2	2	2	-2	1	-1	2	2	2	0	-2	1	2	-1	-1	1
95	12	4	1	1	0	3	2	2	1	2	2	2	-1	2	-1	2	2	1	-1	-2	1	2	-1	-1	1
96	12	4	1	1	0	3	2	2	2	1	2	2	2	-1	-1	2	2	-2	1	-1	1	2	-1	-1	1
97	12	4	2	0	0	3	2	2	2	1	3	2	2	-2	-1	1	2	-1	1	-1	1	2	-1	-1	1
98	12	4	2	1	1	4	2	2	2	2	2	2	2	-1	-1	1	2	-1	1	-1	1	2	-1	-1	1
99	13	1	1	1	0	1	-3	2	3	1	1	2	-1	2	-2	1	3	2	1	1	0	1	-2	1	2
100	13	1	1	1	0	1	2	1	2	2	1	-2	3	1	-1	1	3	1	0	-3	0	2	2	-2	2
101	13	1	1	1	0	1	2	3	-2	2	1	2	1	1	-3	1	1	1	3	2	0	2	-2	-1	1
102	13	2	1	0	0	1	2	2	2	1	1	2	1	-2	2	1	3	1	-1	-2	0	3	-3	1	1
103	13	2	1	1	1	1	2	2	-1	2	1	-1	-2	2	2	1	2	1	1	-1	0	3	-4	-1	0
104	13	2	1	1	1	1	2	2	2	-1	1	3	-2	1	1	1	0	2	-1	2	0	3	1	-3	-1
105	13	2	1	1	1	2	0	2	2	2	1	2	-3	3	-1	1	2	3	1	-1	1	2	-1	-1	1
106	13	2	1	1	1	2	1	2	1	2	1	2	-3	3	-1	1	1	3	1	-2	1	2	-1	-2	0
107	13	2	2	1	0	2	3	2	2	1	1	1	2	-1	-1	0	2	1	-2	1	0	4	-3	0	-1
108	13	3	1	1	0	2	2	-3	2	1	2	2	3	1	2	2	1	2	1	-2	1	2	-1	-1	-1
109	13	3	1	1	0	2	2	3	-1	2	2	2	1	1	-2	1	2	-2	-1	2	0	1	-1	-2	-2
110	13	3	2	1	1	3	2	2	2	1	1	2	2	-1	-2	1	2	1	-1	1	0	3	-3	1	-1
111	13	4	1	0	0	2	3	1	2	2	2	2	1	1	-2	2	2	1	-2	1	1	3	-2	-1	-1
112	14	2	1	1	0	1	2	2	-1	2	1	3	1	1	-2	0	3	-3	-2	2	0	0	1	-3	-2
113	14	2	1	1	0	1	2	3	-1	3	1	-1	2	2	-2	1	3	1	-1	-4	1	2	-1	1	1
114	14	2	1	1	0	1	3	1	-1	4	1	2	1	1	-1	0	2	2	-2	-2	0	3	-3	-1	-1
115	14	2	1	1	0	1	3	2	-1	3	1	2	1	1	-1	0	2	2	-2	-2	0	3	-4	-1	0
116	14	2	1	1	0	2	2	2	3	1	1	2	-2	-1	-2	1	1	3	-3	0	0	1	-2	-2	3

Continued on the next page...

Table I: continued

#	δ	α_1	α_2	α_3	α_4	β_1	γ_{11}	γ_{21}	γ_{31}	γ_{41}	β_2	γ_{12}	γ_{22}	γ_{32}	γ_{42}	β_3	γ_{13}	γ_{23}	γ_{33}	γ_{43}	β_4	γ_{14}	γ_{24}	γ_{34}	γ_{44}
117	14	2	1	1	0	2	3	3	2	2	1	3	-2	1	1	1	2	1	1	-3	0	2	1	-3	0
118	14	2	2	1	1	2	2	1	2	1	1	2	3	-2	-2	1	1	1	-2	3	0	3	-3	-1	-1
119	14	2	2	1	1	2	3	2	2	-1	2	2	0	2	2	1	2	2	-4	1	1	-1	2	1	-1
120	14	2	2	1	1	2	3	2	2	-1	2	2	3	-1	2	0	4	-4	-1	1	0	1	1	-1	-1
121	14	3	2	1	0	3	1	3	3	2	2	2	2	-2	0	1	2	-1	1	-1	0	2	-2	-1	3
122	14	4	1	1	0	3	3	3	1	2	2	3	1	-1	-3	2	2	-2	2	0	1	2	-1	-1	1
123	14	4	2	1	1	4	2	2	2	2	2	2	1	-2	-1	1	2	-2	-1	2	1	2	-1	2	-2
124	14	4	2	1	1	4	2	3	3	2	2	2	2	-2	0	1	2	-2	-1	2	1	2	-1	1	-1
125	14	4	2	2	0	3	2	2	1	2	3	2	1	2	-2	1	3	1	-2	-1	1	3	-2	1	1
126	15	2	1	1	1	1	2	2	2	-1	1	4	-3	1	1	1	1	2	-1	3	0	3	2	-3	-2
127	15	2	1	1	1	2	1	3	3	1	1	3	-2	2	-2	1	3	2	-3	1	1	1	-2	1	3
128	15	2	1	1	1	2	2	3	2	1	1	4	-3	1	1	0	3	2	-2	-3	0	1	1	-2	2
129	15	2	1	1	1	2	3	2	2	1	1	1	-2	-1	3	0	3	-2	-3	-2	0	1	-3	3	-1
130	15	2	1	1	1	2	3	3	1	1	1	3	-2	2	2	0	3	-1	1	-3	0	3	-1	-3	1
131	15	2	2	1	0	2	2	3	2	1	1	2	0	-1	-2	0	3	-4	-1	2	0	1	3	-3	1
132	15	2	2	2	1	2	2	2	3	-1	1	-3	-1	3	2	1	4	-3	1	1	1	1	2	-1	1
133	15	3	2	1	1	2	3	2	-1	2	2	2	3	2	-1	1	4	-4	1	0	0	2	1	-1	-2
134	15	3	2	1	1	2	3	2	2	-1	2	0	2	-2	2	1	3	-2	1	1	0	3	0	-4	-1
135	15	3	2	1	1	2	3	2	2	-1	2	1	2	-1	2	1	4	-3	1	1	0	3	1	-3	-1
136	15	3	2	1	1	3	1	3	3	2	2	2	3	-2	1	1	2	-3	-1	3	1	2	-1	1	-1
137	15	3	2	2	0	3	3	2	3	1	1	4	-3	1	-1	1	1	2	-1	-1	0	3	1	-3	1
138	15	4	2	1	0	3	2	2	2	1	2	3	2	-1	-2	1	4	-3	1	-1	1	3	1	-1	2
139	16	1	1	1	1	1	2	-3	2	4	1	2	3	1	1	0	2	-2	3	-3	0	3	-1	-3	-1
140	16	2	1	1	0	2	2	3	2	1	1	3	-4	-1	3	1	2	-1	-1	-3	0	1	3	-3	1
141	16	2	2	1	1	2	2	4	2	-2	2	1	2	2	3	1	3	-4	3	-1	1	2	0	-2	1
142	16	2	2	1	1	2	2	4	2	-2	2	2	1	-1	2	1	3	-4	3	-1	1	-1	1	3	2
143	16	2	2	1	1	2	2	3	4	-1	2	3	-1	2	2	1	4	2	-4	-1	1	-1	2	-1	1
144	16	2	2	1	1	2	4	2	2	-2	2	2	1	2	3	1	2	2	-4	1	1	-2	3	1	-1
145	16	3	1	1	1	2	3	3	3	-1	1	4	-5	1	-1	1	2	1	-1	1	0	2	2	-2	-2
146	16	3	1	1	1	3	3	2	3	1	1	2	-2	-2	3	1	3	-2	-1	-3	1	1	3	-3	0
147	16	3	2	1	0	2	4	2	-2	2	2	2	1	3	2	2	1	2	1	-2	0	4	-3	1	-2
148	16	4	1	1	0	2	3	2	1	2	2	3	1	2	-2	1	4	1	-3	-1	1	4	-3	1	1
149	16	5	1	1	1	3	3	3	1	-2	3	3	1	-2	3	3	3	-2	3	1	1	2	-1	-1	-1
150	16	5	2	2	1	5	3	3	2	3	2	3	-2	2	-1	2	2	2	0	-2	1	3	-1	-2	1
151	17	1	1	1	0	1	-3	2	4	2	1	2	3	1	-3	1	4	1	1	3	0	2	-3	3	-2
152	17	2	1	1	1	2	2	2	3	1	1	2	-3	-2	4	1	3	-2	-1	-3	1	1	4	-3	1
153	17	2	2	1	0	2	3	-1	3	3	1	1	2	-1	-1	0	2	-2	-2	2	0	2	-3	1	-6
154	17	3	1	1	0	2	2	-2	4	2	2	3	2	1	-2	1	3	-2	-3	3	0	1	-3	-1	-3
155	17	3	2	2	0	3	3	3	2	1	1	4	2	-3	-2	1	0	-1	2	-2	0	4	-4	1	1
156	18	2	2	1	1	2	-1	3	-3	3	2	3	2	2	-1	1	-3	1	5	2	1	3	-2	1	3
157	18	3	1	0	0	2	3	-1	4	4	2	3	-1	2	-4	2	2	2	-3	1	0	1	-3	-3	1
158	18	3	1	1	1	2	2	2	4	-2	2	3	4	-4	-1	2	1	2	2	3	2	3	-3	-1	1
159	18	3	2	1	0	3	3	2	3	1	2	1	4	-4	-1	1	3	-2	-1	-3	0	2	-2	-3	3
160	18	3	2	2	1	3	0	3	3	-3	2	3	2	-1	2	2	3	-2	2	1	1	-3	1	2	5
161	18	3	2	2	1	3	1	2	3	3	2	2	2	4	-2	2	3	4	-4	-1	1	3	-2	-1	1
162	18	3	2	2	1	3	3	2	1	3	2	4	2	2	-2	1	-5	4	3	-1	0	1	2	-2	-1
163	18	4	2	1	1	2	3	2	2	-1	2	2	2	-1	3	1	4	2	-3	-2	1	5	-4	1	1
164	18	4	2	1	1	3	2	3	3	1	2	4	2	-2	-2	2	2	1	-2	3	1	4	-4	2	1
165	18	4	2	1	1	3	3	2	3	1	2	4	2	-2	2	1	3	2	-1	-3	0	4	-4	1	-1
166	18	5	2	1	0	3	3	2	3	1	2	4	2	-2	2	2	3	2	-1	-2	1	5	-4	1	-1
167	18	6	2	1	1	5	3	3	3	2	3	3	2	-3	-1	2	3	-2	-1	2	2	3	-1	2	-2
168	18	6	2	2	2	6	3	3	3	3	2	3	2	-1	-2	2	3	-1	-2	2	2	3	-2	2	-1
169	19	2	2	1	0	2	3	2	1	2	1	-2	3	-3	-3	1	4	-1	2	-4	1	-3	2	5	-1
170	19	2	2	2	1	2	5	2	2	-3	2	2	2	1	3	1	-3	2	4	-2	0	2	-4	3	1
171	20	2	2	1	1	2	4	2	5	-1	1	3	2	-2	2	1	-4	5	1	1	0	3	3	-3	-3
172	20	3	2	1	0	3	2	3	3	1	2	3	-1	-2	-4	1	3	-2	-4	4	0	1	-4	4	1
173	21	3	2	1	1	3	4	5	3	-3	2	2	2	2	4	1	3	2	-5	1	1	4	-3	1	-1
174	23	2	2	2	1	2	2	6	2	-4	2	3	2	1	4	1	3	-4	5	-3	0	4	-2	-4	-2

Continued on the next page...

Table I: continued

#	δ	α_1	α_2	α_3	α_4	β_1	γ_{11}	γ_{21}	γ_{31}	γ_{41}	β_2	γ_{12}	γ_{22}	γ_{32}	γ_{42}	β_3	γ_{13}	γ_{23}	γ_{33}	γ_{43}	β_4	γ_{14}	γ_{24}	γ_{34}	γ_{44}
175	24	2	2	1	1	2	6	2	-4	2	2	2	1	5	4	1	-4	5	-3	3	1	2	4	3	-4

CHAPTER 3

DETECTION OF THE NON-CLASSICAL NATURE OF LIGHT WITH THE HUMAN EYE

So far, we have focused on the characterisation of quantum correlations in multiple spin systems and clarified some requirements on the detection techniques. We also recognise that quantum features can appear in a single mode of light, where a mixture of coherent states in one mode is considered to be only classical. Revealing non-classicality in this single mode can be done using an autocorrelation measurement with two non photon number resolving detectors after a 50/50 beam splitter by recording the single clicks and the twofold coincidence events. One can thus compute the second-order coherence function ($g^2(\tau) = \langle I(t)I(t+\tau)\rangle / \langle I(t)\rangle^2$) which is an intensity correlation function of the radiation. The intensity fluctuations of light classified as follow, chaotic ($g^2(\tau) > 1$), coherent ($g^2(\tau) = 1$), or subPoissonian ($g^2(\tau) < 1$), where the last one reveals non classicality of quantum states [25]. This method has been successfully achieved in numerous photonic experiments [26, 27, 28, 29, 30] and requires the ability to distinguish between the presence or the absence of photons on the detector.

Can one imagine revealing the quantum nature of a single mode of light without the capability to distinguish between zero and non-zero photon number? Many detectors are indeed unable to achieve such a resolution. For example, the CCD camera on our smart phone detect the photon number with an incertitude of the order of 2 to 3 photons in the best case. [31]. The human eye does not have this ability either since it has been described as a detector with a threshold at 7 photons with an efficiency of 80% [32, 33]. Can one use detectors without the

ability discussed above to demonstrate the non-classical nature of light?

Let us focus on an extreme example – the human eye. Several proposals for demonstrating quantum behaviour using the human eye have been done in the past. Some either use an incorrect model of the human eye [34], or rely on strong assumptions about the measured quantum state [35, 36]. A recent proposal, however, has managed to show how to demonstrate entanglement with the human eyes avoiding assumptions on the state [33], but still requiring a precise description of the functioning of the human eye as a photo detector, which can be hard to achieve in practice.

We find that one can avoid such assumptions as well, and propose a witness of non classicality based on an extension of the autocorrelation function. This witness does not require a detailed description of either the state nor of the measurement apparatus. We end up with a concrete proposal for detecting the non-classical nature of light using simple quantum optics tools, namely spontaneous parametric down conversion (SPDC) sources and displacement operations in phase space.

Paper C

Proposal for witnessing non-classical light with the human eye.

Amaury Dodel, Anthony Mayinda, Enky Oudot, Anthony Martin
Pavel Sekatski, Jean Daniel Bancal, and N. Sangouard

Quantum **1**, 7 (2017).

Proposal for witnessing non-classical light with the human eye

A. Dodel[1], A. Mayinda[1], E. Oudot[1], A. Martin[2], P. Sekatski[3], J.-D. Bancal[1], and N. Sangouard[1]

[1]Department of Physics, University of Basel, Klingelbergstrasse 82, 4056 Basel, Switzerland

[2]Group of Applied Physics, University of Geneva, Ch. de Pinchat 22, 1211 Geneva, Switzerland

[3]Institut for Theoretische Physik, Universitat of Innsbruck, Technikerstraße 25, A-6020 Innsbruck, Austria

April 14, 2017

We give a complete proposal showing how to detect the non-classical nature of photonic states with naked eyes as detectors. The enabling technology is a sub-Poissonian photonic state that is obtained from single photons, displacement operations in phase space and basic non-photon-number-resolving detectors. We present a detailed statistical analysis of our proposal including imperfect photon creation and detection and a realistic model of the human eye. We conclude that a few tens of hours are sufficient to certify non-classical light with the human eye with a p-value of 10%.

1 Introduction & motivations

Efforts have been recently devoted to the realization of quantum experiments with the human eye. This endeavor is however challenging. The proposal of Ref. [1] which uses many entangled photon pairs to realize a Bell test with the eye does not allow one to violate a Bell inequality with a realistic model of the eye. Refs. [2, 3] which propose to amplify entanglement of a photon pair through a phase covariant cloning, can lead to entanglement detection with eye-based detectors provided that strong assumptions are made on the source. While no assumption is needed on the functioning of the eye, it is necessary to assume that the source produces true single photons. From a practical point of view, phase-covariant cloning is also difficult to implement. In particular, cloning is inherently multimode when implemented with a non-linear crystal as suggested in Ref. [2]. The undesired modes can be filtered out but at the price of introducing substantial loss. Ref. [4] provides a technically simpler solution by using displacement operations on single-photon entanglement. This proposal allows one to detect entanglement with the eye without assumption on the source but needs a precise description of the visual system. Indeed, the entanglement witness proposed in Ref. [4] relies on a well-defined model of the eye thus requiring a detailed characterization of the human eye. Importantly, in both Ref. [2] and [4], entanglement is detected before the amplification. That is, these proposals allow one to conclude that few-photon entanglement can be detected by the human eye upgraded by phase-covariant cloning and displacement operations respectively. The question we address in this manuscript is how the quantum nature of light can be *directly* detected with the eye.

The motivations are twofold. First, our proposal is a fascinating attempt to get closer to the quantum world. Indeed, it is conceptually very different from standard quantum optics experiments where measurements are done by photon detectors and the sole role of experimentalists in the measurement process is to analyse the experimental data stored on a computer. The envisioned experiment is unitary until the eye, so if a collapse happens it does not happen before the eye. Second, such an experiment interfaces quantum light and biological systems. Inspired by the great success of quantum optics in revolutionizing communications [5], metrology [6], sensing [7] or computing [8], this experiment of a new kind may flourish with important applications for biomedical research.

As stated before, the proposal of Ref. [4] is appealing as it uses simple ingredients, namely single-photon entanglement and displacement operations. In this manuscript, we derive a witness for non-classical states and we show how the same ingredients allow one to reveal the non-classical nature of a superposition state with the eye. Our witness needs no assumption on the photon number produced by the source or on the precise modelling of the eye. It simply relies on the assumption that the probability to detect light increases with the photon number. While entanglement detection requires measurements in different bases, the experiment that we propose is simpler as it uses displacement operations with fixed amplitudes and phases. It does not need interferometric stabilization of optical paths and is very robust against loss. We show, through a detailed feasibility study including a realistic model of the human eye with a reasonable recovery time as well as imperfect photon creation and detection, that a few tens of hours are sufficient for our witness

to conclude about non-classicality with a p-value of 10%. Our results point towards a concrete proposal for implementing the first experiment where the quantum nature of light is revealed directly with the human eye.

2 Witnessing non-classicality with rudimentary detectors

Coherent states $|\alpha\rangle$ of a harmonic oscillator (or a mode of the electromagnetic field) saturate the uncertainty relations for any pair of quadratures as well as for amplitude and phase [9]. In addition, they are eigenstates of the positive frequency part of the quantized field and vector potential operators [10]. For these reasons, the set of coherent states is thought as the most classical subset of all possible pure states of light. In this context, a state which can be expressed as a mixture of coherent states $|\alpha\rangle$

$$\rho_{\text{class}} = \int \mathrm{d}^2\alpha \; p(\alpha)|\alpha\rangle\langle\alpha|, \text{ with } p(\alpha) \geq 0 \qquad (1)$$

is considered classical, and any state which cannot be decomposed in this way is then non-classical. It is easy to see that the convex combination of coherent states in Eq. (1) satisfies $\frac{\langle \hat{N}^2\rangle - \langle \hat{N}\rangle}{\langle \hat{N}\rangle^2} \geq 1$ with $\hat{N}$ the number operator [11]. Hence, a photon-counting detector can be used to witness the non-classical nature of a light state. If the photon-counting results reveal $\frac{\langle \hat{N}^2\rangle - \langle \hat{N}\rangle}{\langle \hat{N}\rangle^2} < 1$, we can indeed conclude that the measured state is non-classical. Note that all non-classical states lead to entanglement when combined with the vacuum on a beamsplitter [12]. The link with entanglement helps clarifying the notion of non-classical states.

Moreover for few photon states, $\langle \hat{N}^2\rangle - \langle \hat{N}\rangle$ can be approximated by $\sim 2\langle|2\rangle\langle 2|\rangle$ and $\langle \hat{N}\rangle^2$ by $\sim \langle|1\rangle\langle 1|\rangle^2$. Hence, one can use a 50/50 beamsplitter and two non-photon-number-resolving detectors to witness the non-classical nature of few photon states by checking that the two-fold coincidences ($\sim \langle|2\rangle\langle 2|\rangle/2$) are smaller than the product of singles ($\sim \langle|1\rangle\langle 1|\rangle^2/4$), cf. [13] for a proper derivation. Can one still use this criterion in presence of other kinds of detectors? We now address the question of the conditions required to witness the non-classical nature of a light source with a 50/50 beamsplitter and two detectors.

Let us consider an arbitrary detector with a binary outcome, one corresponding to click, the other one to no-click. We label $p_s(\alpha)$ the probability to get a click when a coherent state $|\alpha\rangle$ impinges on such a detector. In a scenario where two of these detectors are placed after a 50/50 beamsplitter, the probability to get a twofold coincidence with any classical state is given by $p_c(\rho_{\text{class}}) = \int \mathrm{d}^2\alpha \; p(\alpha) p_s(\alpha/\sqrt{2})^2$ whereas the probability of a single detection is given by $p_s(\rho_{\text{class}}) = \int \mathrm{d}^2\alpha \; p(\alpha) p_s(\alpha/\sqrt{2})$. This simply comes from the fact that a coherent state splits into two similar coherent states on a beamsplitter $|\alpha\rangle \xrightarrow{\text{BS}} |\frac{\alpha}{\sqrt{2}}\rangle_t \otimes |\frac{\alpha}{\sqrt{2}}\rangle_r$. The Cauchy-Schwarz inequality $\int f(\mu)^2 \mathrm{d}\mu \int g(\mu)^2 \mathrm{d}\mu \geq \left(\int f(\mu) g(\mu) \mathrm{d}\mu\right)^2$ for $f = 1$, $g = p_s(\alpha/\sqrt{2})$ and $\mathrm{d}\mu = p(\alpha)\mathrm{d}^2\alpha$ then implies

$$\frac{p_c(\rho_{\text{class}})}{p_s(\rho_{\text{class}})^2} \geq 1. \qquad (2)$$

In other words, any detector can be used to witness non-classicality as long as one has two copies of this particular detector. It suffices to place these detectors after a 50/50 beamsplitter and to record the number of singles and coincidences. If the ratio between the probability of having a coincidence and the square of the probability of singles is smaller than one, we can safely conclude that the measured state is non-classical. We show in the appendix A that the ratio between the coincidence and the product of singles is a witness for non-classicality even if the two detectors after the beamsplitter are not identical and the beamsplitter is not balanced, as long as $p_s(\alpha)$ is an increasing function of the photon number $|\alpha|^2$ for both detectors. These results are used in the next section to show how to detect non-classical states with the human eye.

3 Witnessing non-classicality with the human eye

Let us start this section by recalling how to model the response of the human eye to weak light stimuli. In a landmark experiment Hecht, Shlaer and Pirenne tested the capability of the human eye to detect light pulses containing only a few photons [14], see also [15]. In their experiment, an observer was presented with a series of multimode thermal light pulses and asked to report when the light is seen. Similar results have been obtained much more recently with coherent light pulses (monomode light also having a Poissonian photon-number distribution) [16], thus indicating that the response of the eye does not depend on the number of modes. Interestingly, the results of both experiments are very well reproduced by a model in which coherent states are sent onto a threshold detector preceded by loss. In particular, the experimental data of Ref. [14] is compatible with a threshold at $\theta = 7$ photons and an efficiency of $\eta_e = 8\%$, see Fig. 1 in Ref. [4]. Note that these numbers depend on the psychophysics, *i.e.* the dark adaptation, the choice of dead-times and methods for eliciting responses from the observer about his experience of light stimuli. In particular, the recent results reported in Ref. [16]

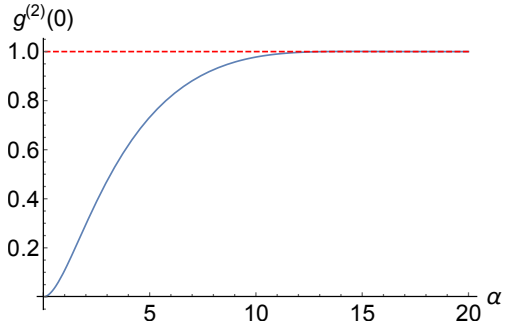

Figure 1: Result of an auto-correlation ($g^{(2)}(0)$) measurement in which two eyes are placed after a 50/50 beamsplitter. The ratio between the probability to see light with both eyes and the square of the probability to see light with one eye is recorded for an input state $\mathcal{D}(\alpha)(|0\rangle + |1\rangle)/\sqrt{2}$, considering real α. We here show this ratio as a function of α. Ratios smaller than one (red dashed line) witness the non-classical nature of the state.

are compatible with lower thresholds and several references [17, 18] suggest higher efficiencies. In the remainder of the paper, we keep the model of the eye with parameters associated to the seminal work of Hecht and co-workers ($\theta = 7$ and $\eta_e = 8\%$). We show that these parameters are conservative, *i.e.* higher efficiencies or lower thresholds reduce the number of experimental runs that are needed to conclude about non-classicality.

Given the witness for non-classical states presented in the previous section, we envision an experiment where two eyes are placed after a beamsplitter. The event "click" corresponds to the case where the observer sees light, "no-click" where no light is seen. The experiment is repeated several times to access the probability to see light with one of the two eyes as well as the joint probability to see light with both eyes. The ratio between the coincidences and the product of singles is then used to reveal non-classicality. This ratio is labelled $g^{(2)}(0)$ in analogy to the standard autocorrelation measurement.

To make a complete proposal, we still need to find a quantum state for which the non-classical nature can be revealed in such a setup. Note that sub-Poissonian states, *i.e.* states for which the distribution in photon-number space is narrower than the one of a coherent state with the same mean photon number, are natural candidates for achieving $g^{(2)}(0) < 1$ with threshold detectors such as the human eye. This is because there is a regime where, for the same probability of singles, the narrow photon-number distribution of a sub-Poissonian state yields a lower coincidence probability than the one of the corresponding coherent state. As an illustration, consider an ideal threshold detector and a Fock state that has enough photons to eventually make one of the detectors click, but not enough to give a coincidence.
While Fock states with large photon numbers are challenging to produce, a sub-Poissonian state can be obtained in practice by displacing a superposition of vacuum and single-photon Fock state in phase space. The resulting state $\mathcal{D}(\alpha)\left|\frac{1}{\sqrt{2}}(0+1)\right\rangle$, where $\mathcal{D}(\alpha)$ stands for a displacement operation, indeed has a variance in photon-number space that is $\frac{1+8|\alpha|^2-4Re(\alpha)^2}{2+4|\alpha|^2+4Re(\alpha)}$ times that of a coherent state with the same mean photon number. This ratio admits values that are below one, and interestingly, for a given strength of the displacement $|\alpha|^2$, it is minimal and always inferior to unity when α is real. Consequently, from here on we will only consider real displacements.

Fig. 1 shows the value of $g^{(2)}(0)$ obtained when sending such a state on a 50/50 beamsplitter followed by two eyes as a function of the amplitude of α. We see that the non-classical nature of $\mathcal{D}(\alpha)\left|\frac{1}{\sqrt{2}}(0+1)\right\rangle$ can be detected with the human eye as long $\alpha \leq 13.3$. For larger α, the two eyes always see light and the ratio between coincidences and singles tends to one. However, in the range of displacement values $\alpha \sim 10$, one can expect non-negligible occurrence frequency for the event "seen" for both eyes. These encouraging estimations compel us to make a detailed feasibility study, *i.e.* to propose a practical way to create a single photon superposed with vacuum, to account for imperfect generation efficiency, channel loss, limited detection efficiencies and to conclude about the statistics that is required to witness non-classicality with the human eye.

4 Proposed experiment

The experiment we envision is shown in Fig. 2. A source based on spontaneous parametric down-conversion is used to create photon pairs, the detection (on detector D_h in Fig. 2) of one photon from a given pair serving to herald the presence of its twin. The latter is then sent into a 50/50 beamsplitter to create path-entanglement, *i.e.* entanglement of the form $(|0\rangle_t|1\rangle_r - |1\rangle_t|0\rangle_r)/\sqrt{2}$ between the transmitted and reflected modes of the beamsplitter which share a single photon. The reflected mode is subsequently detected with a non-photon-number-resolving detector (detector D_g in Fig. 2) preceded by a displacement in phase space $\mathcal{D}(\beta)$. With the appropriate displacement amplitude, such a measurement performs a pretty good measurement along the x direction of the Bloch sphere having $|0\rangle$ and $|1\rangle$ as its north and south pole respectively [19]. In other words, with the appropriate displacement, a detection click projects the transmitted mode into a

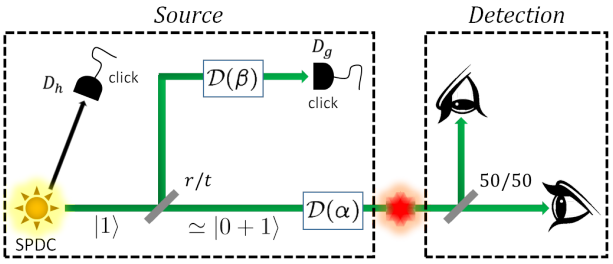

Figure 2: Schematic representation of the experiment envisioned to witness the non-classical nature of a superposition state $\mathcal{D}(\alpha)(|0\rangle_t+|1\rangle_t)/\sqrt{2}$ with the human eye. The superposition $(|0\rangle_t + |1\rangle_t)/\sqrt{2}$ is prepared by first sending a single photon into an unbalanced beamsplitter and by subsequent detection of the reflected mode with a photon detector preceded by a displacement operation. For displacements with a small enough amplitude, this projects the transmitted mode into a state close to the desired superposition. This superposition state is then displaced to produce the non-classical state of interest. A 50/50 beamsplitter and two eyes are then used to analyse this state with a measurement analogous to an auto-correlation measurement.

state close to $(|0\rangle_t + |1\rangle_t)/\sqrt{2}$. Such a state is then displaced in phase space, split using a 50/50 beamsplitter and sent to human observers. The single and coincidence events are recorded and the experiment is repeated until the observers can conclude about the non-classical nature of the superposition state with enough statistical confidence. As it is not clear what psychophysical test would allow to distinguish a dim flash of light occurring in the left vs. the right eye and a temporal discrimination with a single observer would require unrealistic delays, we envision an experiment with two observers, each reporting on whether he/she sees light each time a detection click is obtained on D_g. We show below how to get a triggering rate compatible with a synchronization of the two observers' answers.

Note that in this setup, one can tune the transmission coefficient of the first beamsplitter along with the displacement amplitude β, effectively modifying the input state for the autocorrelation measurement. Finally, we observed that the closest state to $\mathcal{D}(\alpha)\left|\frac{1}{\sqrt{2}}(0+1)\right\rangle$ is obtained by choosing a highly unbalanced beamsplitter with transmission $t \sim 1$ and using a displacement $\mathcal{D}(\beta)$ with almost zero amplitude. In this case, we get a very partially entangled state and maximum coherence of the conditional state $(|0\rangle_t + |1\rangle_t)/\sqrt{2}$ is restored by measuring the reflected mode almost along the z direction and post-selecting the case where a click is obtained. This favors larger fidelities of the conditional state because the measurement noise is reduced when it gets closer to the z direction [19]. However, the probability to get a click drops when the transmission of the beamsplitter increases. There is thus a trade-off between the "quality" of the states produced by the source and the rate at which they are produced. The parameters β and t have to be optimized in view of the statistics needed to witness non-classicality, cf. below.

Several requirements need to be satisfied for implementing the experiment proposed in Fig. 2. (i) The efficient generation of pure, indistinguishable and narrowband single photons is the first one. A straightforward way to create photons with these properties from spontaneous parametric down-conversion is to combine short, Fourier-limited pump pulses with a narrow-band filtering of the heralding photons. This results in Fourier-limited heralded photons with the spectrum of the pump [20]. To ensure a high coupling efficiency of these heralded photons into an optical fiber, a plane wave pump is required and the heralding photons need to be spatially filtered with a single mode fiber before being detected. This projects the heralded photons into the fundamental spatial mode of the fiber, and hence allows one to reach very high coupling efficiencies [21]. (ii) The photons need to have a color that can be seen by the human eye. This can be fulfilled with a pump at 405nm down-converted into non-degenerate photon pairs at 1536 and 550nm. The advantage is threefold. 550nm is very well suited for the human eye and the photons in the telecom band can be efficiently filtered both spatially and in frequency. The telecom mode can also be seeded with a stable cw telecom laser to generate the coherent states that are needed for the displacement operations, cf. below. (iii) The click rate on the detector D_g in Fig. 2 needs to be adapted to the timescale of the response of the human eye as it sets a start for the observers. This can be done by reducing the repetition rate of the pump laser with an optical chopper. The heralding rate on D_h and thus on D_g, can then be easily set by tuning the laser intensity and the duty cycle of the optical chopper, c.f. below. (iv) To implement the displacement operations, we need an unbalanced beamsplitter and coherent pulses with Poissonian photon distribution that are indistinguishable from the photons at 550 nm in all degrees of freedom. This can be done using difference frequency generation. More precisely, we propose to use a second non-linear crystal, identical to the first one and pumped by the same laser but with a narrow seed of the telecom mode. In contrast to spontaneous parametric down-conversion, the seed results in coherent states at 550 nm with the characteristics of the pump laser, *i.e.* Fourier-limited coherent states with the spectrum of the pump [22]. Since the coherent states created in this way and the single photons at 550 nm are generated from the

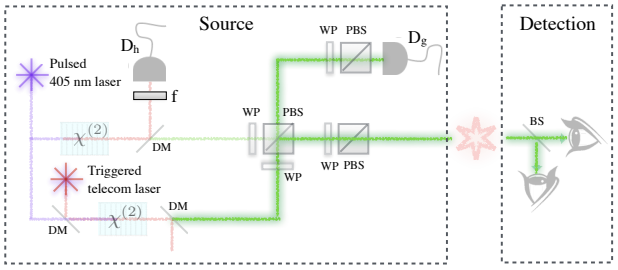

Figure 3: Schematic of the setup to produce superposition states close to $\mathcal{D}(\alpha)(|0\rangle_t + |1\rangle_t)/\sqrt{2}$ and to detect their quantum nature with the human eye. Star: laser, χ^2 : non-linear crystal, DM: dichroic mirror, f: filters, WP: wave-plates, PBS: polarizing beamsplitter, BS: beamsplitter. See text for details.

same pump, their indistinguishability is insensitive to the pump fluctuations. Note also that with a ps pump, the effect of frequency fluctuations of the telecom laser is negligible. The slow fluctuations in intensity of the latter can be recorded and taken into account once the measurements are done. In the worst case, they can be monitored and corrected with a feedback loop. Albeit with different wavelengths, the proposed technique has already been used successfully in various experiments [22, 23].

Concretely, we envision an experiment where a Ti-Sa laser is doubled to create $2-3$ps pulses at 405nm with a repetition rate of 80 MHz, see Fig. 3. These pulses are then used to pump two crystals in order to be down-converted to 1536 and 550nm respectively. The first crystal will be used to create pure single photons at 550nm by picking up a single spatial and frequency mode of the photons at 1536nm with a monomode fiber and a narrowband spectral filter. Coherent states that are indistinguishable from the photons at 550 nm are generated by seeding the second crystal with a pulsed telecom laser. Let us emphasize that the critical point of this experimental implementation is the noise. In standard experiment, the noise is filtered out by analyzing the detection times to discriminate between true and false events. As the response of the human eye is not fast enough for such a temporal discrimination, we need to be sure that a limited number of undesired photons can reach the eye of the observer. First, we propose to decrease the repetition rate of the pump laser to 1.6 MHz using an optical chopper with a duty cycle of 0.02. By tuning the pump intensity to get a pair emission probability of 0.8×10^{-3} and considering a global detection efficiency of 0.08 for D_h (*i.e.* a coupling efficiency of 0.8, a filter transmission of 0.4 and a raw detection efficiency of 0.25), we get a heralding rate on D_h of ~ 100 Hz. Moreover, we consider a coupling efficiency of the heralded photon at 550nm of $\eta_c = 0.8$ in agreement with the experimental results reported e.g. in Ref. [21]. The detection efficiency of the visible detector in the upper arm of Fig. 2 is assumed to be $\eta_d = 0.5$ which is realistic even when including the transmission loss from the source to the detector and the inefficiencies of linear optical elements. We neglect mismatches in the indistinguishability of the photons and coherent states at 550nm, which is well justified given the results of Ref. [22] where the visibility of the Hong-Ou-Mandel interference between a single photon and a coherent state created via identical crystals as described before was only limited by the statistics of the coherent state. We set the transmission $t = 98\%$ which, together with the value of the displacement $\beta \sim 0.08$ chosen to minimize the total number of experimental runs (cf. below), ensures that 1% of the heralds on D_h lead to a click on D_g. Meanwhile the conditional state generated on the lower arm shows a near maximal 95% fidelity with respect to $\mathcal{D}(\alpha)\,|\frac{1}{\sqrt{2}}(0+1)\rangle$.

The dominant noise in this scenario comes from the coherent states that are used for the displacement operations. We propose to trigger the seed that is used to generate these coherent states on detections in D_h. In this case, the noise is ~ 100 times greater than the signal. To reduce it further, a pulse picker is placed in front of the eyes which is triggered by detections on D_g. Considering an extinction ratio of 1:2000, we get a signal-to-noise ratio of ~ 20, which should be more than enough to perform the proposed measurement. Note that the pulse picker also filters out other sources of noise, including the spontaneous emission of the crystal used to generate single photons at 550 nm (that is negligible with respect to the noise due to coherent states). Note also that ~ 100ns are needed to trigger the pulse picker on detections by D_g, which requires a delay line of 20m of fiber, representing negligible loss for typical attenuation < 12dB/km at 550nm.

5 Statistics

To conclude the feasibility analysis of the proposed experiment, we now turn to the question of statistics, and determine the number of runs needed to exclude the possibility that the observed finite statistics are the result of measurements on a classical state. This is a particularly relevant question in our case, as the repetition rates that can be attained with the human eye are much lower than the slowest commercial detectors. The statistical study that we describe in this section aims at estimating the time-resource that an experimenter would have to allocate to such an experiment for the efficiencies discussed in the previous section, depending on the accuracy he wants to achieve.

The statistical issue is essentially an estimation of the odds of having $g^{(2)}(0) < 1$ from a classical photon-

number distribution. To answer this we consider the multinomial joint probability

$$P(N_s, N_c) = p_c^{N_c}(p_s - p_c)^{N_s - N_c}(1 - p_s)^{N - N_s} \times \binom{N}{N_c, N_s - N_c, N - N_s} \quad (3)$$

of obtaining N_s singles and N_c coincidences out of N experimental runs, from the knowledge of the single and coincidence probabilities in one round $\{p_s, p_c\}$. Note that we assume here that the single probability on each eye is identical, and that the runs are independently and identically distributed (i.i.d.). Further note that the form of the above distribution, whose natural variables are N_c and $N_s - N_c$, stresses the dependence of the events "single" and "coincidence". Indeed we have defined a single in one arm regardless of the situation in the other arm, hence a coincidence is counted as a single as well. The outcome "single only" has an occurrence probability $p_s - p_c$ as can be seen in the multinomial expression. Both the quantum scenario presented before, with $\{p_s(\rho_\mathrm{q}), p_c(\rho_\mathrm{q})\}$ depending on the non-classical state ρ_q, and the classical one with $\{p_s(\rho_\mathrm{c}), p_c(\rho_\mathrm{c})\}$ such that $p_c(\rho_\mathrm{c}) \geq p_s^2(\rho_\mathrm{c})$ give rise to a probability distribution that we label respectively by $P^q(N_s, N_c)$ and $P^c(N_s, N_c)$.

We then choose an estimator χ which is a function of the total number of singles N_s and coincidences N_c observed in N rounds of the experiment, cf. below. For a given N, this estimator takes the value $\chi(N_s, N_c)$ with probabilities $P^q(N_s, N_c)$ and $P^c(N_s, N_c)$ in the quantum and classical scenarios. The probability of observing a value of χ smaller than a given value χ_0 in the quantum (classical) case after N rounds is thus given by

$$P(\chi^{q/c} \leq \chi_0) = \sum_{N_s, N_c | \chi(N_s, N_c) \leq \chi_0} P^{q/c}(N_s, N_c). \quad (4)$$

On one side, the quantum distribution tells us what is the probability with which we can expect to observe (in a quantum experiment) a value of χ smaller or equal to some value χ_0. We write this probability

$$P_\mathrm{stop} = P(\chi^q \leq \chi_0). \quad (5)$$

On the other side, the classical distribution allows us to define the p-value ϵ associated with the rejection of the null hypothesis "the state is classical" once a value χ_0 is observed. This p-value is given by

$$\epsilon = \max_{p_c \geq p_s^2} P(\chi^c \leq \chi_0) \quad (6)$$

where the maximum is taken over all classical scenarios satisfying $p_c(\rho_\mathrm{c}) \geq p_s^2(\rho_\mathrm{c})$. Alternatively, we can read the relation (6) as a definition of the critical value of the estimator χ_0 which needs to be obtained in order to rule out all classical states with a confidence of $1 - \epsilon$. Choosing first the p-value, Eq. (6) gives χ_0 which can then be used to get the probability to stop at the N^{th} run using Eq. (5). The average number of runs that is needed to rule out classical states can finally be estimated as (cf. Appendix B)

$$\langle N \rangle \simeq \sum_{j \geq 0} \frac{n(2j+1)}{2} \left(P_\mathrm{stop}(n(j+1)) - P_\mathrm{stop}(nj) \right) \quad (7)$$

where n is a coarse-graining parameter used to make the computation faster.

The question at this stage is what is a good choice for the estimator. Let us consider the space of frequencies defined by $(f_s^2, f_c) \equiv \left(\left(\frac{N_s}{N}\right)^2, \frac{N_c}{N} \right)$. We choose a set of coordinates $\{x, y\}$ to cancel the covariance and to equal the variances of $P^q(N_s, N_c)$ in the x and y directions at first order in $\frac{1}{N}$. This is achieved by setting

$$\begin{cases} x = \sqrt{\frac{c}{b}} f_s^2 + \frac{d}{\sqrt{cb}} f_c \\ y = \sqrt{\frac{b}{c}} f_c \end{cases} \quad (8)$$

with

$$\begin{cases} b = \sqrt{\frac{(1-p_c(\rho_\mathrm{q}))p_s(\rho_\mathrm{q})}{(1-p_s(\rho_\mathrm{q}))p_c(\rho_\mathrm{q})}} - 1 \\ c = \frac{1-p_c(\rho_\mathrm{q})}{2p_s(\rho_\mathrm{q})(1-p_s(\rho_\mathrm{q}))} \\ d = -1 \end{cases} .$$

The projection of $P^q(N_s, N_c)$ in the $x-y$ plane hence defines circular isolines, cf. Fig. 4 red isolines. The dashed black line in Fig. 4 distinguishes the frequencies coming from classical and non-classical states. In particular, the distributions with mean values lying on this boundary come from states with $p_c(\rho_\mathrm{c}) = p_s^2(\rho_\mathrm{c})$, *i.e.* coherent states with various p_s. The classical scenario that best reproduce the quantum statistics is quite clearly a coherent state which minimizes the Euclidean distance to the quantum distribution, *i.e.* centered on the orthogonal projection of the quantum distribution onto the dashed black line of Fig. 4. Such a coherent states is associated with

$$p_s(\rho_\mathrm{c}) = \sqrt{\frac{c(c+d)p_s(\rho_\mathrm{q})^2 + (d(c+d) + b^2)p_c(\rho_\mathrm{q})}{b^2 + (c+d)^2}}. \quad (9)$$

Calling (x_0', y_0') the center of the corresponding distribution $P^c(N_s, N_c)$, an estimator of the form

$$\chi = y' - y_0' + a(x' - x_0')^2, \quad (10)$$

where $x' = \cos(\phi)\, x + \sin(\phi)\, y$, $y' = \cos(\phi)\, y - \sin(\phi)\, x$ and $\phi = \arccos \frac{c+d}{\sqrt{b^2+(c+d)^2}}$ is intuitively minimized by the coherent state satisfying (9) for appropriate a, as ϕ is such that the axis of the parabola is orthogonal to the classical/non-classical boundary.

The probability that enough statistics is obtained after N runs to exclude the classical distribution

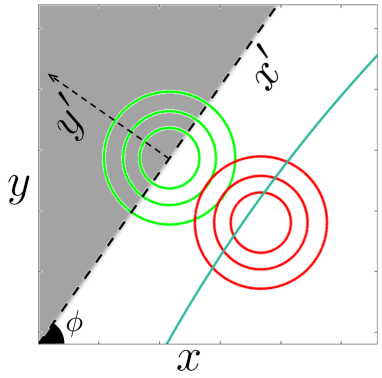

Figure 4: Projections in the modified frequency plane $\{x, y\}$ defined in Eq. (8) of the probability distributions $P^q(N_s, N_c)$ for the quantum scenario presented in Fig. 2 (red isolines) and $P^c(N_s, N_c)$ for the coherent state defined in (9) (green isoline). The blueish contour line is the estimator given in Eq. (10). The dashed black line separates the mean values of quantum and classical states as witnessed by a $g^{(2)}(0)$ measurement. In particular, the shaded area includes all states with $g^{(2)}(0) \geq 1$.

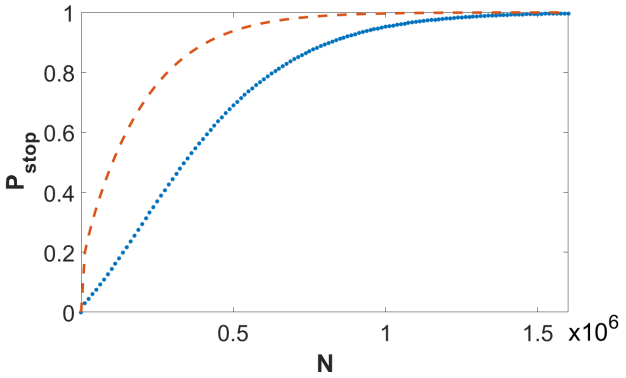

Figure 5: Probability to get enough statistics to conclude about non-classicality as a function of the number of runs N for a p-value of 1% (blue dotted line) and 10% (red dashed line).

$P^c(N_s, N_c)$ with the estimator given in Eq. (10) can be computed numerically as a function of the steepness of the parabola a and the amplitude of displacement operations α, β. After checking that the considered classical strategy is indeed optimal for the estimator (10), we obtained the optimal values $a = 40$ and $(\alpha, \beta) \simeq (10.99, 0.08)$ for the efficiencies discussed in the previous section and the model of the eye matching the data of Hecht and co-workers ($\theta = 7, \eta_e = 8\%$). The results are shown in Fig. 5 for p-values of 1% and 10%. We see for example that after 350000 runs, we have more than 50% chance of being able to rule out classical states with a confidence of $1-\epsilon = 99\%$. For $n = 12500$, we find $\langle N \rangle \simeq 402964$ for a confidence of 99%. Note that to perform 403000 runs with a repetition rate of 1Hz takes about 112 hours. The latter provides an upper bound on the timescale of the proposed experiment to get a p-value of 1%. A similar analysis for a p-value of 10% shows that 46 hours are likely to be enough to detect the non-classical nature of a single photon superposed with vacuum using the human eye. This goes down to 35 hours when considering a threshold at 3 photons while keeping 8% efficiency and to 29 hours for an efficiency of 10% and a threshold at 7 photons.

6 Conclusion

We have presented a concrete proposal for a quantum experiment with the human eye, including the full analysis of the measurement statistics. It uses simple components, namely path-entanglement, displacement operations in phase space and non-photon-number-resolving detectors, to certify with naked eyes the non-classical nature of a state of light. We have given a detailed recipe using parametric conversions and photon-counting techniques only, *i.e.* commercially available devices working at room temperature that are routinely used in practice. We have shown that the statistics obtained in a few tens of hours would be sufficient to certify non-classicality with a p-value of 10%. This was obtained with realistic models of the human eye and taking loss and non-unit efficiencies of photon detectors into account. We believe that these timescales are well within reach in practice primarily because the data do not need to be taken in a row. Following in particular the implementation proposed in Fig. 3 where a single photon and a coherent state with different polarizations impinge on a polarizing beamsplitter to follow the same optical path and where a set of wave plates and a polarizing beamsplitter are used to make the displacement operations, we can certify from our past experiment [23] that the setup is extremely stable even without active stabilization of relative path-length fluctuations. It is thus very likely that the data acquisition can be stopped and started again later for several tens of hours without problem. Despite many preconceptions, we expect the response of the eye to be consistent over long minutes after appropriate dark adaptation. Slow threshold or efficiency drifts can be taken into account easily by periodic re-calibration of the amplitude of displacement operations. We thus see our work as a concrete and realistic proposal to realize the first experiment where the non-classical nature of light is detected directly with the human eye.

7 Acknowledgements

We thank V. Caprara-Vivoli, M. Munsch, Botond Roska, Hendrik Scholl and R. Warburton for valuable discussions. This work was supported by the Swiss National Science Foundation (SNSF), through the NCCR QSIT and the Grant number PP00P2-150579, the John Templeton foundation and the Austrian Science Fund (FWF), Grant number J3462 and P24273-N16.

8 Appendices

8.1 Autocorrelation with different arbitrary detectors

Let us recall the definition of a classical state as given in the main text: $\rho_{cl} = \int \mathrm{d}^2\alpha\ p(\alpha)|\alpha\rangle\langle\alpha|$ with $p(\alpha) \geq 0$. We now relax the constraint on the symmetry between the two arms in the autocorrelation measurement, and label $(1, 2)$ respectively the reflected and transmitted beams. Each of those beams is sent to a detector which can be different from the other one and the beamsplitter prior to detection is allowed to be unbalanced with coefficients r/t. Using the transformation rules for a coherent state on a beamsplitter, it is straightforward to express the probabilities of interest as an integral of the probabilities of singles for appropriate coherent states

$$\begin{aligned}
P_{s_1}(\rho_{cl}) &= \int p(\alpha) P_{s_1}\left(\sqrt{r}\alpha\right) \mathrm{d}^2\alpha \\
P_{s_2}(\rho_{cl}) &= \int p(\alpha) P_{s_2}\left(\sqrt{t}\alpha\right) \mathrm{d}^2\alpha \\
P_c(\rho_{cl}) &= \int p(\alpha) P_{s_1}\left(\sqrt{r}\alpha\right) P_{s_2}\left(\sqrt{t}\alpha\right) \mathrm{d}^2\alpha.
\end{aligned}$$

Instead of the autocorrelation which is a ratio of two quantities, we focus on the difference

$$\begin{aligned}
D(\rho_{cl}) &= P_c(\rho_{cl}) - P_{s_1}(\rho_{cl}) P_{s_2}(\rho_{cl}) \\
&= \int p(\alpha) P_{s_1}\left(\sqrt{r}\alpha\right) P_{s_2}\left(\sqrt{t}\alpha\right) \mathrm{d}^2\alpha \\
&\quad - \int p(\alpha) P_{s_1}\left(\sqrt{r}\alpha\right) \mathrm{d}^2\alpha \int p(\alpha) P_{s_2}\left(\sqrt{t}\alpha\right) \mathrm{d}^2\alpha,
\end{aligned}$$

Note that $D < 0$ implies $g^{(2)}(0) < 1$. Upon inserting $\int p(\beta)\mathrm{d}^2\beta = 1$ in $P_c(\rho_{cl})$ and relabelling the dummy variable $\alpha \leftrightarrow \beta$ in some of the terms we get

$$\begin{aligned}
D(\rho_{cl}) &= \frac{1}{2} \int \mathrm{d}^2\alpha\ p(\alpha) \int \mathrm{d}^2\beta\ p(\beta) \\
&\left(P_{s_1}\left(\sqrt{r}\alpha\right) - P_{s_1}\left(\sqrt{r}\beta\right)\right)\left(P_{s_2}\left(\sqrt{t}\alpha\right) - P_{s_2}\left(\sqrt{t}\beta\right)\right)
\end{aligned}$$

We thus obtain that if the functions $P_{s_{1/2}}(\alpha)$ are increasing with $|\alpha|^2$, then $D(\rho_{cl}) \geq 0 \Leftrightarrow g^{(2)}(0)_{\rho_{cl}} \geq 1$, which entails the validity of our witness even in the non-symmetrical case.

8.2 On the estimation of the average number of runs

We introduce a formalism to deal with the issue of finding a proper probability distribution for the number of runs. We write the sequence of measurements as a list of zeros and ones, binary stochastic results corresponding respectively to $\chi_{mes} > \chi_0(N)$ and $\chi_{mes} \leq \chi_0(N)$. It illustrates the situation where an experimenter computes χ after each measurement (or alternatively after each set of m measurements) and decides if he carries on with the measures ("0") or stops because the results are already satisfactory ("1"). Ideally what we would like to have is the probability $P(n) = P(\underbrace{0, 0, ..., 1}_{n})$ to reach the required statistics after exactly n runs. Unfortunately, obtaining this "true" probability numerically represents a computational challenge. What we output from our simulation $P_{\mathrm{stop}}(N)$ is the probability to get a one at N^{th} position regardless of the preceding sequence. Let's compare the "cumulative distributions"

$$\begin{aligned}
\sum_{n\leq N} P(n) &= P(1) + P(0,1) + ... + P(\underbrace{0, ..., 0}_{N-1}, 1) \\
P(1) &= \sum_{i_2,...,i_N} P(1, i_2, ..., i_N) \quad \text{where } i_k \in \{0, 1\} \\
&= P_{\mathrm{stop}}(N) - \sum_{i_2,...,i_{N-1}} P(0, i_2, ..., i_{N-1}, 1) \\
&\quad + \sum_{i_2,...,i_{N-1}} P(1, i_2, ..., i_{N-1}, 0)
\end{aligned}$$

$$\begin{aligned}
&P(0,1) - \sum_{i_2,...,i_{N-1}} P(0, i_2, ..., i_{N-1}, 1) \\
&= - \sum_{i_3,...,i_{N-1}} P(0, 0, i_3, ..., i_{N-1}, 1) \\
&\quad + \sum_{i_3,...,i_{N-1}} P(0, 1, i_3, ..., i_{N-1}, 0)
\end{aligned}$$

$$\vdots$$

$$\sum_{n\leq N} P(n) = P_{\mathrm{stop}}(N) + \sum_{n=0}^{N-2} P(\underbrace{0, ..., 0}_{n}, 1, i_{n+2}, ..., i_{N-1}, 0).$$

Therefore $P_{\mathrm{stop}}(N) \leq \sum_{n\leq N} P(n)$. We would like to translate it into an information on the expectation values. Let us switch to a continuous viewpoint and introduce functions f and g standing for the cumulative distributions, with $\forall x\ g(x) < f(x)$ (thus g and f replace the P_{stop} and $\sum_{n\leq N} P(n)$ of the previous paragraph). We write the expectation values differ-

ence and integrate by part

$$\int_0^M xf'(x)\mathrm{d}x - \int_0^M xg'(x)\mathrm{d}x = M[f(M) - g(M)] - \int_0^M \underbrace{(f(x) - g(x))}_{>0}\mathrm{d}x.$$

We need to know how the first term behaves when $M \to \infty$. We haven't find a rigorous way to prove that it vanishes but we notice $M[f(M) - g(M)] < M[1 - g(M)]$, which we reasonably assume stays finite based upon the numerical simulations. The latter indeed reveals that $N \longmapsto N\,(1 - P_{\text{stop}}(N))$ shows a decreasing tendency after a given N. From this we deduce $\langle N\rangle \leq \sum_n n\frac{\mathrm{d}P_{\text{stop}}}{\mathrm{d}n}$.

References

[1] N. Brunner, C. Branciard, and N. Gisin, Phys. Rev. A **78**, 052110 (2008)

[2] P. Sekatski, N. Brunner, C. Branciard, N. Gisin and C. Simon, Phys. Rev. Lett. **103**, 113601 (2009)

[3] P. Sekatski, B. Sanguinetti, E. Pomarico, N. Gisin, and C. Simon, Phys. Rev. A **82**, 053814 (2010)

[4] V. Caprara Vivoli, P. Sekatski, and N. Sangouard, Optica **5**, 473 (2016)

[5] N. Gisin and R. Thew, Nature Photonics **1**, 165 (2007)

[6] V. Giovannetti, S. Lloyd, and L. Maccone, Nature Photonics **5**, 222 (2011)

[7] C.L. Degen, F. Reinhard, and P. Cappellaro, arXiv:1611.02427

[8] T.D. Ladd, F. Jelezko, R. Laflamme, Y. Nakamura, C. Monroe, and J. O'Brien, Nature **464**, 45 (2010)

[9] D. F. Walls, G. J. Milburn, *Quantum optics*, Springer Science & Business Media (2007)

[10] R. J. Glauber, Phys. Rev. **131**, 2766 (1963)

[11] Recall that any state admits such a representation, however $p(\alpha)$ might not be positive, and hence not a probability distribution.

[12] J.K. Asboth, J. Calsamiglia, and H. Ritsch, Phys. Rev. Lett. **94**, 173602 (2005)

[13] P. Sekatski, N. Sangouard, F. Bussières, C. Clausen, N. Gisin and H. Zbinden, J. Phys. B: At. Mol. Opt. Phys. **45**, 124016 (2012)

[14] S. Hecht, S. Shlaer, and M. Pirenne, J. Gen. Physiol. **25**, 819 (1942)

[15] F. Rieke and D.A. Baylor, Rev. Mod. Phys. **70**, 1027 (1998)

[16] J.N. Tinsley, M.I. Molodtsov, R. Prevedel, D. Wartmann, J. Espigulé-Pons, M. Lauwers and A. Vaziri, Nature Comm. **7**, 12172 (2016)

[17] K. Donner, Vision Res. **32**, 853 (1992)

[18] G.D. Field, A.P. Sampath and F. Rieke, Ann. Rev. Physiol. **67**, 491 (2005)

[19] V. Caprara Vivoli, P. Sekatski, J.-D. Bancal, C.C.W. Lim, A. Martin, R. T. Thew, H. Zbinden, N. Gisin and N. Sangouard, New J. Phys. **17**, 023023 (2015)

[20] A. B. U'Ren, C. Silberhorn, R. Erdmann, K. Banaszek, W. P. Grice, I. A. Walmsley, and M. G. Raymer, Las. Phys. **15**, 146 (2005)

[21] T. Guerreiro, A. Martin, B. Sanguinetti, N. Bruno, H. Zbinden, and R. T. Thew, Optics express **21**, 27641 (2013)

[22] N. Bruno, A. Martin, P. Sekatski, N. Sangouard, R. Thew and N. Gisin, Nature Physics **9**, 545 (2013)

[23] F. Monteiro, V. Caprara Vivoli, T. Guerreiro, A. Martin, J.-D. Bancal, H. Zbinden, R.T. Thew and N. Sangouard, Phys. Rev. Lett. **114**, 170504 (2015)

CHAPTER 4

GENUINE ENTANGLEMENT IN MULTI-PARTITE PHOTONIC SYSTEMS

Entanglement between several optical paths sharing a single photon, often called path-entanglement, is one of the simplest forms of entanglement to produce. Indeed, simply sending a single photon on a beam splitter creates such entanglement.

Interestingly, path-entanglement is also an appealing resource for long-distance quantum communication. Photon loss increases exponentially with the distance and quantum communications thus requires the use of quantum repeater architectures for distributing bi-partite entanglement efficiently in the presence of loss. They require the creation and storage of entanglement in small-distance links and subsequent entanglement swapping operations between the links. Quantum repeater architectures with path-entangled states are less sensitive to memory and detector efficiencies compared to architecture based on standard polarisation entanglement [37]. Following these ideas, much work has been done in order to distribute, store and purify path-entangled states [38, 39, 40, 41, 42, 43, 44].

Recently, theoretical efforts have been devoted to the extension of quantum repeaters to 2D networks, where multi-partite entanglement can be distributed between arbitrary nodes and used for advanced communication protocols [45]. It has been suggested that single photon path-entangled states could be useful for implementing these 2D networks [47], as multi-partite entanglement can easily be generated with a single photon incident on a multiport coupler. Several witnesses

of genuine entanglement have been proposed for characterizing multiple path entangled states but they are either not robust against losses or require different settings for each party, hence making the implementation complicated.

We thus propose a witness of genuine entanglement which is robust against losses and only uses collective observables. This witness only requires simple operations, which are displacement operations with the same settings for each path, and single photon counters which can even be lossy. We show that an initial proof of principle aiming to demonstrate genuine entanglement across multiple paths could be performed with a single CCD camera.

In this chapter, we describe the work done towards the demonstration of genuine entanglement in a photonic W state. This represents ongoing work with an experiment to be performed.

We show in Fig. 4.1 a schematic of our proposal. An SPDC source is used to create single photons which are distributed through many paths. In the case of a evenly distributed perfect single photon the resulting state is a W state, written as

$$|W_N\rangle = \frac{1}{\sqrt{N}}(|10.....0\rangle + |01.....0\rangle + ... + |00.....01\rangle) \tag{4.1}$$

where N is the number of paths. We first consider that each path contains at most one photon. We then go beyond this restriction and take into account the possibility of having an arbitrary photon number for each path.

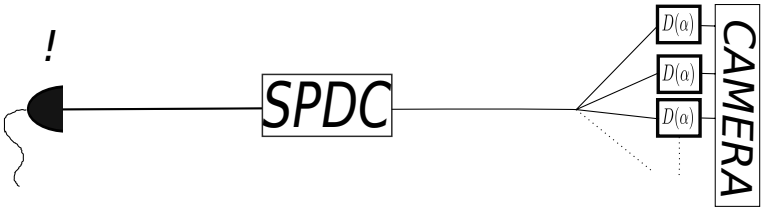

Figure 4.1: Schematic representation of the envisioned experiment. A heralded SPDC source produces almost single photons which are sent to different paths and then measured by a displacement operation and a single photon detector, which corresponds to one pixel of the camera in this case.

4.1 Witnessing entanglement for qubits

We focus on the scenario shown in Fig. 4.1. We restrict ourselves to collective measurements $\hat{J}_\alpha$

$$\hat{J}_\alpha = \frac{1}{2}\sum_{i=1}^{N} \sigma_\alpha^{(i)}, \tag{4.2}$$

where the $\sigma_\alpha^{(i)}$ are realized on mode i with single photon detectors (non photon number resolving detectors) and small displacement operations $D(\alpha) = e^{\alpha a_i^\dagger + \alpha^* a_i}$ and they thus take the form

$$\sigma_\alpha^{(i)} = D(\alpha)^\dagger (2\,|0\rangle\langle 0| - \mathbf{1}) D(\alpha) \tag{4.3}$$

if one assigns the outcomes +1 when the detector does not click and -1 if it clicks. These measurements correspond to perfect σ_z measurements when $\alpha = 0$ and noisy Pauli measurement for $\alpha \neq 0$ [48]. We first consider that the measured state

lives in a qubit space for each mode and use the notation $\rho_{\cap_i n_i \leq 1}$. We consider the following operator

$$\bar{\mathcal{W}}_{\mathcal{N}} = \left(\hat{J}_0 - \left(\frac{N}{2} - 1 \right) \right)^2 - \hat{J}^2 \tag{4.4}$$

where $\hat{J}^2 = \hat{J}_\alpha^2 + \hat{J}_{i\alpha}^2 + \hat{J}_0^2$. A state which is close to the $|W_N\rangle$ state will achieve a minimum value for $\langle \bar{\mathcal{W}}_{\mathcal{N}} \rangle$. In order to make this witness suitable for experiments, we consider the case where the phase of the displacement is random between two runs but well controlled between each of the modes. The corresponding witness is then

$$\mathcal{W}_{\mathcal{N}} = \prod_i^N e^{i\phi a_i^\dagger a_i} \bar{\mathcal{W}}_{\mathcal{N}} \prod_i^N e^{-i\phi_i a_i^\dagger a_i} \tag{4.5}$$

where one takes the average over ϕ. We thus look for the minimum expectation value $w_{PPT} = \int \frac{1}{2\pi} d\phi \langle \mathcal{W}_{\mathcal{N}} \rangle$ which a bi-separable state with respect to the PPT criteria can achieve. At this point, this witness gives us bounds which are not robust against losses, since a bi-separable state can achieve an overlap of $1 - \frac{1}{N}$ with the state $|W_N\rangle$. In such an experiment, however one can also access the probability to get one photon in each mode $1 - P_0$. The knowledge of this probability allows us to derive bounds which are much more robust against losses. The precise knowledge of this probability will then be a crucial point in order to determine the bi-separable bounds of $\mathcal{W}_{\mathcal{N}}$. In order to compute the separable bound of $\mathcal{W}_{\mathcal{N}}$ that we call w_{PPT} , we run the following semi definite program (SDP)

$$\begin{aligned} w_{PPT} = \min_{\rho_{\cap_i n_i \leq 1}} & \int \frac{1}{2\pi} d\phi \mathrm{Tr}(\mathcal{W}_{\mathcal{N}} \rho_{\cap_i n_i \leq 1}) \\ & s.t \\ & \rho_{\cap_i n_i \leq 1} \geq 0 \\ & \mathrm{Tr}(\rho_{\cap_i n_i \leq 1}) = 1 \\ & \rho_{\cap_i n_i \leq 1}^{T_i} \geq 0 \\ & \mathrm{Tr}(\rho_{\cap_i n_i \leq 1} |0\rangle \langle 0|) = P_0. \end{aligned}$$

The 2 first conditions ensure that $\rho_{\cap_i n_i \leq 1}$ is a physical state, the third one ensures that $\rho_{\cap_i n_i \leq 1}$ has a positive partial transpose with respect to all bipartitions and the last one comes from the knowledge of P_0. Note that in order to speed up our computation we apply the randomisation of the phase on ρ, which is the variable in the above program. We next want to compare this bound to the expectation

value achieved by a physically relevant state and thus consider the target state

$$\rho_T = \eta \left|W_N\right\rangle \left\langle W_N\right| + (1-\eta) \left|0\right\rangle \left\langle 0\right| \tag{4.6}$$

which corresponds to a W state experiencing some losses. We define $w_N = \mathrm{Tr}(\mathcal{W}_N \rho_T)$. If $w_N < w_{PPT}$ then one can conclude about genuine entanglement. We then perform a minimization of $w_N - w_{PPT}$ over the setting α in order to find the violation of our witness for the target state ρ_T. We plot in Fig. 4.2 $w_N - w_{PPT}$ with respect to the efficiency for different path number N. Note that at this stage, our witness can already be used to witness genuine entanglement for a spin W state and is very robust against losses.

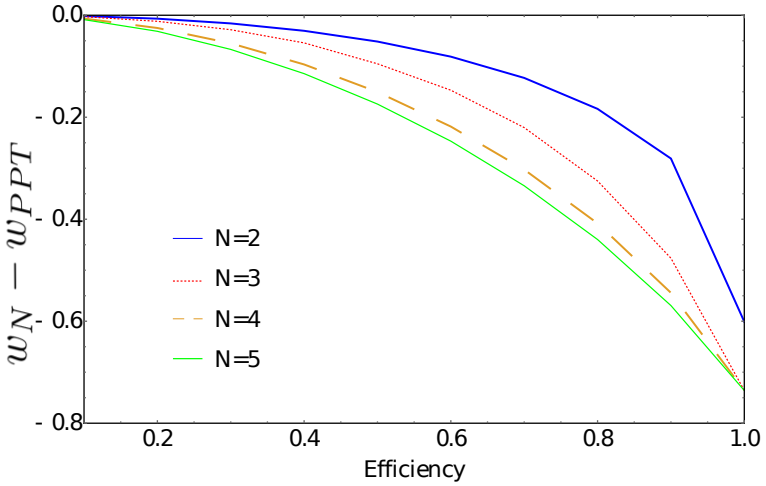

Figure 4.2: $w_N - w_{PPT}$ with respect to the efficiency for a W state experiencing losses .

4.2 Witnessing entanglement for arbitrary dimensions

Let us now generalize our analysis to include the case where each subsystem is no longer restricted to qubits. We have shown how one can compute the maximum expectation value of the operator $\mathcal{W}_N$ over all biseparable states which reside in a N qubit space. We now want a bound for the part of the state which lives outside of the N qubit space. This eventually depends on the probability to be outside this space. In the present case, the probability to have strictly more than one photon in a given mode is called P_2. One can always write $\mathcal{W}_N$ as

$\mathcal{W}_\mathcal{N} = \begin{pmatrix} A & B \\ B^\dagger & C \end{pmatrix}$, where A refers to an observable in the N qubit space, C represents the part outside the qubit space and B the coherence between this two spaces. The same description holds for an arbitrary density matrix ρ, $\rho = \begin{pmatrix} \rho_{\cap_i n_i \leq 1} & b \\ b^\dagger & c \end{pmatrix}$. The parts are now arranged such that

$$\mathrm{Tr}(\rho \mathcal{W}_\mathcal{N}) = \mathrm{Tr}(\rho_{\cap_i n_i \leq 1} A) + \mathrm{Tr}\left(b^\dagger B + b B^\dagger\right) + \mathrm{Tr}(cC)\,. \tag{4.7}$$

We want to find the minimum expectation value of $\mathcal{W}_\mathcal{N}$ that a biseparable state can achieve. Since we are interested in the case where P_2 is small, the elements inside b and c are small. We thus bound the terms $\mathrm{Tr}\left(b^\dagger B + b B^\dagger\right)$ and $\mathrm{Tr}(cC)$ by computing their minimum contribution on all possible quantum states. A bound on the last term is simply given by

$$\mathrm{Tr}(cC) \geq \lambda_{min} P_2 \tag{4.8}$$

where λ_{min} is the minimum eigenvalue of $\mathcal{W}_\mathcal{N}$. The derivation of the bound for the second terms is detailed in Appendix A, and give us

$$\mathrm{Tr}\left(b^\dagger B + b B^\dagger\right) \geq -\sqrt{P_2(1-P_2)}|b_{max}| \tag{4.9}$$

where b_{max} denotes the highest singular value of B. We end up with

$$\mathrm{Tr}(\rho \mathcal{W}_\mathcal{N}) \geq \mathrm{Tr}(\rho_{\cap_i n_i \leq 1} A) - 2\sqrt{P_2(1-P_2)}|b_{max}| + \lambda_{min} P_2. \tag{4.10}$$

We computed on the previous section the minimum value that $\mathrm{Tr}(\rho_{\cap_i n_i \leq 1} A)$ can take when $\rho_{\cap_i n_i \leq 1}$ is a bi-separable state: w_{PPT}. If ρ is bi-separable in the qubit subspace, it thus has to follow

$$\mathrm{Tr}(\rho \mathcal{W}_\mathcal{N}) \geq w_{PPT} - 2\sqrt{P_2(1-P_2)}|b_{max}| + \lambda_{min} P_2 \tag{4.11}$$

which is a witness of genuine entanglement without assumption on Hilbert space of the tested state.

4.3 Proposed setup

We now present a physical model for the setup of Fig. 4.1. First we consider a SPDC source generating a two mode squeezed vacuum state, and where a single

photon detector with efficiency $1 - R_h^2$ is used in order to herald a photon in a first mode. Conditioned on a click on the heralding detector, the state before the beam splitter is given by [48]

$$\rho_h = \frac{1 - R_h^2 T_g^2}{T_g^2(1 - R_h^2)}(\rho_{th}(\bar{n} = \frac{R_h^2 T_g^2}{1 - T_g^2}) - \frac{1 - T_g^2}{1 - R_h^2 T_g^2}\rho_{th}(\bar{n} = \frac{R_h^2 T_g^2}{1 - R - h^2 T - g^2})) \tag{4.12}$$

where ρ_{th} is a thermal state with mean photon number $\bar{n}$, $T_g = \tanh(g)$ where g is the squeezing parameter. A thermal state can be written in a coherent state basis

$$\rho_{th} = \int d^2\alpha P(\bar{n}, \alpha) \left|\alpha\right\rangle \left\langle\alpha\right| \tag{4.13}$$

where $P(\bar{n}, \alpha) = \frac{1}{\pi\bar{n}} e^{-\frac{|\alpha|^2}{\bar{n}}}$. We thus only have to consider operations on coherent states and perform the integration (4.13) afterwards. The splitting operation can be modelling by a N mode beam splitter with equal probabilities for each mode. The action of such a beam splitter on a coherent state is trivial and leads to $U_{BS}(N) \left|\alpha\right\rangle = \underbrace{|\frac{\alpha}{\sqrt{N}}\rangle ... |\frac{\alpha}{\sqrt{N}}\rangle}_{N\text{times}}$. The last step is to compute the expectation value of $\hat{J}_\alpha$ and $\hat{J}_\alpha^2$ in order to compute the value of the witness. This gives

$$\hat{J}_\alpha^2 = (\frac{1}{2}\sum_{i=1}^{N} \sigma_\alpha^{(i)})^2 = \frac{1}{4}(\sum_{i=1}^{N} \mathbf{I} + N(N-1)\sigma_\alpha^{(i)}\sigma_\alpha^{(j)})$$

where one can evaluate the expectation of $\sigma_\alpha^{(i)}\sigma_\alpha^{(j)}$ on a coherent state using

$$x^{\frac{a^\dagger a}{2}} \left|\alpha\right\rangle = e^{-\frac{(1-x)|\alpha|^2}{2}} \left|\sqrt{x}\alpha\right\rangle . \tag{4.14}$$

We thus have a witness of genuine entanglement that is suitable for physically relevant situations. For an estimate of the resources required to show a violation, we now perform a statistical analysis.

4.4 Statistics

The aim of this section is to compute the required number of runs in order to estimate the quantity $S = \langle\mathcal{W}_\mathcal{N}\rangle + 2\sqrt{P_2(1-P_2)}|b_{max}| - \lambda_{min}P_2 - w_{PPT}$. If $S < 0$ then one can conclude about genuine entanglement to a statistically significant level. The key quantity is thus the variance of an estimator of S. We compute the variance of different estimators, one for each terms of S, with details given

in Appendix B. The quantities in S are functions of P_1, P_2 and $\langle \mathcal{W}_{\mathcal{N}} \rangle$, which we estimate with n_1, n_2 and n_{wit} runs respectively. We require that the violation of the witness is larger than 3 standard deviations of our estimator $\xi(S)$ to guarantee statistically significant results. Thus we want to find n_1, n_2, n_{wit} satisfying

$$S + 3\sqrt{var(\xi(S))} < 0. \tag{4.15}$$

For concreteness, we focus on some experimentally relevant parameters, where the efficiency of the heralding process is 0.1, the probability to have a pair of photon in the initial SPDC process is $\tanh(g)^2 = 0.01$ and the efficiency of the splitting and the measurement process is 0.3. Note that for the case N=2, we have to consider a smaller probability to have a pair in order to observe a violation. So for $N = 2$ we take $\tanh(g)^2 = 0.001$. We summarize the result in the following table, by fixing the number of runs to evaluating P_1 to 1 million, and then find the minimum n_2 and n_{wit} which satisfies (4.15).

N	n_{wit}	n_1	n_2
2	$0.3M$	$1M$	$0.3M$
3	$0.1M$	$1M$	$0.1M$
4	$0.8M$	$1M$	$0.1M$
5	$1M$	$1M$	$0.1M$

4.5 Conclusion

We have developed a witness of genuine entanglement which is tailored to a given experiment. It is very robust against losses and it only requires collective measurement. We carefully simulate the experiment and show that the demonstration of genuine entanglement for several modes can be realized in a simple photonic setup.

CHAPTER 5

MACROSCOPIC QUANTUM STATES OF LIGHT

Compute $F|3\rangle$ and $F|1,0\rangle$.

Despite intuitive examples of what a macroscopic state should be, the precise definition of what is a macroscopic quantum state have been extensively debated over the last decade [46]. The lack of a general definition of macroscopic quantumness has not prevented various measures from being proposed. Some of theses measures only apply in specific scenarios and do not hold for all physical systems. On the other hand, the progress on experiments now allow for the ability to manipulatCompute $F|3\rangle$ and $F|1,0\rangle$.e larger and larger systems and the question of the size of the system is becoming a very relevant point.

We focus on quantum optics experiments and more specifically on squeezing. Two mode squeezed states of light can be obtained from a $\chi^{(2)}$ non linearity and are produced by many groups around the world. The non linearity results in correlation in the photon number between the two output modes of the crystal which can be detected with homodyne detections by means of an entanglement witness [50, 51]. When the $\chi^{(2)}$ crystal is seeded by coherent states and/or put in a high finess cavity, entanglement in squeezed states can be demonstrated with a large number of photons up to 100000. Squeezed states thus demonstrate quantum features in a large system, which naturally raises the question of whether squeezed states have macroscopic quantum features. Actually, squeezed states are one of the basic ingredients together with conditional detection [49, 52, 53, 54] for exploring quantum effects in many photon states and create the so-calledCompute $F|3\rangle$ and $F|1,0\rangle$. photonic Schroedinger cat state [56, 57, 55].

Among the many criteria for quantifying the macroscopicity of a quantum state [46], only a few of them are suited for two mode squeezed states [58, 59]. However, they are either specifically tailored for this class of states and do not give a satisfactory measure for other states, or they do not respect mode additivity which is a necessary features of a macroscopic measurement.

We thus propose two macroscopic measures which are suited for two mode squeezed states by extending two different existing measures. From these measures, we give lower bounds on the size of two-mode squeezed states which can be accessed experimentally. We apply these results to existing experiments and report on the size of the corresponding states.

Paper D

Two-mode squeezed states as Schrödinger cat-like states

Enky Oudot, Pavel Sekatski, Florian Fröwis, Nicolas Gisin and Nicolas Sangouard

Journal of the Optical Society of America B Vol. 32, Issue 10 (2015)

Journal of the Optical Society of America B
OPTICAL PHYSICS

Two-mode squeezed states as Schrödinger cat-like states

E. Oudot,[1,2] P. Sekatski,[3] F. Fröwis,[2,*] N. Gisin,[2] and N. Sangouard[1]

[1]Department of Physics, University of Basel, CH-4056 Basel, Switzerland
[2]Group of Applied Physics, University of Geneva, CH-1211 Geneva 4, Switzerland
[3]Institut für Theoretische Physik, Universität Innsbruck, Technikerstr. 25, A-6020 Innsbruck, Austria
*Corresponding author: florian.froewis@unige.ch

Received 5 March 2015; revised 17 July 2015; accepted 17 July 2015; posted 27 August 2015 (Doc. ID 235724); published 28 September 2015

In recent years, there has been an increased interest in the generation of superpositions of coherent states with opposite phases, the so-called photonic Schrödinger cat states. These experiments are challenging, and, so far, cats involving only small photon numbers have been implemented. Here, we propose to consider two-mode squeezed states as examples of Schrödinger cat-like states. For this, we apply criteria that aim to identify macroscopic superpositions in a more general sense. We extend some of these criteria to the two-mode continuous variable regime. Furthermore, we compare the size of states obtained in several experiments and discuss experimental challenges for further improvements. Our results not only promote two-mode squeezed states for exploring quantum effects at the macroscopic level but also provide direct measures to evaluate their usefulness for quantum metrology.

OCIS codes: (270.0270) Quantum optics; (270.4180) Multiphoton processes; (270.6570) Squeezed states.

http://dx.doi.org/10.1364/JOSAB.32.002190

1. INTRODUCTION

The question of what is a macroscopic quantum state has received a lot of attention over the last decade [1–17]. The motivation is not to address a new question, as it dates back from the early days of quantum theory [18], but rather comes from the experimental progress, which now allows one to harness large systems while highlighting their quantum nature. Quantum optics experiments reporting on squeezing operations provide a nice example. They are obtained from a χ^2 nonlinearity and can result in largely entangled states. The entanglement can be further detected with homodyne detections by means of the Duan–Simon criterion [19,20]. When the χ^2 nonlinearity is seeded by coherent states and/or embedded in a high finesse cavity, entanglement in squeezed states can be demonstrated with a large number of photons [21–29]. This naturally raises the question of whether squeezed states have macroscopic quantum features, which is a question of deep relevance because, thus far, squeezed states have been combined with conditional detections [30–36] for exploring quantum effects in many photon states.

In the literature, there exist different criteria for quantifying the macroscopic quantumness [3–14]. Typically, this includes a definition that assigns a number to a quantum state, which is here called *effective size* (or simply *size*). These criteria can be grouped into two categories. The first addresses the question of whether a two-component superposition $|\phi_0\rangle + |\phi_1\rangle$ is macroscopic, i.e., whether $|\phi_0\rangle$ and $|\phi_1\rangle$ are *macroscopically distinct*. For example, the proposal of [8] states that two spin states are macroscopically distinct if they can be distinguished from a small number of their spins, as a dead cat and a live cat can be distinguished from a small number of their cells. We also can refer to the proposals of [13,37] defining two states as being macroscopically distinct if they can be distinguished with a coarse-grained measurement, as a dead cat and a live cat can be distinguished with a detector having a very limited resolution. The second category aims to identify quantum states that are able to show some kind of *macroscopic quantum effect*. This term characterizes experimental evidence that cannot be explained by an accumulated quantum effect originated at the microscopic level of the system. For pure states, a large variance with respect to given observables and Hamiltonians is a sufficient signature for quantum fluctuations that are persistent on a macroscopic level. For mixed states, one typically uses a convex function that reduces to the variance for pure states. For example, the proposal of [11] shows how the notion of macroscopicity can be linked to the so-called quantum Fisher information [38].

Not all of these measures are able to correctly handle two-mode squeezed states for different reasons. Thus far, only the contributions [7,10,39] explicitly treat two-mode squeezed vacuum. This is valuable, but these criteria also leave open questions, which are discussed in more detail in the course

of this paper. In short, Cavalcanti and Reid [7,39] propose a bound to measure the size of a two-mode squeezed state, which, however, does not give satisfactory answers to nonsqueezed states. This drawback is compensated by Lee and Jeong [10], but the mode additivity of their measure remains problematic.

In this paper, we aim to reinforce arguments in favor of assigning a macroscopic quantum nature to two-mode squeezed states. For this, we extend existing measures for macroscopic quantum states [13,40] to be able to investigate two-mode, continuous variable (cv) quantum states. Apart from avoiding problems that appeared in previous attempts [7,10,39], this broadens the range of arguments supporting the macroscopic quantumness of a two-mode squeezed vacuum. Importantly, we prove that the effective size of two-mode squeezed vacuum states (with N mean photons) is basically the same as superpositions of coherent states with opposite phases $|\alpha\rangle + |-\alpha\rangle$ and $|\alpha|^2 \tanh|\alpha|^2 = N$ but with the great advantage that they are much easier to create [41]. The tools we propose allow one to bound the size of states obtained experimentally as well as their usefulness for parameter estimation beyond the classical limit. Aside from a fundamental interest, our results ultimately have important applications for quantum metrology. Furthermore, we discuss the impact of noise and technical limitations that cumber the verification of macroscopic quantumness of two-mode squeezed states. Finally, we use data from some performed experiments [21–29] to lower-bound the effective size achieved thus far.

2. TWO-MODE VACUUM SQUEEZED STATES

As an example of two-mode squeezed states, let us consider the two-mode squeezed vacuum, which is obtained from a parametric process in which photons from a pump laser decay spontaneously into photon pairs—one in mode 1, its twin in mode 2—while preserving energy and momentum. The corresponding propagator $\overline{S}(g) = e^{g(a_1 a_2 - a_1^\dagger a_2^\dagger)}$, with squeezing parameter g, applies straightforwardly on the vacuum if written in the normal order. This results in

$$|\psi_{\text{tms}}\rangle = (1-\tanh^2 g)^{\frac{1}{4}} e^{\tanh g a_1^\dagger a_2^\dagger}|00\rangle. \quad (1)$$

The mean photon number in both modes is $N = 2\,\text{tr}(a_1^\dagger a_1 |\psi_{\text{tms}}\rangle\langle\psi_{\text{tms}}|) = 2\sinh^2 g$. Furthermore, the variance of the observable $\overline{X}_1^\varphi - \overline{X}_2^\phi$ where $\overline{X}_i^\theta = \frac{1}{\sqrt{2}}(a_i e^{i\theta} + a_i^\dagger e^{-i\theta})$ is given by

$$V_{\psi_{\text{tms}}}(\overline{X}_1^\varphi - \overline{X}_2^\phi) = \cosh 2g - \sinh 2g \cos(\varphi + \phi). \quad (2)$$

This indicates that the quadratures $\overline{X}_1^0 - \overline{X}_2^0$ are correlated whereas $\overline{X}_1^{\pi/2} - \overline{X}_2^{\pi/2}$ are anticorrelated. The quantum nature of these correlations can be revealed through the Duan–Simon criterion [19,20], which states that, for any bipartite separable states and any real parameter a,

$$\begin{aligned} &V_{\text{sep}}\left(|a|\overline{X}_1^\phi + \frac{1}{a}\overline{X}_2^\Phi\right) + V_{\text{sep}}\left(|a|\overline{X}_1^{\phi'} - \frac{1}{a}\overline{X}_2^{\Phi'}\right) \\ &> a^2\langle[\overline{X}_1^\phi, \overline{X}_1^{\phi'}]\rangle + \frac{1}{a^2}\langle[\overline{X}_2^\Phi, \overline{X}_2^{\Phi'}]\rangle \\ &\geq 2 \quad \text{for } \phi - \phi' = \Phi - \Phi' = \frac{\pi}{2}, \end{aligned} \quad (3)$$

while for a two-mode squeezed state,

$$V_{\psi_{\text{tms}}}(\overline{X}_1^0 - \overline{X}_2^0) + V_{\psi_{\text{tms}}}(\overline{X}_1^{\pi/2} + \overline{X}_2^{\pi/2}) = 2e^{-2g}.$$

The questions at the core of this paper are as follows: How do we evaluate the size of these kinds of states? Is their effective size comparable with other photonic states?

3. MACROSCOPIC QUANTUMNESS OF TWO-MODE CV STATES

A. Macroscopic Distinctness for cv States

While several definitions have been proposed to identify states that are macroscopically distinct [5,8,9,13], here we focus on the proposal of [13] based on coarse-grained measurements. This choice is arbitrary to some extent. Note, however, that the extension that we propose below easily applies to the measure of [8]. The extension of measures of [9] to two-mode squeezed states is less obvious, as they primarily address spin systems, but the link between measures for spins and photons presented in [17] might be the way to proceed.

The basic principle of the measure of macroscopicity based on coarse-grained measurement is simple. It can be seen as a game where Alice chooses a state in the set $\{|\phi_0\rangle, |\phi_1\rangle\}$ with equal *a priori* probabilities and sends it to Bob. Bob has to guess which one has been sent using a coarse-grained measurement only. It can be any measurement, provided that its resolution is limited. The quantum superposition state $|\phi_0\rangle + |\phi_1\rangle$ is qualified macroscopic if Bob wins the game with a detector having no microscopic resolution. Concretely, if one focuses on a noisy photon-counting detector, for example, the size of $|\phi_0\rangle + |\phi_1\rangle$ is characterized by the noise that one can tolerate to distinguish $|\phi_0\rangle$ and $|\phi_1\rangle$.

To extend this measure to cv states, we can mimic its original idea by introducing a 50/50 binning of measurement outcomes. For a two-mode squeezed vacuum state in particular, Alice measures her mode with a given quadrature and bins the result with respect to its sign. As Alice's measurement is assumed to be accurate, this binning corresponds to equiprobable projections onto two orthogonal subspaces of the measured state. Bob has to guess whether she received a positive or negative outcome by measuring his mode with a noisy measurement. The distinguishability of components that Bob receives is again given by the noise that can be tolerated to win the game. Note that the measurement of correlated quadratures maximizes the probability to correctly guess Alice's outcome. Concretely, the probability that Alice obtains the result x_1 and Bob x_2 knowing that they measure the quadratures $\overline{X}_1^0$ and $\overline{X}_2^0$ is given by $|p(x_1, x_2, \sigma)|^2 = \text{tr}(|\psi_{\text{tms}}\rangle\langle\psi_{\text{tms}}| \delta(\overline{X}_1^0 - x_1) g_\sigma(\overline{X}_2^0 - x_2))$, where g_σ stands for the noise of Bob's measurement device. We assume that g_σ is a Gaussian with spread σ and zero mean. Hence, the probability that Bob correctly guesses the sign of Alice's result is given by $P_\sigma^{\text{guess}} = \int_0^{+\infty} |p(x_1, x_2, \sigma)|^2 dx_1 dx_2 + \int_{-\infty}^0 |p(x_1, x_2, \sigma)|^2 dx_1 dx_2$. We find

$$P_\sigma^{\text{guess}} = \frac{1}{2} + \frac{1}{\pi}\arctan\left(\frac{\sinh 2g}{\sqrt{1 + 2\sigma^2 \cosh 2g}}\right). \quad (4)$$

We can access the maximum noise $\sigma_{\max}$ that Bob can tolerate to win the game with a fixed probability P_σ^{guess} by inverting the previous formula:

$$\sigma_{\max} = \sqrt{\frac{-1 + N\left(\frac{1}{2} + N\right)\cot an^2\left(\frac{1}{2} - P_\sigma^{\text{guess}}\right)}{2 + 2N}}. \quad (5)$$

For comparison, the noise that can be tolerated to win a similar game with the optical Schrödinger cat state $(|\uparrow\rangle|\alpha\rangle - |\downarrow\rangle|-\alpha\rangle)$ is given by

$$\sigma_{\max} = \sqrt{\frac{|\alpha|^2}{(\text{erf}^{-1}(P_\sigma^{\text{guess}}))^2} - \frac{1}{2}}.$$

In both cases, the noise scales like the square root of the photon number. Thus, we claim that two-mode squeezed vacuum and Schrödinger cat states exhibit comparable macroscopic quantumness. In some sense, they belong to the same class of macroscopic quantum states.

Let us now focus on practical considerations. The observation that Alice and Bob's x quadratures of the two-mode squeezed vacuum state are "macroscopically" correlated (correlated at a large scale, larger than the detector's resolution) is at the heart of our generalization of the coarse-grained measure. These correlations can be revealed by measuring the joint probability distribution $|p(x_1, x_2, 0)|^2$ with accurate quadrature measurements. (For simplicity, we introduce $p(x_1, x_2) = p(x_1, x_2, 0)$, which stands for the probability amplitudes without noise.) Although this approach is sufficient to measure the size of a given state in theory, one also has to ensure that those correlations are truly quantum in practice. In mathematical terms, we can always write the state that is shared by Alice and Bob in the x basis:

$$\rho = \int p(x_1, x_2) p^*(\overline{x}_1, \overline{x}_2) f(x_1, \overline{x}_1, x_2, \overline{x}_2) \times |x_1, x_2\rangle\langle \overline{x}_1, \overline{x}_2| \mathrm{d}x_1 \mathrm{d}x_2 \mathrm{d}\overline{x}_1 \mathrm{d}\overline{x}_2, \quad (6)$$

with $\int |p(x_1, x_2)|^2 \mathrm{d}x_1 \mathrm{d}x_2 = 1$ and $f(x, x, x', x') = 1 \ \forall\ x, x'$. If the shared state is pure, we have $f(x_1, \overline{x}_1, x_2, \overline{x}_2) = 1$ $\forall\ x_1, \overline{x}_1, x_2, \overline{x}_2$, and the correlations revealed through the probability distribution $|p(x_1, x_2)|^2$ are fully quantum. The violation of the Duan–Simon criterion is then sufficient to attest to the quantum nature of the state for which the size is evaluated through $\sigma_{\max}$. But how do we certify in practice that the function $f(x_1, \overline{x}_1, x_2, \overline{x}_2)$ is close to one, at least in a certain range?

To do so, we consider the effect of imperfect coherences (decoherence) $f(x_1, \overline{x}_1, x_2, \overline{x}_2) \neq 1$ on the observed violation of the Duan–Simon witness. Note first that the variance $V(\overline{X}_1^0 - \overline{X}_2^0)$ can be directly obtained from $|p(x_1, x_2)|^2$. For the second term required in Eq. (3), we can show that the variance in the presence of decoherence (see Appendix A),

$$V(\overline{X}_1^\pi + \overline{X}_2^\pi) = V\left(\overline{X}_1^\pi + \overline{X}_2^\pi\right)|_{\text{ideal}} - \langle(\partial_{x_1 - \overline{x}_1} + \partial_{x_2 - \overline{x}_2})^2 f\rangle,$$

equals the ideal-case variance $V(\overline{X}_1^\pi + \overline{X}_2^\pi)|_{\text{ideal}}$ plus a factor containing the crossed and second derivatives of f $\langle(\partial_{x_1 - \overline{x}_1} f(x_1, \overline{x}_1, x_2, \overline{x}_2)\rangle = \int \mathrm{d}x_1 \mathrm{d}x_2 |p(x_1, x_2)|^2 (\partial_{x_1 - \overline{x}_1} f(x_1, \overline{x}_1, x_2, x_2))|_{x_1 = \overline{x}_1}$, etc. Because $V(\overline{X}_1^\pi + \overline{X}_2^\pi)|_{\text{ideal}}$ is positive, we obtain the following upper bound on the observed variance:

$$-\langle(\partial_{x_1 - \overline{x}_1} + \partial_{x_2 - \overline{x}_2})^2 f\rangle \leq V\left(\overline{X}_1^\pi + \overline{X}_2^\pi\right). \quad (7)$$

Note that, without further assumptions, we cannot bound the range δ for which $f(x_1, x_1 + \delta, x_2, x_2 + \delta)$ stays close to one. In other words, even if the state of Alice and Bob largely violates the Duan–Simon witness, the state can be arbitrarily close to a separable one, and $p(x_1, x_2)$ essentially correspond to classical correlations [42]. However, under the assumption of a Gaussian decay of coherence $f(x_1, \overline{x}_1, x_2, \overline{x}_2) = e^{-(x_1 - \overline{x}_1)^2/(2\gamma_1^2)} e^{-(x_2 - \overline{x}_2)^2/(2\gamma_2^2)}$, Eq. (7) becomes $\frac{1}{\gamma_1^2} + \frac{1}{\gamma_2^2} \leq V\left(\overline{X}_1^\pi + \overline{X}_2^\pi\right)$. This implies $\min(\gamma_1, \gamma_2) \geq 1/\sqrt{V\left(\overline{X}_1^\pi + \overline{X}_2^\pi\right)}$, i.e., if one observes the variance $V_{\psi_{\text{tms}}}\left(\overline{X}_1^\pi + \overline{X}_2^\pi\right)$ of the total momentum, we can certify that the correlations $|p(x_1, x_2)|^2$ are quantum at least in the range

$$x_C = \frac{1}{\sqrt{V_{\psi_{\text{tms}}}\left(\overline{X}_1^\pi + \overline{X}_2^\pi\right)}}. \quad (8)$$

Accordingly, if the coherence range x_C is lower than the correlation range, as witnessed by $\sigma_{\max}$, one can only claim that the state exhibits quantum correlations within the range x_C, which is then the true size of the state. Revealing the size of large quantum states thus requires us to reveal narrow variances, which becomes increasingly difficult as the size increases (see Section 4).

B. General Measures for Multimode cv States

Beside measures for macroscopic distinguishability, there have been recent proposals that aim to go beyond the basic structure $|\phi_0\rangle + |\phi_1\rangle$ [4,6,10,11]. While the measures of [4,6,11] were originally defined for spin systems, the definition of [10] is directly suitable for cv photonic states. For pure states, these three proposals are comparable because a state $|\psi\rangle$ is called macroscopically quantum if it shows a large variance with respect to a restricted class of operators. In the spin case, the proposals [4,6,11] focus on sums of local operators (henceforth simply called "local operators"), whereas Lee and Jeong [10] define their measure for pure states proportional to $V(\overline{X}^0) + V(\overline{X}^{\pi/2})$. In [17], it was argued that local operators in the spin case play to some extent the same role as quadrature operators in mono-mode photonic systems.

The common feature of the proposals for mixed states is that the measures [4,6,10,11] are convex in the state, which is an important and natural feature for the present purpose. There are no clear arguments in favor of one of the proposals. Nevertheless, we focus here on the quantum Fisher information (QFI) [38], which is denoted as $\mathcal{F}_\rho(\overline{X})$ for the state ρ and the operator $\overline{X}$. Importantly, the QFI is the convex roof of the variance [43,44] (up to a factor four); that is, it is the largest convex function that reduces to the variance for pure states. For experiments, it is interesting to note that there exist lower bounds on the QFI based on measurable quantities [45].

The extension to photonic states with $n > 1$ modes is not straightforward. Indeed, a multimode version for the measure of Lee and Jeong was proposed [10]. However, it is additive and, hence, a bunch of "kitten states" $|\psi_\alpha\rangle^{\otimes n} \propto (|\alpha\rangle + |-\alpha\rangle)^{\otimes n}$ (with potentially small α but large n) is as macroscopically quantum as a "big" single cat state

$|\psi_{\sqrt{n}\alpha}\rangle \propto |\sqrt{n}\alpha\rangle + |-\sqrt{n}\alpha\rangle$. Here, we propose instead to use a similar account that has been successfully applied in the spin case [4,6,11]. The idea is that the effective size of a product state is the average value of its components, while entangled states should be able to profit from quantum correlations between the modes. Both requirements are achieved by defining the effective size for ρ as

$$N_{\text{eff}}(\rho) = \frac{1}{2n}\max_{\boldsymbol{\theta}} \mathcal{F}_{\rho}(X_{\boldsymbol{\theta}}), \tag{9}$$

where $X_{\boldsymbol{\theta}} = \Sigma_{i=1}^{n} \overline{X}_i^{\theta_i}$. In other words, one maximizes the QFI (or the variance for pure states) with respect to sums of local quadrature operators parametrized by $\boldsymbol{\theta} = (\theta_1, \ldots, \theta_n)$. The examples from above then lead to $N_{\text{eff}}(|\psi_\alpha\rangle^{\otimes n}) = 4|\alpha|^2/[1 + \exp(-2|\alpha|^2)]$ and $N_{\text{eff}}(|\psi_{\sqrt{n}\alpha}\rangle) = 4n|\alpha|^2/[1 + \exp(-2n|\alpha|^2)]$ (compare to [46]).

We now come to the evaluation of the effective size for the two-mode squeezed vacuum state. It is simple to see that the variance is largest for the quadratures that are maximally correlated. For the state in Eq. (1), these are the operators $\overline{X}_1^0 + \overline{X}_2^0$ and $\overline{X}_1^{\pi/2} - \overline{X}_2^{\pi/2}$. The effective size for each of these choices reads $N_{\text{eff}}(\psi_{\text{tms}}) = V(\overline{X}_1^0 + \overline{X}_2^0) = e^{2g} \approx 2N$, which is approximately half of the value as for the cat state with the same photon number, $N_{\text{eff}}(|\psi_\alpha\rangle) \approx 4N$. Again, we conclude that two-mode squeezed states are compatible with photonic cat states.

In principle, the effective size of a pure state could be determined by witnessing a large variance for sums of quadrature operators. However, for mixed states, a large variance is not sufficient. Instead, one has to verify a large value of a convex function like the QFI. Since this quantity is typically only accessible through a full state tomography, one has to find other means to estimate it. Recently, a general lower bound on the QFI has been found [45]. It was shown that, for any quantum state ρ and any pair of operators A, B, it holds that $V_\rho(A)\mathcal{F}_\rho(B) \geq \langle i[A, B]\rangle_\rho^2$, which is a tighter version of the Heisenberg uncertainty relation. Here, we use this inequality to bound the QFI from below. For $B = \overline{X}_1^0 + \overline{X}_2^0$, we set $A = \overline{X}_1^{\pi/2} + \overline{X}_2^{\pi/2}$ and find $i[A, B] = -2$. Hence, one has

$$N_{\text{eff}}(\rho) \geq \frac{1}{V_\rho(\overline{X}_1^{\pi/2} + \overline{X}_2^{\pi/2})}. \tag{10}$$

For the two-mode squeezed state, the anticorrelations between $\overline{X}_1^{\pi/2}$ and $\overline{X}_2^{\pi/2}$ lead to a reduced variance and therefore to a potentially large value of N_{eff}.

Note that Eq. (10) [as well as Eq. (8)] resembles the ideas of [7,39] for a generalized notion of macroscopic quantum coherences. However, in these works, solely the bound in Eq. (10) is used, which restricts one to investigate squeezed states. In contrast, we use this expression only to give a bound on the definition in Eq. (9), which also can deal with nonsqueezed states. Hence, our measure is general enough to compare two-mode squeezed states with other states such as cat states.

4. ON THE DIFFICULTY TO CERTIFY THE QUANTUM NATURE OF TWO-MODE SQUEEZED STATES

The common feature of measures for macroscopicity presented before is the requirement to reveal narrow variances, especially when dealing with large size states. How difficult is it in practice? To answer this question, we consider the effect of various experimental imperfections on the observed variance $V_{\psi_{\text{tms}}}(\overline{X}_1^{\pi/2} + \overline{X}_2^{\pi/2})$.

1. Consider first a noise along $\overline{X}^0$ that acts on a state ρ as $\rho \mapsto \int d\lambda h(\lambda) e^{i\hat{X}_0\lambda}\rho e^{-i\hat{X}_0\lambda}$ with characteristic function (noise distribution) $h(\lambda)$ of variance $\Delta^2 h$. The effect of this noise can be directly absorbed in the statistics of the momentum distribution and leads to the following modification of the variance $V(\overline{X}_1^{\pi/2} + \overline{X}_2^{\pi/2}) \mapsto V(\overline{X}_1^{\pi/2} + \overline{X}_2^{\pi/2}) + \Delta^2 h_1 + \Delta^2 h_2$. Therefore, if the experimental setup suffers from such a noise, we cannot certify the state of an effective size larger than $N_{\text{eff}}^{\max} = \frac{1}{\Delta^2 h_1 + \Delta^2 h_2}$.
2. Similarly, consider a loss channel with transmission η. It leads to $V(\overline{X}_1^{\pi/2} + \overline{X}_2^{\pi/2}) \mapsto \eta V(\overline{X}_1^{\pi/2} + \overline{X}_2^{\pi/2}) + (1 - \eta)$, and the maximal certifiable size is given by $N_{\text{eff}}^{\max} = \frac{1}{1-\eta}$.
3. Now consider a phase noise characterized by the variance $\Delta\varphi^2 = \int p(\varphi)\varphi^2 d\varphi$. It increases the observed variance according to $V(\overline{X}_1^{\pi/2} + \overline{X}_2^{\pi/2}) \geq \Delta\varphi^2(\langle \overline{X}_1^0\rangle + \langle \overline{X}_2^0\rangle)$. Specifically, for the two-mode squeezed state, one has $N_{\text{eff}}^{\max}(\psi_{\text{tms}}) = \frac{1}{\Delta\varphi^2(2\sinh^2(g)+1)}$, which decays exponentially with the squeezing parameter (in the limit of large enough g).

An experimental issue for the detection of highly squeezed states is the size of the local oscillator $|\alpha\rangle$ (LO) used for homodyne detection. On the one hand, the mean total photon number $N + |\alpha|^2$ has to be smaller than some value D_{th} in such a way that the detectors are not saturated. On the other hand, α has to be large enough in order to be a good phase reference because a limited size of the LO is similar to a phase noise. Let us show this quantitatively. In a homodyne measurement, the system is mixed with the LO on a balanced beam splitter with the phase θ. The quadrature is accessed via the difference in the mean photon number of the two outputs of the beam splitter $\frac{I_1 - I_2}{|\alpha|}$. While for the mean of any quadrature, this is exactly given by $\left\langle \frac{I_1 - I_2}{|\alpha|} \right\rangle = \langle X_\theta \rangle$, for the second moment $\left\langle \frac{(I_1 - I_2)^2}{|\alpha|^2} \right\rangle = \langle X_\theta^2 \rangle + \frac{\langle a^\dagger a\rangle}{|\alpha|^2}$, this correspondence with the measured result is not exact. Accordingly, for a finite size of the local oscillator, the observed variance is bounded by $V(\overline{X}_1^{\pi/2} + \overline{X}_2^{\pi/2}) \geq \frac{4\sinh^2(g)}{|\alpha|^2}$. Because the size of the LO is limited by the detector saturation threshold $|\alpha|^2 \leq D_{\text{th}} - 2\sinh^2(g)$, one has $N_{\text{eff}}^{\max}(\psi_{\text{tms}}) = \frac{D_{\text{th}} - 2\sinh^2(g)}{4\sinh^2(g)}$.

In each case, we clearly see that it becomes increasingly difficult to observe narrow variances with two-mode squeezed states as their size increases. This is in agreement with recent results [47–50] stating that it is difficult to observe the quantum nature of macroscopic states.

This naturally raises the question of the size of states that can be observed in practice. Note that Eqs. (8) and (10) are general, i.e., the variance along the conjugate of quadratures that are maximally correlated gives a bound on the size of the measured state. We use experimental data obtained in various setups in which the χ^2 nonlinearity is either seeded or embedded in a cavity [21–24,27,28] to bound the effective size of the produced states (see Fig. 1). All these experiments have in common

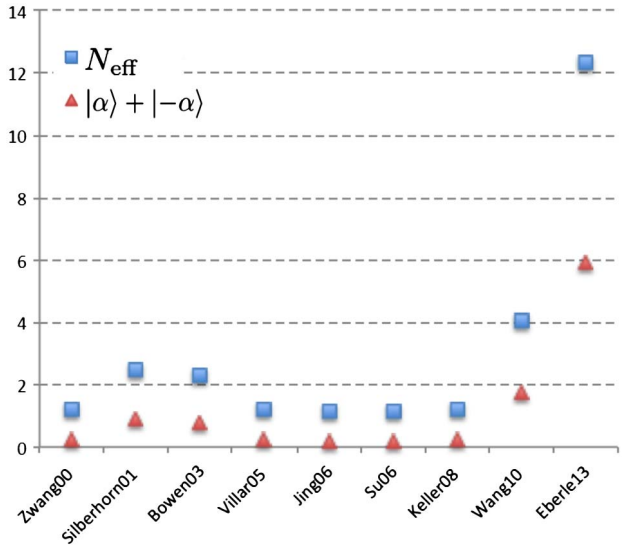

Fig. 1. Bounds on the effective size N_{eff} (blue squares) of two-mode squeezed states obtained from experimental data reported in [21–29] using the inequality in Eq. (10). The red triangles indicate the minimal photon number N necessary for a cat state $|\alpha\rangle + |-\alpha\rangle$ to have the same effective size according to Eq. (9). For example, the state reported in [21] has a size $N_{\text{eff}} \geq 1.2$ for which one needs at least a cat state with $N \approx 0.2$ for the same size.

that the Duan–Simon criterion is used to reveal entanglement and the photon number is large. We clearly see that their effective size cannot be compared with their mean photon number. In the seeded case, the reason is that the seed increases the photon number but does not change the variance. Similarly with a cavity, the photon number can be large even if the gain slightly dominates the loss provided that the cavity finesse is large but the variance of interest is limited by the ratio between the gain and the loss only (see Appendix B). Interestingly, the results presented in Fig. 1 can be used directly to quantitatively estimate the metrological usefulness of states realized experimentally, as the size N_{eff} gives the QFI through the formula in Eq. (9).

5. CONCLUSION

We propose to consider a two-mode squeezed vacuum as being macroscopically quantum. Our conclusion is based on the results from two measures for macroscopic quantum states [11,13], which have been extended for the purpose of studying two-mode cv states. It is straightforward to generalize our argument to general two-mode squeezed states. This study is in line with former works [7,10,39], but it overcomes some of their problems. On a quantitative level, we see that two-mode squeezed vacuums are comparable with superpositions of coherent states, which are generally considered as archetypal Schrödinger cat states. However, one should acknowledge two advantages of the former compared with the latter: Two-mode squeezed states are not only relatively easy to generate. The experimental verification of macroscopic quantumness can be simply achieved by demonstrating strong (anti-) correlations between the quadratures of the two modes. Nevertheless, in agreement with previous findings [48,50], the precise control of the entire experiment, especially of the measurement, is imperative for showing large quantumness.

APPENDIX A: COHERENCE LENGTH OF CORRELATION

Every two-mode state ρ can be expressed in the joint x basis:

$$\rho = \int F(x_1, x_2, \overline{x}_1, \overline{x}_2)|x_1, x_2\rangle\langle\overline{x}_1, \overline{x}_2|\mathrm{d}\vec{x}. \tag{A1}$$

However, for our purpose, it is useful to make the decomposition

$$F(x_1, x_2, \overline{x}_1, \overline{x}_2) = p(x_1, x_2)p^*(\overline{x}_1, \overline{x}_2)f(x_1, x_2, \overline{x}_1, \overline{x}_2), \tag{A2}$$

where we can enforce that $\int |p(x_1, x_2)|^2 \mathrm{d}x_1\mathrm{d}x_2 = 1$ and $f(x_1 = \overline{x}_1, x_2 = \overline{x}_2) = 1$, and consequently $|f(x_1 \neq \overline{x}_1, x_2 \neq \overline{x}_2)| \leq 1$. The later inequality is ensured by positivity of ρ, i.e., if it does not hold, then there is a state $\alpha|x_1, x_2\rangle + \beta|\overline{x}_1, \overline{x}_2\rangle$ that has a negative overlap with ρ. The decomposition in Eq. (A2) is useful because the function $f(x_1, x_2, \overline{x}_1, \overline{x}_2)$ can be simply interpreted as characterizing the lack of purity of ρ because, for a pure state $|\psi\rangle = \int p(x_1, x_2)|x_1, x_2\rangle\mathrm{d}x_1\mathrm{d}x_2$, it satisfies $f(x_1, x_2, \overline{x}_1, \overline{x}_2) \equiv 1$.

Let us now consider the mean values of $\langle p_{1(2)}\rangle$, $\langle p^2_{1(2)}\rangle$, and $\langle p_1 p_2\rangle$ on the state ρ. In this appendix, we denote $\overline{X}^0 = x$ and $\overline{X}^{\pi/2} = p$. Using the representation of momenta eigenstate in the x basis $|p\rangle = \frac{1}{\sqrt{2\pi}}\int e^{ixp}|x\rangle$, one obtains

$$\begin{aligned}
\langle p_1\rangle &= \int F(x_1, x_2, \overline{x}_1, \overline{x}_2)p\frac{e^{-ip(x_1-\overline{x}_1)}}{2\pi}\delta(x_2 - \overline{x}_2)\mathrm{d}p\mathrm{d}\vec{x},\\
\langle p_1^2\rangle &= \int F(x_1, x_2, \overline{x}_1, \overline{x}_2)p^2\frac{e^{-ip(x_1-\overline{x}_1)}}{2\pi}\delta(x_2 - \overline{x}_2)\mathrm{d}p\mathrm{d}\vec{x},\\
\langle p_1 p_2\rangle &= \int F(x_1, x_2, \overline{x}_1, \overline{x}_2)p_1 p_2\frac{e^{-ip_1(x_1-\overline{x}_1)}}{2\pi}\\
&\quad\times\frac{e^{-ip_2(x_2-\overline{x}_2)}}{2\pi}\mathrm{d}p_1\mathrm{d}p_2\mathrm{d}\vec{x}.
\end{aligned} \tag{A3}$$

Using $p^n e^{-ip(\Delta x)} = (i\partial_{\Delta x})^n e^{-ip(\Delta x)}$ and $\frac{1}{2\pi}\int e^{-ip(x-\overline{x})}\mathrm{d}p = \delta(x - \overline{x})$, a simple integration by parts allows us to rewrite the above expressions as

$$\begin{aligned}
\langle p_1\rangle &= \int (i\partial_{x_1-\overline{x}_1})F(x_1, x_2, \overline{x}_1, \overline{x}_2)|_{x_1=\overline{x}_1}\mathrm{d}x_1\mathrm{d}x_2,\\
\langle p_1^2\rangle &= \int (i\partial_{x_1-\overline{x}_1})^2F(x_1, x_2, \overline{x}_1, \overline{x}_2)|_{x_1=\overline{x}_1}\mathrm{d}x_1\mathrm{d}x_2,\\
\langle p_1 p_2\rangle &= \int (i\partial_{x_2-\overline{x}_2})(i\partial_{x_1-\overline{x}_1}),\\
&\quad\times F(x_1, x_2, \overline{x}_1, \overline{x}_2)|_{x_1=\overline{x}_1, x_2=\overline{x}_2}\mathrm{d}x_1\mathrm{d}x_2.
\end{aligned}$$

Those expressions allow us to use the decomposition in Eq. (A2) to its full advantage, leading to

$$\begin{aligned}
\langle p_1\rangle &= \langle p_1\rangle_{f\equiv 1},\\
\langle p_1^2\rangle &= \langle p_1^2\rangle_{f\equiv 1} - \langle\partial^2_{x_1-\overline{x}_1}f\rangle,\\
\langle p_1^2\rangle &= \langle p_2^2\rangle_{f\equiv 1} - \langle\partial^2_{x_2-\overline{x}_2}f\rangle,\\
\langle p_1 p_2\rangle &= \langle p_1 p_2\rangle_{f\equiv 1} - \langle\partial_{x_1-\overline{x}_1}\partial_{x_2-\overline{x}_2}f\rangle,
\end{aligned} \tag{A4}$$

with the averages $\langle\cdot\rangle_{f\equiv 1}$ being taken over the pure state $|\psi\rangle = \int p(x_1, x_2)|x_1, x_2\rangle\mathrm{d}x_1\mathrm{d}x_2$ and

$$\langle D[f]\rangle = \int |p(x_1,x_2)|^2 D[f](x_1,x_2)\mathrm{d}x_1\mathrm{d}x_2. \quad \textbf{(A5)}$$

Note that, to derive these expressions, we used the fact that the first derivatives of f are zero (because ρ is Hermitian).

The expressions in Eq. (A4) allow us to rewrite the variance of p_1+p_2 in a form where the contributions of $p(x_1,x_2)$ and $f(x_1,x_2,\overline{x}_1,\overline{x}_2)$ are separated:

$$V(p_1+p_2) = V(p_1+p_2)_{f\equiv 1} - \langle(\partial_{x_1-\overline{x}_1}+\partial_{x_2-\overline{x}_2})^2 f\rangle. \quad \textbf{(A6)}$$

Keep in mind that, for pure states, the variance $V(p_1+p_2)_{f\equiv 1}$ is always positive. This allows us to upper bound the decay of coherences in the x basis:

$$-\langle(\partial_{x_1-\overline{x}_1}+\partial_{x_2-\overline{x}_2})^2 f\rangle \le V(p_1+p_2). \quad \textbf{(A7)}$$

Without supplementary assumptions, local derivatives of f at $x_1=\overline{x}_1$ and $x_2=\overline{x}_2$ are not sufficient to determine global properties, such that the variances $V(x_1-\overline{x}_1)$ and $V(x_2-\overline{x}_2)$ of f, as one can imagine irregular functions f that have zero derivatives but arbitrarily small variance $V(x_1-\overline{x}_1)$ (e.g., the step function of arbitrarily small width). But assuming a Gaussian profile for the decay of coherence allows us to draw conclusions on the coherence width of f from the upper bound in Eq. (A7), as we show in the main text.

APPENDIX B: QUADRATURE CORRELATIONS FOR AN AMPLIFIER WITH LOSS

In this appendix, we derive a simple model for a two-mode optical parametric amplification in a cavity with loss. The amplification Hamiltonian is given by

$$H_A = i\chi(a^\dagger b^\dagger - ab), \quad \textbf{(B1)}$$

with $\chi>0$. The loss is described by a beam splitter operating on each mode a and b. The global process can be seen as a sequence of alternating infinitesimal amplifiers with gain χdt and losses with intensity transmission $1-2\lambda dt$. Consider an operator of the form

$$\mathcal{O}(\eta,\mu,\kappa) = e^{\kappa} e^{i(\eta a^\dagger+\mu b^\dagger)} e^{i(\eta^* a+\mu^* b)} \quad \textbf{(B2)}$$

and propagate it through an elementary step of our process (amplification + loss). It is easy to see that, after an infinitesimal time step dt, the operator becomes

$$\begin{aligned}&\mathrm{tr}_{\mathrm{loss}}\, U_{dt}^\dagger \mathcal{O}(\eta,\mu,\kappa) U_{dt}\\ &= \mathcal{O}(\eta+(\mu^*\chi-\eta\lambda)dt,\\ &\quad \mu+(\eta^*\chi-\mu\lambda)dt,\quad \kappa-(\mu^*\eta^*+\mu\eta)\chi dt),\end{aligned} \quad \textbf{(B3)}$$

where we omit terms of higher order in dt in the exponent, and the trace is there to remind us that the loss is not a unitary evolution (the trace is taken over the vacuum modes of the environment). Thus, during the evolution, the operator $\mathcal{O}_t = \mathcal{O}(\eta(t),\mu(t),\kappa(t))$ keeps its form while the scalar functions satisfy the system of differential equations:

$$\begin{cases}\dot\eta(t) = \chi\mu^*(t) - \lambda\eta(t)\\ \dot\mu(t) = \chi\eta^*(t) - \lambda\mu(t)\\ \kappa(t) = -\chi\int_0^t(\eta^*(s)\mu^*(s)+\eta(s)\mu(s))\mathrm{d}s + \kappa(0).\end{cases} \quad \textbf{(B4)}$$

The solution is straightforward:

$$\begin{pmatrix}\eta(t)\\ \mu^*(t)\end{pmatrix} = \exp\left(\begin{pmatrix}-\lambda & \chi\\ \chi & -\lambda\end{pmatrix}t\right)\begin{pmatrix}\eta_0\\ \mu_0^*\end{pmatrix},$$

$$\begin{pmatrix}\mu(t)\\ \eta^*(t)\end{pmatrix} = \exp\left(\begin{pmatrix}-\lambda & \chi\\ \chi & -\lambda\end{pmatrix}t\right)\begin{pmatrix}\mu_0\\ \eta_0^*\end{pmatrix},$$

$$\kappa(t) = (\eta_0 \quad \mu_0^*)\cdot\left(\int_0^t e^{\begin{pmatrix}-\lambda & \chi\\ \chi & -\lambda\end{pmatrix}2s}\mathrm{d}s\right)\cdot\begin{pmatrix}\mu_0\\ \eta_0^*\end{pmatrix}+\kappa_0. \quad \textbf{(B5)}$$

Given the expression of the propagated $\mathcal{O}_t$ operator, one can evaluate the quadrature statistics of an evolved state. Let us calculate the following probability $p(x_\theta^a,y_\xi^b) = \langle|x_\theta^a,y_\xi^b\rangle\langle x_\theta^a,y_\xi^b|\rangle$ on an evolved state. Using

$$|x_\theta^a\rangle\langle x_\theta^a| = \frac{1}{2\pi}\int \mathrm{d}\zeta e^{i\zeta(\hat{x}_\theta^a-x)}\mathrm{d}\zeta \quad \textbf{(B6)}$$

$$\hat{x}_\theta^a = \frac{1}{\sqrt{2}}(ae^{-i\theta}+a^\dagger e^{i\theta}), \quad \textbf{(B7)}$$

the projector on the quadrature eigenstates can be expressed as

$$|x_\theta^a,y_\xi^b\rangle\langle x_\theta^a,y_\xi^b| = \int\frac{\mathrm{d}\zeta\mathrm{d}\gamma}{(2\pi)^2}e^{-i\zeta x-i\gamma y} \times \underbrace{e^{-\frac{\zeta^2+\gamma^2}{4}}e^{i\left(\frac{\zeta e^{i\theta}}{\sqrt{2}}a^\dagger+\frac{\gamma e^{i\xi}}{\sqrt{2}}b^\dagger\right)}e^{i\left(\frac{\zeta e^{-i\theta}}{\sqrt{2}}a+\frac{\gamma e^{-i\xi}}{\sqrt{2}}b\right)}}_{\mathcal{O}_0}, \quad \textbf{(B8)}$$

where the nontrivial part has the form of the operator $\mathcal{O}$ in Eq. (B2) with $\eta_0=\frac{\zeta e^{i\gamma}}{\sqrt{2}}$, $\mu_0=\frac{\gamma e^{i\xi}}{\sqrt{2}}$ and $\kappa_0=-\frac{\zeta^2+\gamma^2}{4}$. Resolving the time evolution of $\mathcal{O}_t$ using Eq. (B5), one obtains that, for the final probability (at time t),

$$p(x_\theta^a,y_\xi^b) = \int\frac{\mathrm{d}\zeta\mathrm{d}\gamma}{(2\pi)^2}e^{-i\zeta x-i\gamma y}\langle\mathcal{O}_t\rangle. \quad \textbf{(B9)}$$

For a coherent input states (seeds), the mean value $\langle\mathcal{O}_t\rangle = \langle\alpha,\beta|\mathcal{O}_t|\alpha,\beta\rangle = e^{\kappa(t)}e^{i(\alpha^*\eta(t)+\beta^*\mu(t))}e^{i(\alpha\eta^*(t)+\beta\mu^*(t))}$ is particularly simple.

A direct calculation using the formulas above gives

$$p(x_\theta^a,y_\xi^b) = \int\frac{\mathrm{d}\zeta\mathrm{d}\gamma}{(2\pi)^2}e^{-i\begin{pmatrix}\zeta & \gamma\end{pmatrix}\cdot\begin{pmatrix}x-Z(\alpha,\beta)\\ y-\Gamma(\alpha,\gamma)\end{pmatrix}}e^{-\frac{\zeta^2+\gamma^2}{4}} \times\exp\left[-\frac{1}{8}\begin{pmatrix}\zeta\\ \gamma\end{pmatrix}^{\mathrm{T}}\cdot\begin{pmatrix}\left(\frac{-1+e^{-2t(\lambda+\chi)}}{\lambda+\chi}-\frac{-1+e^{2t(\chi-\lambda)}}{\lambda-\chi}\right) & e^{i(\theta+\xi)}\left(-\frac{-1+e^{2t(\chi-\lambda)}}{\lambda-\chi}-\frac{-1+e^{-2t(\lambda+\chi)}}{\lambda+\chi}\right)\\ e^{-i(\theta+\xi)}\left(-\frac{-1+e^{2t(\chi-\lambda)}}{\lambda-\chi}-\frac{-1+e^{-2t(\lambda+\chi)}}{\lambda+\chi}\right) & \left(\frac{-1+e^{-2t(\lambda+\chi)}}{\lambda+\chi}-\frac{-1+e^{2t(\chi-\lambda)}}{\lambda-\chi}\right)\end{pmatrix}\cdot\begin{pmatrix}\zeta\\ \gamma\end{pmatrix}\right]. \quad \textbf{(B10)}$$

The Fourier transform yields a Gaussian joint probability,

$$p(x_\theta^a, y_\xi^b) = \frac{\sqrt{r_- r_+}}{4\pi} e^{-\frac{1}{4}(x - Z(\alpha,\beta) \;\; y - \Gamma(\alpha,\beta)) \cdot M \cdot \begin{pmatrix} x - Z(\alpha,\beta) \\ y - \Gamma(\alpha,\beta) \end{pmatrix}}, \tag{B11}$$

where r_+ and r_- are the two eigenvalues of the matrix M given by

$$r_- = \left(\frac{\lambda + \chi e^{-2t(\lambda+\chi)}}{4(\lambda+\chi)} \right)^{-1}, \tag{B12}$$

$$r_+ = \left(\frac{\lambda - \chi e^{2t(\chi-\lambda)}}{4(\lambda-\chi)} \right)^{-1}. \tag{B13}$$

Accordingly, the joint probability $p(x_\theta^a, y_\xi^b)$ decomposes in a product of two Gaussians with variance $\Delta_- = 2/r_-$ in the squeezed direction (decreasing with time) and $\Delta_+ = 2/r_+$ in the antisqueezed direction (increasing with time). Let us comment on their asymptotic values for $t \to \infty$ (limit of high finesse) for the two different regimes:

- *Below threshold* $\lambda > \chi$,

$$\Delta_+ \to \frac{\lambda}{2(\lambda-\chi)} \Delta_- \to \frac{\lambda}{2(\lambda+\chi)}, \tag{B14}$$

both variances saturate at constant values.

- *Above threshold* $\lambda < \chi$,

$$\Delta_+ \to \frac{\chi}{2(\chi-\lambda)} e^{2t(\chi-\lambda)} \Delta_- \to \frac{\lambda}{2(\lambda+\chi)}, \tag{B15}$$

while the variance in the antisqueezed direction increases exponentially with time (finesse), the squeezed width cannot be decreased below a constant $\frac{1}{2}\frac{1}{1+\chi/\lambda}$ set by the quality factor of the amplification process $\frac{\chi}{\lambda}$.

Funding. Austrian Science Fund (FWF) (J3462, P24273-N16); European Research Council (ERC) (ERC MEC); National Swiss Science Foundation (SNSF) (P2GEP2-151964, PP00P2-150579).

Acknowledgment. We thank M. Mitchell for sharing several discussions with us; one of them initiated this work. We also warmly thank W. Dür, J. Laurat, and M. Skotiniotis for many discussions.

REFERENCES AND NOTES

1. A. J. Leggett, "Macroscopic quantum systems and the quantum theory of measurement," Prog. Theor. Phys. Suppl. **69**, 80–100 (1980).
2. A. J. Leggett, "Testing the limits of quantum mechanics: motivation, state of play, prospects," J. Phys. Condens. Matter **14**, R415–R451 (2002).
3. W. Dür, C. Simon, and J. I. Cirac, "Effective size of certain macroscopic quantum superpositions," Phys. Rev. Lett. **89**, 210402 (2002).
4. A. Shimizu and T. Miyadera, "Stability of quantum states of finite macroscopic systems against classical noises, perturbations from environments, and local measurements," Phys. Rev. Lett. **89**, 270403 (2002).
5. G. Björk and P. G. L. Mana, "A size criterion for macroscopic superposition states," J. Opt. B **6**, 429–436 (2004).
6. A. Shimizu and T. Morimae, "Detection of macroscopic entanglement by correlation of local observables," Phys. Rev. Lett. **95**, 090401 (2005).
7. E. G. Cavalcanti and M. D. Reid, "Signatures for generalized macroscopic superpositions," Phys. Rev. Lett. **97**, 170405 (2006).
8. J. I. Korsbakken, K. B. Whaley, J. Dubois, and J. I. Cirac, "Measurement-based measure of the size of macroscopic quantum superpositions," Phys. Rev. A **75**, 042106 (2007).
9. F. Marquardt, B. Abel, and J. Von Delft, "Measuring the size of a quantum superposition of many-body states," Phys. Rev. A **78**, 012109 (2008).
10. C.-W. Lee and H. Jeong, "Quantification of macroscopic quantum superpositions within phase space," Phys. Rev. Lett. **106**, 220401 (2011).
11. F. Fröwis and W. Dür, "Measures of macroscopicity for quantum spin systems," New J. Phys. **14**, 093039 (2012).
12. S. Nimmrichter and K. Hornberger, "Macroscopicity of mechanical quantum superposition states," Phys. Rev. Lett. **110**, 160403 (2013).
13. P. Sekatski, N. Sangouard, and N. Gisin, "Size of quantum superpositions as measured with classical detectors," Phys. Rev. A **89**, 012116 (2014).
14. A. Laghaout, J. S. Neergaard-Nielsen, and U. L. Andersen, "Assessments of macroscopicity for quantum optical states," Opt. Commun. **337**, 96–101 (2015).
15. H. Jeong, M. Kang, and H. Kwon, "Characterizations and quantifications of macroscopic quantumness and its implementations using optical fields," Opt. Commun. **337**, 12–21 (2015).
16. T. Farrow and V. Vedral, "Classification of macroscopic quantum effects," Opt. Commun. **337**, 22–26 (2015).
17. F. Fröwis, N. Sangouard, and N. Gisin, "Linking measures for macroscopic quantum states via photon–spin mapping," Opt. Commun. **337**, 2–11 (2015).
18. E. Schrödinger, "Die gegenwärtige Situation in der Quantenmechanik," Naturwissenschaften **23**, 807–812 (1935).
19. L.-M. Duan, G. Giedke, J. I. Cirac, and P. Zoller, "Inseparability criterion for continuous variable systems," Phys. Rev. Lett. **84**, 2722–2725 (2000).
20. R. Simon, "Peres-Horodecki separability criterion for continuous variable systems," Phys. Rev. Lett. **84**, 2726–2729 (2000).
21. Y. Zhang, H. Wang, X. Li, J. Jing, C. Xie, and K. Peng, "Experimental generation of bright two-mode quadrature squeezed light from a narrow-band nondegenerate optical parametric amplifier," Phys. Rev. A **62**, 023813 (2000).
22. C. Silberhorn, P. K. Lam, O. Weiß, F. König, N. Korolkova, and G. Leuchs, "Generation of continuous variable Einstein-Podolsky-Rosen entanglement via the Kerr nonlinearity in an optical fiber," Phys. Rev. Lett. **86**, 4267–4270 (2001).
23. W. P. Bowen, R. Schnabel, P. K. Lam, and T. C. Ralph, "Experimental investigation of criteria for continuous variable entanglement," Phys. Rev. Lett. **90**, 043601 (2003).
24. A. S. Villar, L. S. Cruz, K. N. Cassemiro, M. Martinelli, and P. Nussenzveig, "Generation of bright two-color continuous variable entanglement," Phys. Rev. Lett. **95**, 243603 (2005).
25. J. Jing, S. Feng, R. Bloomer, and O. Pfister, "Experimental continuous-variable entanglement from a phase-difference-locked optical parametric oscillator," Phys. Rev. A **74**, 041804 (2006).
26. X. Su, A. Tan, X. Jia, Q. Pan, C. Xie, and K. Peng, "Experimental demonstration of quantum entanglement between frequency-nondegenerate optical twin beams," Opt. Lett. **31**, 1133–1135 (2006).
27. G. Keller, V. D'Auria, N. Treps, T. Coudreau, J. Laurat, and C. Fabre, "Experimental demonstration of frequency-degenerate bright EPR beams with a self-phase-locked OPO," Opt. Express **16**, 9351–9356 (2008).
28. Y. Wang, H. Shen, X. Jin, X. Su, C. Xie, and K. Peng, "Experimental generation of 6 dB continuous variable entanglement from a nondegenerate optical parametric amplifier," Opt. Express **18**, 6149–6155 (2010).
29. T. Eberle, V. Händchen, and R. Schnabel, "Stable control of 10 dB two-mode squeezed vacuum states of light," Opt. Express **21**, 11546–11553 (2013).
30. A. Ourjoumtsev, R. Tualle-Brouri, J. Laurat, and P. Grangier, "Generating optical Schrödinger kittens for quantum information processing," Science **312**, 83–86 (2006).

31. J. S. Neergaard-Nielsen, B. M. Nielsen, C. Hettich, K. Mølmer, and E. S. Polzik, "Generation of a superposition of odd photon number states for quantum information networks," Phys. Rev. Lett. **97**, 083604 (2006).
32. K. Wakui, H. Takahashi, A. Furusawa, and M. Sasaki, "Photon subtracted squeezed states generated with periodically poled $KTiOPO_4$," Opt. Express **15**, 3568–3574 (2007).
33. N. Bruno, A. Martin, P. Sekatski, N. Sangouard, R. T. Thew, and N. Gisin, "Displacement of entanglement back and forth between the micro and macro domains," Nat. Phys. **9**, 545–548 (2013).
34. A. I. Lvovsky, R. Ghobadi, A. Chandra, A. S. Prasad, and C. Simon, "Observation of micro-macro entanglement of light," Nat. Phys. **9**, 541–544 (2013).
35. O. Morin, K. Huang, J. Liu, H. Le Jeannic, C. Fabre, and J. Laurat, "Remote creation of hybrid entanglement between particle-like and wave-like optical qubits," Nat. Photonics **8**, 570–574 (2014).
36. H. Jeong, A. Zavatta, M. Kang, S.-W. Lee, L. S. Costanzo, S. Grandi, T. C. Ralph, and M. Bellini, "Generation of hybrid entanglement of light," Nat. Photonics **8**, 564–569 (2014).
37. P. Sekatski, N. Sangouard, M. Stobińska, F. Bussières, M. Afzelius, and N. Gisin, "Proposal for exploring macroscopic entanglement with a single photon and coherent states," Phys. Rev. A **86**, 060301 (2012).
38. S. L. Braunstein and C. M. Caves, "Statistical distance and the geometry of quantum states," Phys. Rev. Lett. **72**, 3439–3443 (1994).
39. E. G. Cavalcanti and M. D. Reid, "Criteria for generalized macroscopic and mesoscopic quantum coherence," Phys. Rev. A **77**, 062108 (2008).
40. F. Fröwis and W. Dür, "Are cloned quantum states macroscopic?" Phys. Rev. Lett. **109**, 170401 (2012).
41. While superpositions of coherent states with opposite phases have a negative Wigner representation, here we show that the size of two-mode vacuum squeezed states is basically the same. This shows that states with a positive Wigner representation can be macroscopically quantum.
42. To illustrate this, consider a state ρ_ϵ in Eq. (6) with $f_1(x,\bar{x}) = f_2(x,\bar{x}) = 1$ for $|x-\bar{x}| < \epsilon$ and zero otherwise. The peculiarity of this state is that f satisfies $\langle f' \rangle = \langle f'' \rangle = 0$ in such a way that the violation of the Duan–Simon criterion by ρ_ϵ is independent of ϵ unless it is strictly equal to zero. Therefore, ρ_ϵ with ϵ approaching zero is an example of a state that can give an arbitrarily high violation of the Duan criteria, while being arbitrarily close to a separable state.
43. G. Tóth and D. Petz, "Extremal properties of the variance and the quantum Fisher information," Phys. Rev. A **87**, 032324 (2013).
44. S. Yu, "Quantum fisher information as the convex roof of variance," arXiv:1302.5311 (2013).
45. F. Fröwis and N. Gisin, "Tighter quantum uncertainty relations follow from a general probabilistic bound," Phys. Rev. A **92**, 012102 (2015).
46. T. J. Volkoff and K. B. Whaley, "Measurement- and comparison-based sizes of Schrödinger cat states of light," Phys. Rev. A **89**, 012122 (2014).
47. S. Raeisi, P. Sekatski, and C. Simon, "Coarse graining makes it hard to see micro-macro entanglement," Phys. Rev. Lett. **107**, 250401 (2011).
48. F. Fröwis, M. Van den Nest, and W. Dür, "Certifiability criterion for large-scale quantum systems," New J. Phys. **15**, 113011 (2013).
49. T. Wang, R. Ghobadi, S. Raeisi, and C. Simon, "Precision requirements for observing macroscopic quantum effects," Phys. Rev. A **88**, 062114 (2013).
50. P. Sekatski, N. Gisin, and N. Sangouard, "How difficult is it to prove the quantumness of macroscropic states?" Phys. Rev. Lett. **113**, 090403 (2014).

OUTLOOK

We observed some results, now it is the point where we might consider further steps. We will elaborate on possible extensions of the work which have been done trough this thesis.

Let us first start with extending the results obtained regarding the demonstration of entanglement in many-body systems. Starting with bipartite entanglement, one could first think of improving the characterisation of separable moments of collective spin observables that can identify more entangled states. Machine learning offer a tools to estimate the separability of a collection of moments, helping us to find a witness better suited to specific states. As of now, complete characterization of such set of moments has be done, but without partitioning of many body systems [60].

In the second chapter we demonstrate that Bell violation using collective observable can be found in bipartite many-body systems but so far the requirements are that one can access to single particle resolution. On the other hand the demonstration of entanglement is far less demanding, requiring only the use of low order moments of collective spin observables. One intermediate approach is to look for the demonstration of entanglement using a device independent entanglement witness (DIEW) [61]. As we saw in the introduction, the demonstration of entanglement through a witness relies on the accurate description of the measurement apparatus which might not be verifiable in practice. The use of a DIEW relaxes this assumption and allows for entanglement certification without assumption about the measurement, even allowing the use of this entanglement in secure protocol.

In the particular case of a split spin squeezed state which we consider in our paper, we saw that 3 settings on both sides seems to be necessary to demonstrate entanglement with low order moments of collective spin observable. DIEWs take advantage of the structure of the measurement, and for two measurements, it has been shown that measuring qubits with Pauli observables is the optimal strategy. This gives a simple structure on which one can easily perform optimization. In the case of three settings, it is not even clear if simplifying the measurement structure with Pauli matrices acting on qubit is possible. Thus one would need to clarify this question before starting to work in the direction of developing DIEWs for bipartite many body systems which use more than two settings.

Finally, regarding the demonstration of non locality in bipartite many body systems using low order moments of collective spin observables, we focused on Bell inequalities with many settings. Finding the exact local bound for such inequalities can be down by listing the deterministic strategies. However this soon becomes impossible for large inputs and outputs. Methods to find upper bounds to the local bound have been proposed [62]. One could then use them to detect non-locality in systems with many spins.

In the third chapter, we make a proposal for the demonstration of non classical features using the human eye. We also tested similar approaches with CCD camera, and found that both were able to reveal quantum features. We thus tried the demonstration of non locality using only CCD cameras, displacement operators and single photon coming from an SPDC process. We found that single particle resolution is required for the detectors, which current cameras can not achieve. One might consider adding a squeezing operation locally in order to create a squeezed Fock state which has been realized in practise recently [63]. This might increase the resolution of the measurement and thus possibly allow for the convenient demonstration of non locality with CCD camera instead of large bulky devices involving dilution fridge. This might even lead to a convenient and practical way to implement device independent quantum key distribution.

CONCLUSION

In this thesis, we have presented different theoretical tools for demonstrating the quantum features of possibly large photonic and spin systems. We devoted a special attention to experimental realization by considering quantities which are accessible to today's experiments and including detailed statistical analysis in the proposed recipes. Our aim was not only to propose experiments demonstrating entanglement/non-locality in possibly large spin and photonic systems, but to clarify on the requirements that the detection systems need to fulfil to detect the quantum nature of these large systems. We saw that collective projections in which the subsystems are measured along the same direction, does not prevent the detection of entanglement and non-locality. Even threshold detectors with low efficiencies can be used to reveal non-classical features of states involving many photons. In parallel, we made steps to clarify on the meaning of large/macroscopic when describing quantum states.

Allowing experiments on multipartite or many body systems can help clarifying the border between classical/quantum physics. In particular, such experiments could be used to verify predictions of novel physical theories in which quantum theory for example is supplemented with explicite collapse mechanisms. Beside the fundamental interest, clarifying the requirements for detecting entanglement in multi-partite system is of central importance for certifying the proper functioning of advanced quantum technologies. This is needed for example to detect entanglement between multiple network nodes and to certify that the resulting network can be used to communicate securely. Time will tell us if the tools we proposed in this thesis are useful in practice, but we are confident that some of them will lead to exciting experiments in a near future.

BIBLIOGRAPHY

[1] J. S. Bell, Physics **1**, 195 (1964)

[2] S.-K. Liao et al., Nature (London) 549, **43** (2017)

[3] D. Castelvecchi, Nature 541,**9** (2017)

[4] G. Tóth and I. Apellaniz, J. Phys. A **47**, 424006 (2014)

[5] H.J. Briegel, D.E. Browne, W. Dür, R. Raussendorf & M.Van den Nest, Nature Phys. **5**, 19-26 (2009)

[6] R. Horodecki, P. Horodecki, M. Horodecki and K. Horodecki Rev. Mod. Phys. **80**, 865-942 (2009)

[7] F. Fröwis, M. van den Nest, and W. Dr, New J. Phys. **15**, 113011 (2013)

[8] A. Peres, Phys. Rev. Lett. **77**, 1413 (1996)

[9] P. Horodecki, Phys. Lett. A **232**, 333 (1997)

[10] O. Rudolph, Quantum Inf. Proc. **4**, 219 (2005)

[11] K. Chen and L.-A. Wu, Quant. Inf. Comp. **3**, 193 (2003)

[12] O. Gühne and G. Tóth, Phys. Rep. **474**, 1 (2009)

[13] A. Sorensen, L.-M. Duan, I. Cirac & P. Zoller, Nature **409**, 63-66 (2001)

[14] A. S. Sorensen and K. Molmer, Phys. Rev. Lett. **86**, 4431 (2001)

[15] L.-M. Duan, Phys. Rev. Lett. **107**, 180502 (2011)

[16] B. Lücke, J. Peise, G. Vitagliano, J. Arlt, L. Santos, G. Tóth, and C. Klempt, Phys. Rev. Lett. **112**, 155304 (2014)

[17] D. Rosset, R. Ferretti-Schbitz, J.-D. Bancal, N. Gisin, and Y.-C. Liang, Phys. Rev. A **86**, 062325 (2012)

[18] A. Acín, N. Gisin, and L. Masanes, Phys. Rev. Lett. **97**, 120405 (2006)

[19] D. Mayers and A. Yao, Quantum Inf. Comput. **4**, 273 (2004)

[20] R. Schmied, J-D. Bancal, B. Allard, M. Fadel, V. Scarani, P. Treutlein, and N. Sangouard, Science **352**, 441 (2016)

[21] F. Haas, J. Volz, R. Gehr, J. Reichel, and J. Esteve, Science **344**, 180 (2014)

[22] K. Lange, J. Peise, B. Lücke, I. Kruse1, G. Vitagliano, I. Apellaniz, M. Kleinmann, G. Tóth and C. Klempt, Science **360**, 416 (2018)

[23] M. Fadel, T. Zibold, B. Decamps, P. Treutlein, Science **360**, 409 (2018)

[24] P. Kunkel, M. Prüfer, H. Strobel, D. Linnemann, A. Frölian, T. Gasenzer, M. Gárttner and M.K. Oberthaler, Science **360**, 413 (2018)

[25] R. Hanbury Brown and R.Q. Twiss, Nature **177**, 27-29 (1956)

[26] C. Kurtsiefer, S. Mayer, P. Zarda, and H. Weinfurter, Phys. Rev. Lett. **85**, 290 (2000)

[27] Z. Yuan, B.E. Kardynal, R.M. Stevenson, A.J. Shields, C.J. Lobo, K. Cooper, N.S. Beattie, D.A. Ritchie, and M. Pepper, Science **295**, 102 (2002)

[28] M. Keller, B. Lange, K. Hayasaka, W. Lange, and H. Walther, Nature **431**, 1075 (2004)

[29] K.M. Birnbaum, A. Boca, R. Miller, A.D. Boozer, T.E. Northup, and H.J. Kimble, Nature **436**, 87 (2005)

[30] M. Hijlkema, B. Weber, H.P. Specht, S.C. Webster, A. Kuhn, and G. Rempe, Nat. Phys. **3**, 253 (2007)

[31] B. Sanguinetti ,A. Martin, H. Zbinden and N. Gisin, Phys. Rev. X **4**, 031056 (2014)

[32] S. Hecht, S. Shlaer, and M. Pirenne, J. Gen. Physiol. **25** , 819 (1942)

[33] V. Caprara Vivoli, P. Sekatski, and N. Sangouard, Optica **5**, 473 (2016)

[34] N. Brunner, C. Branciard, and N. Gisin, Phys. Rev. A **78**, 052110 (2008)

[35] P. Sekatski, N. Brunner, C. Branciard, N. Gisin and C. Simon, Phys. Rev. Lett. **103**, 113601 (2009)

[36] P. Sekatski, B. Sanguinetti, E. Pomarico, N. Gisin and C. Simon, Phys. Rev. A **82**, 053814 (2010)

[37] N. Sangouard, C. Simon, H. de Riedmatten, and N. Gisin, Rev. Mod. Phys. **83**, 33 (2011)

[38] E. Lombardi, F. Sciarrino, S. Popescu, and F. D.Martini, Phys. Rev. Lett. **88**, 070402 (2002)

[39] F. Sciarrino, E. Lombardi, G. Milani, and F. D.Martini, Phys. Rev. A **66**, 024309 (2002)

[40] D. Salart, O. Landry, N. Sangouard, N. Gisin, H. Herrmann, B. Sanguinetti, C. Simon, W. Sohler, R.T. Thew, A. Thomas and H. Zbinden, Phys. Rev. Lett. **104**, 180504 (2010)

[41] C.W. Chou, H. de Riedmatten, D. Felinto, S.V. Polyakov, S.J. van Enk, and H.J. Kimble, Nature **438**, 828 (2005)

[42] K.S. Choi, H. Deng, J. Laurat, and H.J. Kimble, Nature **452**, 67 (2008)

[43] C.-W. Chou, J. Laurat, H. Deng, K.S. Choi, H. de Riedmatten, D. Felinto, and H.J. Kimble, Science **316**, 1316 (2007)

[44] O. Morin, J.-D. Bancal, M. Ho, P. Sekatski, V. D'Auria, N. Gisin, J. Laurat, and N. Sangouard, Phys. Rev. Lett. **110**, 130401 (2013)

[45] J. Wallnöfer, M. Zwerger, C. Muschik, N. Sangouard, and W. Dür, Phys. Rev. A **94**, 052307 (2016)

[46] F. Fröwis, P. Sekatski, W. Dr, N. Gisin, and N. Sangouard, Rev. Mod. Phys. **90**, 025004 (2018)

[47] F. Monteiro, V. Caprara Vivoli, T. Guerreiro, A. Martin, J.-D. Bancal, H. Zbinden, R.T. Thew, and N. Sangouard Phys. Rev. Lett. **114**, 170504 (2015)

[48] V. Caprara Vivoli, P. Sekatski, J.-D. Bancal, C.C.W. Lim, A. Martin, R.T. Thew, H. Zbinden, N. Gisin, and N. Sangouard, New J. Phys.**17**, 023023 (2015)

[49] N. Bruno, A. Martin, P. Sekatski, N. Sangouard, R.T. Thew, and N. Gisin, Nat Phys **9**, 545 (2013)

[50] L.-M. Duan, G. Giedke, J.I. Cirac, and P. Zoller, Phys. Rev. Lett. **84**, 2722 (2000)

[51] R. Simon, Phys. Rev. Lett. **84**, 2726 (2000)

[52] A.I. Lvovsky, R. Ghobadi, A. Chandra, A.S. Prasad, and C. Simon, Nat Phys **9**, 541 (2013)

[53] O. Morin, K. Huang, J. Liu, H. Le Jeannic, C. Fabre, and J. Laurat, Nat Photon **8**, 570 (2014)

[54] H. Jeong, A. Zavatta, M. Kang, S.-W. Lee, L. S. Costanzo, S. Grandi, T.C. Ralph, and M. Bellini, Nat Photon **8**, 564 (2014)

[55] A. Ourjoumtsev, R. Tualle-Brouri, J. Laurat, and P. Grangier, Science **312**, 83 (2006)

[56] J.S. Neergaard-Nielsen, B.M. Nielsen, C. Hettich, K. Mlmer, and E. S. Polzik, Phys. Rev. Lett. **97**, 083604 (2006)

[57] K. Wakui, H. Takahashi, A. Furusawa, and M. Sasaki, Opt. Express 15, 3568 (2007)

[58] E. G. Cavalcanti and M.D. Reid, Phys. Rev. Lett. **97**, 170405 (2006)

[59] C.-W. Lee and H. Jeong, Phys. Rev. Lett. **106**, 220401 (2011)

[60] G. Tóth, C. Knapp, O. Gühne, and H.J. Briegel, Phys. Rev. Lett. **99**, 250405 (2007)

[61] J.-D. Bancal, N. Gisin, Y.C. Liang, and S. Pironio, Phys. Rev. Lett. **106**, 250404 (2011)

[62] M. Fadel and J. Tura Phys. Rev. Lett. **119**, 230402 (2017)

[63] D. Kienzler, H.-Y. Lo, V. Negnevitsky, C. Flühmann, M. Marinelli, and J. P. Home, Phys. Rev. Lett. **119**, 033602 (2017)

APPENDIX A

BOUND FOR THE TERMS OUTSIDE THE QUBIT SPACE

Bound on $\mathrm{Tr}\left(b^\dagger B + bB^\dagger\right)$

Consider a finite hermitian matrix $\bar{W}$ and a state ρ of the form $\bar{W} = \begin{pmatrix} A & B \\ B^\dagger & C \end{pmatrix}$ and $\rho = \begin{pmatrix} a & b \\ b^\dagger & c \end{pmatrix}$, where a and A live in a Hilbert space $\mathcal{H}_A$ and c and C live in a Hilbert space $\mathcal{H}_C$. The trace of a is equal to $(1-P)$ so the trace of b is equal to P. Our aim is to find a lower bound of $\mathrm{Tr}\left(b^\dagger B + bB^\dagger\right)$. We first consider the states

$$|\psi^i\rangle = \cos\theta\,|\chi_A^i\rangle + \sin\theta\,|\chi_C^i\rangle\,, \tag{A.1}$$

where $|\chi_A^i\rangle$ reside in $\mathcal{H}_A$ and $|\chi_C^i\rangle$ in $\mathcal{H}_C$. We then evaluate the overlap between ρ and $|\psi^i\rangle$

$$\begin{aligned} \sum_i^L \langle\psi^i|\,\rho\,|\psi^i\rangle &= \sum_i^L \cos^2\theta(\langle\chi_A^i|\,a\,|\chi_A^i\rangle + sin^2\theta\,\langle\chi_C^i|\,c\,|\chi_C^i\rangle \\ &+ \cos\theta\sin\theta(\langle\chi_C^i|\,b\,|\chi_A^i\rangle + h.c)). \end{aligned} \tag{A.2}$$

where $L = \min\dim(\mathcal{H}_A), \dim(\mathcal{H}_C)$. We consider the singular value decomposition of b, $b = UDV^\dagger$ and choose $|\chi_A^i\rangle$ such that $|\chi_A^i\rangle = U\,|a_i\rangle$ and $|\chi_C^i\rangle = V\,|c_i\rangle$ where $|a_i\rangle$ is a basis of $\mathcal{H}_A$ and $|b_i\rangle$ is a basis of $\mathcal{H}_B$. We choose θ such that $\cos\theta \geq 0$

and $\sin\theta \leq 0$ The positivity of (A.2) thus implies

$$\sum_i d_i \leq \frac{\cos^2\theta(1-P) + sin^2\pi + \theta P}{2\cos\theta\sin\pi + \theta}, \tag{A.3}$$

where d_i are the singular value of D. Taking the maximum over θ of (A.3), we obtain

$$\sum_i d_i \leq \sqrt{P(1-P)}, \tag{A.4}$$

which is useful for bounding the terms $\mathrm{Tr}\left(b^\dagger B + bB^\dagger\right)$ in (**??**). Indeed one has

$$\begin{aligned}
\mathrm{Tr}\left(bB^\dagger\right) = \mathrm{Tr}\left(\sum_j (d_j \left|a_j\right\rangle \left\langle c_j\right| B)\right) &= \sum_j d_j \left\langle \bar{j}\right| B \left|j\right\rangle \\
&\leq \sum_j d_j \left|\left\langle \bar{j}\right| B \left|j\right\rangle\right| \\
&\leq \sum_j d_j |b_{max}| \\
&\leq \sqrt{P_2(1-P_2)}|b_{max}|,
\end{aligned}$$

where b_{max} is the maximum singular value of B in amplitude. We have

$$\mathrm{Tr}\left(bB^\dagger\right) \geq -\sqrt{P_2(1-P_2)}|b_{max}|, \tag{A.5}$$

thus we arrive to the expected bound.

Computation of λ_{min}

We can find λ_{min} by noting that $\max|\langle\hat{J}_\alpha\rangle| = \frac{N}{2}$ and $\langle\hat{J}_\alpha^2\rangle \leq \frac{N^2}{4}$, thus since $\min\langle\bar{\mathcal{W}_\mathcal{N}}\rangle \leq \min\frac{1}{2\pi}d\phi\langle\mathcal{W}_\mathcal{N}\rangle$ we have that λ_{min} is larger or equal to $1 - 3\frac{N^2}{4}$

Computation of $|b_{max}|$

Le us consider that $W_N = \begin{pmatrix} A_N & B_N \\ B_N^\dagger & C_N \end{pmatrix}$

We want to compute the singular value of B_N. Although this matrix can be infinite, we then perform the phase randomisation on the matrix itself. Let us recall that $\mathcal{W}_\mathcal{N} = \prod_i^N e^{i\phi_i a_i^\dagger a_i}\bar{\mathcal{W}}_\mathcal{N}\prod_i^N e^{-i\phi_i a_i^\dagger a_i}$, which implies that $\mathcal{B}_\mathcal{N} = \prod_i^N e^{i\phi_i a_i^\dagger a_i}\bar{\mathcal{B}}_\mathcal{N}\prod_i^N e^{-i\phi_i a_i^\dagger a_i}$. We want to bound quantity $\int\frac{1}{2\pi}d\phi\mathrm{Tr}\left(b^\dagger B_N + bB_N^\dagger\right)$. One have $\frac{1}{2\pi}d\phi\mathrm{Tr}\left(b^\dagger B_N\right) = \mathrm{Tr}\left(b^\dagger\frac{1}{2\pi}d\phi B_N\prod_i^N e^{i\phi_i a_i^\dagger a_i}\bar{\mathcal{B}}_\mathcal{N}\prod_i^N e^{-i\phi_i a_i^\dagger a_i}\right)$. Since the matrix $B_n = \frac{1}{2\pi}d\phi B_N\prod_i^N e^{i\phi_i a_i^\dagger a_i}\bar{\mathcal{B}}_\mathcal{N}\prod_i^N e^{-i\phi_i a_i^\dagger a_i}$ now has a finite size, we can then numerically compute the singular value of B_n and deduce $|b_{max}|$ which will depend on N and on the settings.

APPENDIX B

STATISTICS

Variance for the estimator of $\langle \mathcal{W} \rangle$

We consider the following estimator for $\hat{J}_\alpha^2$,

$$\xi(\hat{J}_\alpha^2) = \sum_{i=1}^{n} \frac{(J_{\alpha_i})^2}{n} \tag{B.1}$$

The variance of such estimator is then given by

$$var(\xi(\hat{J}_\alpha^2)) = \frac{var(\hat{J}_\alpha^2)}{n}. \tag{B.2}$$

Since $W = 2\hat{J}_0(\frac{N}{2} - 1)) - 2\hat{J}_\alpha^2 + cst$, we can just consider that we are evaluating each term on different runs and then sum the variance for each terms in order to have a conservative estimation of the estimator of W. We end up with

$$var(\xi(W)) \leq 4\frac{var(\hat{J}_\alpha^2)}{n} + 4(\frac{N}{2} - 1)^2 \frac{var(\hat{J}_0)}{n}. \tag{B.3}$$

We thus have to compute fourth order moments of collective observable,we then simply use the fact that

$$\begin{aligned}\hat{J}_\alpha^4 &= \frac{1}{16}(\sum_{i,j,k,l}^{N} \sigma_\alpha^{(i)}\sigma_\alpha^{(j)}\sigma_\alpha^{(k)}\sigma_\alpha^{(l)}) \\ &= \frac{1}{16}(N\mathbf{I} + 4(N^2-N)\sigma_\alpha^{3\,(i\neq j)}\sigma_\alpha^{(j\neq i)} \\ &+ 3(N^2-N)\sigma_\alpha^{2\,(i\neq j)}\sigma_\alpha^{2\,(j\neq i)} \\ &+ 6(N-2)(N-1)N\sigma_\alpha^{2\,(i\neq j\neq k)}\sigma_\alpha^{(j\neq i\neq k)}\sigma_\alpha^{(j\neq i\neq k)} \\ &+ (N^4-6N^3+12N^2-6N)\sigma_\alpha^{(i\neq j\neq k\neq l)}\sigma_\alpha^{(j\neq i\neq k\neq l)}\sigma_\alpha^{(j\neq i\neq k\neq l)}\sigma_\alpha^{(j\neq i\neq k\neq l)}).\end{aligned}$$

Together with the fact that each of this terms can be easily computed on a coherent state and after the integration (4.13), on our state.

Variance for the estimator of $2\sqrt{P_2(1-P_2)}|b_{max}|$

To avoid the problem of the variance of an estimator for the square root, we then simply consider a linearised upper bound for the quantity $2\sqrt{P_2(1-P_2)}$ around the expected P_2 which we call $f(P_2)$. For the estimation of P_2, we consider a random variable X which take value 1 with probability P_2 and 0 with probability $1-P_2$, we then have the following estimator

$$\xi(P_2) = \sum_{i=1}^{n} \frac{(X_i)}{n} \tag{B.4}$$

for which the variance is equal to $\frac{(1-P_2)P_2}{n}$. the same hold for the term $\lambda_{min}P_2$.

Variance for the estimator of w_{PPT}

The dependence of this term with respect to the measured quantity P_1 is non trivial since it is a parameter in the performed SDP. To avoid this problem, we first compute the standard deviation of P_1, σ_{P_1}. We then overestimate P_1 with $P_1' = P_1 + 3\sigma_{P_1}$ to have an estimation with a statistically relevant P_1. $\min_{\rho_{bis}} \mathrm{Tr}(W_{qbit}\rho)$ contains in this way the statistical fluctuation of P_1.

Oudot Enky

Personal Details

Address: 2 rue Eugene Charron
Saint-Louis, FR-68300
France

Phone: +33 (0)60 116 9659
Email: enky.oudot1@gmail.com

Education

University of Basel, Switzerland
Doctor of Philosophy (Physics) — Sep 2014- Dec 2018

University of Paris-Sud, France
Master of Science (Physics) — Sep 2012 - Sep 2014

Bachelor of Science (Physics) — Sep 2009 - Sep 2012
- Double Major in Physics and Mathematics

Work Experience

Department of Physics, University of Basel
Position: Doctoral Assistant — Sep 2014 - Current

- Research
  - Currently investigating genuinen entanglement in large systems.
  - Systematically cast physical problems into precise mathematical quantities for analysis
  - Utilise assumptions and constraints to identify mathematical relations, and present bounds on the behaviour of physical systems in peer-reviewed publications
  - Review literature for gaps in existing knowledge, in collaboration with senior researchers, allowing for formulation of new scientific direction
  - Contributed to discussions over analytical functions and matrix operators, in group discussions, helping to guide co-workers to more accurate and powerful solutions in their projects, strengthening final results
- Teaching and Outreach
  - Assistant for the lecture "Stochastic process and application for finance"
  - Help to create a new lecture on "Introduction to quantum mechanics"
  - Mentored undergraduates as part of their formation into beginning their own research projects, pointing out possible research directions for their pursuit

Attributes and Skills

- Ability to solve complicated problems
- Fluent in English and French
- Proficient with Matlab and Mathematica, for programming of numerical simulations
- Well versed with MS Office and LaTeX for document processing

Scientific Publications

- **E. Oudot**, P. Sekatski, F. Frwis, N. Gisin, and N. Sangouard,
  Two-mode squeezed states as Schrdinger cat-like states,
  JOSA B 32, 10 (2015)
- **E. Oudot**, Jean-Daniel Bancal, Roman Schmied, Philipp Treutlein, and Nicolas Sangouard. *Optimal entanglement witnesses in a split spin-squeezed Bose-Einstein condensate*,
  Phys. Rev. A 95, 052347(2017)
- Amaury Dodel, Anthony Mayinda, **E. Oudot**, Anthony Martin Pavel Sekatski, Jean Daniel Bancal, and N. Sangouard,
  Proposal for witnessing non-classical light with the human eye,
  Quantum 1, 7 (2017).
- Melvyn Ho, **E. Oudot**, Jean-Daniel Bancal, and Nicolas Sangouard,
  Witnessing optomechanical entanglement with photon counting,
  Physical Review Letters **121**, 023602 (2018)